1982

Vibrational characteristics and seismic analysis of cylindrical liquid storage tanks, May 1982 (Tedesco's PhD dissertation)

Joseph W. Tedesco

Celal N. Kostem

Lehigh University

VIBRATIONAL CHARACTERISTICS AND SEISMIC ANALYSIS OF CYLINDRICAL LIQUID STORAGE TANKS

BY

JOSEPH W. TEDESCO

CELAL N. KOSTEM

Fritz Engineering Laboratory

FRITZ ENGINEERING LABORATORY REPORT NO. 433.5

VIBRATIONAL CHARACTERISTICS AND SEISMIC ANALYSIS

OF

CYLINDRICAL LIQUID STORAGE TANKS

by

Joseph W. Tedesco

Celal N. Kostem

Fritz Engineering Laboratory

Department of Civil Engineering

Lehigh University

Bethlehem, Pennsylvania

May, 1982

Fritz Engineering Laboratory Report No. 433.5

TABLE OF CONTENTS

TABLE OF CONTENTS (continued)

TABLE OF CONTENTS (continued)

ABSTRACT

This dissertation presents the results of an in-depth investigation concerning the vibrational characteristics and seismic analysis of ground supported, circular cylindrical liquid storage tanks subject to a horizontal component of earthquake ground motion. The scope of the study includes empty, partially full, and completely full tanks.

Simple analytical expressions, in the form of cubic polynomials, are developed for empty tanks which accurately predict frequencies and radial mode shapes corresponding to the fundamental mode of vibration. These expressions form the basis of simplified procedures for determining shell stresses and displacements, base shears, and overturning moments induced in empty cylindrical tanks by earthquake ground motion. The effects of a roof structure and support conditions upon the vibrational characteristics of cylindrical tanks are also examined.

Analytical expressions, also in the form of cubic polynomials, are developed which accurately determine the fundamental natural frequency of the shell and the impulsive fluid mass. These expressions are applicable to tanks both half full and completely full with liquid. Simple procedures for assessing impulsive hydrodynamic wall pressures, and the resulting shell stresses, base shears, and overturning moments induced in flexible tanks by a horizontal component of earthquake ground motion are presented. Numerical comparisons which verify the accuracy of the procedures developed in this investigation are provided.

1. INTRODUCTION

1.1 Introduction

The performance of liquid storage tanks during a seismic event is well documented in the literature (Refs. 10, 19, 25 and 57). Special importance is assigned to this matter because of the potentially disastrous results associated with liquid storage tank failures. For example, uncontrolled fires in the wake of a major earthquake could result if the water supply is disrupted, and cause more damage than the earthquake itself. Spillage of flammable petroleum products and toxic chemicals can cause damage which extends far beyond the values of the affected tanks and contents.

The circular cylindrical tank, built on grade and usually constructed in steel (or aluminum) or prestressed concrete is one of the most common forms of liquid storage vessels. Damage surveys of tanks that were subjected to actual earthquakes have shown various modes of failure for these tanks (Refs. 25, 48, 55 and 57). For steel tanks the most common form of failure observed has been the buckling of the tank walls due to the development of high compressive stresses, induced by seismic forces causing an overturning moment at the base of the tank. Damage to concrete tanks ranges from cracking (produced by tensile hoop stresses which develop due to shaking induced hydrodynamic pressures between the liquid and the tank wall)

to total collapse. Damage to fixed or floating roofs can also result from liquid sloshing if sufficient freeboard does not exist.

The foregoing examples illustrate the need for simple, accurate, and practical analytical methods capable of predicting pressures exerted by the liquid on the tank wall and of determining the resulting shell stresses, base shear, and overturning moment. The present study addresses this need.

The following sections of this chapter present the objectives and scope of the present investigation, and a brief review of previous research conducted in the subject area.

1.2 Previous Research

The development of the early seismic response theories of liquid storage tanks considered the container to be rigid. One of the first investigators, Jacobsen (Refs. 31 and 32), developed equations for effective hydrodynamic mass and mass moment for the contents of cylindrical tanks subject to horizontal translation.

Graham and Rodriguez (Ref. 23) simulated the behavior of the liquid contents of rectangular tanks by an equivalent multi-degree-of-freedom mechanical spring-mass system, where the different masses and spring stiffnesses represented the contributions of the different sloshing modes of vibration (Ref. 30).

Housner (Refs. 27 and 28) developed a simplified procedure for estimating liquid response in seismically excited rigid,

rectangular and cylindrical tanks. In that study, the response was considered to be composed of separate convective and impulsive components. The Housner procedure was later refined and amplified by the Atomic Energy Commission (Ref. 63).

The aerospace industry has also made significant contributions to research on the dynamic behavior of liquid storage vessels. The "slosh problem" as related to liquid propellants for rockets or space vehicles was thoroughly investigated, both analytically and experimentally, by Abramson (Ref. 1). The problem was further studied by Bauer who developed a comprehensive mathematical model for applications in the design of fuel tanks in space vehicles (Ref. 9).

Edwards (Ref. 20) was the first investigator to consider tank flexibility in establishing the hydrodynamic forces exerted on ground supported, cylindrical tanks subject to horizontal earthquake ground motions. He was also the first of several investigators to employ the finite element technique to the dynamic analysis of liquid storage tanks. Subsequent finite element investigations were conducted by Shaban and Nash (Ref. 60), and Haroun (Ref. 26). In his study, Haroun also considered effects which complicate the dynamic behavior of liquid storage tanks such as the effect of initial hoop stress due to hydrostatic pressure, the effect of coupling between liquid sloshing and shell vibration, and the effect of soil flexibility. In all three of the aforementioned finite element investigations it was assumed that the base of the tank was uniformly and

continuously connected about its periphery to a rigid foundation, and that the tank had no roof structure.

Veletsos (Ref. 64) presented a simple procedure for evaluating the hydrodynamic forces induced in flexible liquid filled cylindrical tanks. This method was based on the assumptions that the tank behaved as a single-degree-of-freedom system, that the cross-section of the tank remained circular during vibration, and that the heightwise distribution of the deflection was of a prescribed form. Simplified formulas to obtain the fundamental natural frequencies of both empty and completely filled (with liquid) cylindrical storage tanks by the Rayleigh-Ritz method were later presented by Veletsos and Yang (Ref. 65). In both of these studies it was also assumed that the periphery of the tank base was uniformly and continuously attached to a rigid foundation and that the tank had no roof structure.

The dynamic response of flexible, liquid-filled cylindrical tanks subject to a vertical excitation of the base was investigated by Yang (Ref. 68), and then by Kumar (Ref. 45). In his study Kumar presented a general modal superposition procedure for the analysis of the shell-liquid system subject to a vertical transient excitation of arbitrary time variations.

Limited experimental investigations of the behavior of shallow cylindrical liquid storage tanks were conducted by Clough (Ref. 13), and similar investigations of tall cylindrical liquid storage tanks were conducted by Niwa (Ref. 54). The results of these experiments indicated that higher order circumferential modes

of vibration (i.e. cos $n\theta$; refer to Section 2.1 for detailed explanation) may be excited by a lateral earthquake-like disturbance of the base of the cylindrical tanks, due to inherent imperfections in the geometry of the shell.

1.3 Objectives

The primary objectives of the present investigation are:

1. To provide information for a better understanding of the vibrational characteristics of both empty and liquid-filled cylindrical storage tanks.
2. To develop simplified procedures applicable to the dynamic (response spectrum) seismic analysis of cylindrical liquid storage tanks subject to lateral earthquake ground motion.

Among the unique contributions of the reported study are:

1. An evaluation of the effects of boundary conditions on the vibrational characteristics of cylindrical tanks,
2. Assessment of the effect of roof structures on the vibrational characteristics of cylindrical tanks,
3. Development of simple analytical expressions which accurately determine the vibrational characteristics (frequency and mode shape) of flexible cylindrical storage tanks, and

4. The development of simplified procedures for assessing the seismic response (i.e. hydrodynamic pressures, shell stresses, base shears, and overturning moments) of flexible cylindrical liquid storage tanks.

The investigation described herein was performed in four phases:

Phase I - Vibrational characteristics of empty cylindrical tanks

Phase II - Vibrational characteristics of liquid-filled cylindrical tanks

Phase III - Seismic analysis of empty cylindrical storage tanks

Phase IV - Seismic analysis of liquid-filled cylindrical storage tanks

The subject matter of these studies is covered in four chapters, the scope of which is defined in the following section. Each chapter is written in a self-contained manner, and may be read essentially independently of the others.

1.4 Scope of Study

The vibrational characteristics (i.e. natural frequencies and mode shapes) of empty cylindrical storage tanks both with and without roof structures are examined in Chapter 2. This comprehensive study encompasses a class of tanks having a height to diameter ratio,

H_o/D_o, within the range of 0.1 to 1.5, inclusive, thus including the transition from shallow ($H_o/D_o \leq 0.5$) to tall ($H_o/D_o \geq 0.75$) tanks. Special emphasis is placed upon the free vibration aspects associated with a circumferential wave number, n, equal to one, and an axial wave number, m, equal to one (refer to Section 2.1 for details). Simple analytical expressions, in the form of cubic polynomials, are developed which accurately determine the natural frequencies and mode shapes of empty cylindrical tanks associated with the n = 1 and m = 1 mode.

An evaluation of the effects of discrete boundary (or support) conditions at the tank base upon the vibrational characteristics of cylindrical tanks are also provided in Chapter 2. The effects of roof structure on the vibrational characteristics of empty tanks are also assessed in this chapter. Analytical expressions, similar to those developed for open-top cylindrical tanks, for predicting natural frequencies and mode shapes of tanks with roof structure are also presented.

Chapter 3 deals with the vibrational characteristics of liquid-filled cylindrical storage tanks without roof structure possessing a height to diameter ratio within the range 0.1 to 1.5 inclusive. Tanks both completely full and half-full with liquid are considered. Simple analytical expressions, also in the form of cubic polynomials, for estimating the natural frequencies associated with the n = 1, m = 1 mode are introduced.

In Chapter 4 simplified procedures for assessing the dynamic seismic response, by the response spectrum technique, of empty cylindrical storage tanks, both with and without a roof structure, are presented. For simplicity in the analysis, the tank is idealized as a continuous, single-degree-of-freedom system. Simple expressions to estimate shell displacements and membrane stresses, base shears, and overturning moments induced by a horizontal component of earthquake ground motion are presented.

The dynamic seismic (via the response spectrum technique) response of both rigid and flexible liquid-filled, open-top cylindrical tanks subjected to horizontal earthquake ground motion is considered in Chapter 5. Both the impulsive and convective effects in rigid tanks are analyzed. Simplified procedures for assessing the impulsive effects (i.e. hydrodynamic pressures, shell membrane stresses, base shears, and overturning moments) induced in flexible tanks due to earthquake ground motions are developed. The convective effects are considered to be independent of tank flexibility and therefore may be assessed by existing methods available for rigid tanks.

2. VIBRATIONAL CHARACTERISTICS OF EMPTY TANKS

2.1 Introduction

A cylindrical shell undergoing free vibration may be deformed in a variety of ways as shown in Figs. 1 and 2, where several configurations are given. The natural modes of free vibration are defined by two integers: the number of circumferential waves, n; and the number of axial waves, m. Cases of n equal to 0, 1, 2 and 3 are represented in Fig. 1 and the axial wave forms corresponding to m equal to 1, 2, 3 and 4 are presented in Fig. 2. (The variation of the circumferential response is defined by cos ($n\theta$)). Theoretically an infinite number of such modes defined by n and m are possible.

Of particular interest in this investigation are the modes of free vibration associated with circumferential wave number n equal to 1, which may be excited by unidirectional lateral excitation of the base of a uniformly supported cylindrical shell (Fig. 3). The lowest mode of this type (that corresponding to axial wave number m equal to 1) is referred to as the flexural mode in which the radial displacement of the middle surface, w, is predominant (Fig. 3).

Modes of vibration corresponding to circumferential wave numbers, n, greater than one are usually not associated with the classical case of the lateral vibration of a cantilever cylindrical shell with uniform boundary conditions at its base (Refs. 68 and 43).

However, as often occurs in practice, the base of the shell is attached to its foundation at discrete locations about the circumference. This practice introduces imperfections into the systems, causing the mode of vibrations to deviate somewhat from the mode shape which corresponds to n = 1 and be influenced by higher order circumferential modes (n greater than 1). Such infiltration of higher circumferential modes, due to noncontinuous boundary conditions at the base of the shell, is among the aspects of the free vibration of cylindrical shells also examined in this investigation.

2.2 Mathematical Model for a Shell

The geometry of shells (i.e., where one dimension, the thickness, is much smaller than the other dimensions) does not warrant, in general, the consideration of the complete three dimensional elasticity equations. In the development of thin shell theories, simplification is accomplished by reducing the shell problem to the study of the deformations of the reference surface of the shell (Fig. 4). The geometry of a shell is entirely defined by specifying the form of the reference surface and the thickness of the shell at each point.

The two-dimensional reference surface which describes the shell, is specified mathematically by (Ref. 35)

$$\begin{aligned} x &= f_1(\zeta_1, \zeta_2) \\ y &= f_2(\zeta_1, \zeta_2) \\ z &= f_3(\zeta_1, \zeta_2) \end{aligned} \tag{2.1}$$

where x, y and z are Cartesian coordinates and ζ_1 and ζ_2 are coordinates on the reference surface (Fig. 4). The parameters ζ_1 and ζ_2 constitute a system of curvilinear coordinates for points on the reference surface, the position of any point on the surface being determined by the values of ζ_1 and ζ_2 at that point (Fig. 5). The parameter ζ_3 defines the thickness of the shell at the specified point.

The governing equations for a shell require the following information about the reference surface (Ref. 35):

1. The components of metric
2. The components of curvature

The "metric" describes the geometry of the chosen coordinate system ζ_1, ζ_2 on the reference surface (Ref. 35). It gives the relationship between an increment in a coordinate and the arclength along the coordinate curve between the points separated by the increment. Curvature describes how the surface curves.

The ζ_1 curve alone is first considered (Fig. 5). The metric component of the ζ_1 coordinate, denoted by α_1, is defined as the quantity by which $d\zeta_1$ must be multiplied to obtain the length $ds_1 = (PQ_1)$; thus

$$ds_1 = \alpha_1 \, d\zeta_1 \tag{2.2}$$

Introducing the unit tangent vector for the ζ_1 curve as $\vec{t}_1$, then

$$ds_1 \, \vec{t}_1 = \frac{d\vec{r}}{d\zeta_1} \, d\zeta_1 \tag{2.3}$$

where $\vec{r}$ is the position vector from the origin of the Cartesian coordinate systems to the point P on the reference surface. Substituting ds_1 from Eq. 2.2 into Eq. 2.3, the result is

$$\alpha_1 \vec{t}_1 = \frac{d\vec{r}}{d\zeta_1} \tag{2.4}$$

Thus the metric component α_1 is the magnitude of $\frac{d\vec{r}}{d\zeta_1}$, and can be determined from

$$\alpha_1 = \sqrt{\frac{d\vec{r}}{d\zeta_1} \cdot \frac{d\vec{r}}{d\zeta_1}} \tag{2.5}$$

Similarly, for the ζ_2 curve, the metric component α_2 is given by

$$\alpha_2 = \sqrt{\frac{d\vec{r}}{d\zeta_2} \cdot \frac{d\vec{r}}{d\zeta_2}} \tag{2.6}$$

The procedure for determination of the metric components, α_1 and α_2, as summarized in Ref. 35, is as follows:

1. Write the position vector $\vec{r}$ of a point on the reference surface as

$$\vec{r} = x\vec{i} + y\vec{j} + z\vec{k} \tag{2.7}$$

where $\vec{i}$, $\vec{j}$ and $\vec{k}$ are constant unit vectors along the x, y and z axes respectively.

2. Substitute for x, y and z in Eq. 2.7, the description of the reference surface given in Eq. 2.1.
3. Differentiate $\vec{r}$ with respect to ζ_1 and ζ_2, and determine α_1 and α_2 from Eqs. 2.5 and 2.6.

Directions on the reference surface are defined by unit tangent vectors $\vec{t}_1$ and $\vec{t}_2$ for the ζ_1 and ζ_2 curves respectively. The direction away from the reference surface is defined by the unit tangent vector $\vec{t}_3$, determined from

$$\vec{t}_3 = \vec{t}_1 \times \vec{t}_2 \tag{2.8}$$

Variables of the shell, such as displacement and forces, can be resolved along these unit vectors.

2.2.1 Axisymmetric Shells

Shells for which the geometry (reference surface) and material properties are symmetric with respect to one straight axis are known as axisymmetric shells. The reference surface of an axisymmetric shell is obtained by drawing any plane curve and revolving it about an axis lying in the plane of the curve (Figs. 6 and 7). This curve is called the meridian. Axisymmetric shells are very common structural elements and are used extensively in various kinds of containers, tanks, and domes (Ref. 66).

The simplification in the analysis, when going from a general shell to an axisymmetric shell, is considerable. This is so because the geometric and material parameters for an axisymmetric shell depend on one coordinate only (rather than two for a general shell). This transition analysis from the general shell to an axisymmetric shell is treated in Refs. 35, 43 and 66.

Because the geometric and material parameters of an axisymmetric shell depend on one coordinate only, the governing equations can be reduced to a one-dimensional form, thus facilitating the applications of methods of analysis that are available for the solutions of boundary value problems which are governed by ordinary differential equations (Refs. 8 and 35).

2.3 Governing Equations for Axisymmetric Shells

As was cited in the previous section, for an axisymmetric shell (Fig. 6) significant simplifications from the general shell model can be made. The curvature components, ζ_1 and ζ_2, for an axisymmetric shell are θ and s, respectively, where θ is the circumferential coordinate angle and s is the arclength along the meridian. The arclength s is defined by

$$ds = R_{\phi}\, d\phi \tag{2.9}$$

where ϕ is the angle between the axis of the shell and the shell normal, $\vec{t}_3$, and R_{ϕ} is the radius of curvature of the meridian. The metric components for an axisymmetric surface, α_1 and α_2, become r (Fig. 6) and 1, respectively (Ref. 35).

Referring to Fig. 8 for identification of force and moment resultants for an element of an axisymmetric shell, the equations of equilibrium are as follows:

$$\frac{1}{r}\frac{dN_\theta}{d\theta} + \frac{N_{\phi\theta}}{ds} + \frac{\cos\phi}{r}(N_{\theta\phi} + N_{\phi\theta}) + \frac{Q_\theta}{R_\theta} + p_\theta = 0 \qquad \text{(a)}$$

$$\frac{1}{r}\frac{dN_{\theta\phi}}{d\theta} + \frac{dN_\phi}{ds} + \frac{\cos\phi}{r}(N_\phi - N_\theta) + \frac{Q_\theta}{R_\phi} + p_\phi = 0 \qquad \text{(b)}$$

$$\frac{1}{r}\frac{dQ_\theta}{d\theta} + \frac{dQ_\phi}{ds} + \frac{\cos\phi}{r}Q_\phi - \left(\frac{N_\theta}{R_\theta} + \frac{N_\phi}{R_\phi}\right) + p_3 = 0 \qquad \text{(c)}$$

$$\frac{1}{r}\frac{dM_\theta}{d\theta} + \frac{dM_{\phi\theta}}{ds} + \frac{\cos\phi}{r}(M_{\theta\phi} + M_{\theta\phi}) - Q_\theta = 0 \qquad \text{(d)}$$

$$\frac{1}{r}\frac{dM_{\theta\phi}}{d\theta} + \frac{dM_\phi}{ds} + \frac{\cos\phi}{r}(M_\phi - M_\theta) - Q_\phi = 0 \qquad \text{(e)}$$

(2.10)

The stress-strain equations are:

$$N_\theta = K(\varepsilon_\theta + \nu\varepsilon_\phi) \qquad \text{(a)}$$

$$N_\phi = K(\varepsilon_\phi + \nu\varepsilon_\theta) \qquad \text{(b)}$$

$$N_{\theta\phi} = N_{\phi\theta} = \frac{(1-\nu)}{2} K(\alpha_\theta + \alpha_\phi) \qquad \text{(c)}$$

$$M_\theta = D(k_\theta + \nu k_\phi) \qquad \text{(d)}$$

$$M_\phi = D(k_\phi + \nu k_\theta) \qquad \text{(e)}$$

$$M_{\theta\phi} = M_{\phi\theta} = \frac{(1-\nu)}{2} D(\delta_\phi + \delta_\theta) \qquad \text{(f)}$$

(2.11)

where $K = \frac{E h^2}{1-\nu^2}$ and $D = \frac{E h^3}{12(1-\nu^2)}$, in which E is Young's modulus h is the shell thickness, and ν is Poisson's ratio.

The strain-displacement relations are:

$$\varepsilon_\theta = \frac{1}{r}\frac{du_\theta}{d\theta} + \frac{\cos\phi}{r}u_\phi + \frac{w}{r} \qquad (a)$$

$$\varepsilon_\phi = \frac{du_\phi}{ds} + \frac{w}{R_\phi} \qquad (b)$$

$$\gamma_\theta = \frac{1}{r}\frac{du_\phi}{d\theta} - \frac{\cos\phi}{r}u_\theta \qquad (c)$$

$$\gamma_\phi = \frac{du_\theta}{ds} \qquad (d)$$

$$\beta_\phi = -\frac{dw}{ds} + \frac{u_\phi}{R_\phi} \qquad (e)$$

$$k_\phi = \frac{d\beta_\phi}{ds} \qquad (f)$$

$$k_\theta = \frac{1}{r}\frac{d\beta_\theta}{d\theta} + \frac{\cos\phi}{r}\beta_\phi \qquad (g)$$

$$\delta_\theta = \frac{1}{r}\frac{d\beta_\theta}{d\theta} - \frac{\cos\phi}{r}\beta_\theta \qquad (h)$$

$$\delta_\phi = \frac{d\beta_\theta}{ds} \qquad (i)$$

$$\beta_\theta = -\frac{1}{r}\frac{dw}{d\theta} + \frac{u_\theta}{R_\theta} \qquad (j)$$

(2.12)

where u_ϕ, u_θ and w are the displacement components parallel to the unit vectors $\vec{t}_\phi$, $\vec{t}_\theta$ and $\vec{t}_3$ respectively (Fig. 6).

Axisymmetric deformation of cylindrical shells (Fig. 9) admit simpler solutions. By making the substitutions $s = z$, $\frac{1}{R_\phi} = 0$, $r = a$, and $\phi = 90^o$, and setting all torsional variables equal to zero, the governing equations for a cylindrical shell are:

1. Equilibrium

$$\frac{dN_z}{dz} + p_z = 0 \tag{2.13}$$

$$\frac{dQ_z}{dz} - \frac{N_\theta}{a} + p_3 = 0 \tag{2.14}$$

$$\frac{dM_z}{dz} - Q_z = 0 \tag{2.15}$$

2. Stress-Strain

$$N_\theta = K(\varepsilon_\theta + \nu\varepsilon_z) = Eh\,\frac{w}{a} + \nu N_z \tag{2.16}$$

$$N_z = K(\varepsilon_z + \nu\varepsilon_0) \tag{2.17}$$

$$M_\theta = D(k_\theta + \nu k_z) \tag{2.18}$$

$$M_z = D\,(k_z + \nu k_\theta) \tag{2.19}$$

3. Strain-Displacement

$$\varepsilon_\theta = \frac{w}{a} \tag{2.20}$$

$$k_\theta = 0 \tag{2.21}$$

$$\varepsilon_z = \frac{du_z}{dz} = -\frac{\nu w}{a} + \frac{N_z}{K} \tag{2.22}$$

$$k_z = -\frac{dw}{dz} \tag{2.23}$$

2.4 Features of Shell Vibration

The common mathematical models for thin shells admit a strain energy expression that consists of two parts: extensional (or stretching, or membrane) and flexural (or bending). In general, the extensional energy is produced by the extensional and shear strains in the middle surface, and it is proportional to the shell thickness. Flexural energy is produced by the changes in curvature and torsion of the middle surface, and it is proportional to the cube of the thickness (Ref. 38). Because of the curvature in a shell, the two systems of differential equations governing the extensional and flexural deformations are coupled, and pure extensional or flexural modes cannot exist.

Lord Rayleigh (Ref. 46) suggested that during vibration the resulting displacement field of a shell will, in general, include terms for both stretching and bending, and any expression for the energy will be of the form

$$Ah\ (\text{extensions})^2 + Bh^3\ (\text{bending})^2$$

where A and B are constants, and h is the shell thickness. The question of whether the flexural or extensional energy terms are the dominant ones in the vibrations of thin shells was finally resolved by Ross (Ref. 59). He found that if the boundary conditions involve any one of the displacements that are tangential to the middle surface, then the lowest frequency is independent of the shell thickness (for a cylindrical shell, the lowest frequency would be that associated with a circumferential wave number n = 1, and an axial wave number

m = 1). Thus, the overall problem of the identification of the parameters that govern the frequency can be directly related to the boundary conditions. If the tangential displacements of the mid-surface are restricted at an edge, the flexural energy will become negligible in comparison to the extensional energy for sufficiently small values of thickness. For shells with free edges, the extensional energy is negligible.

In the present investigation, the vibration of cylindrical storage tanks such as those depicted in Figs. 9, 10 and 11 are primarily extensional in nature. Therefore, the fundamental natural frequencies (m = 1, n = 1) of these shells are independent of their thickness. This critical fact was the underlying principle in the development of the simplified expressions for the determination of the natural frequencies of cylindrical tanks which are presented in Section 2.6 of this investigation.

2.5 Solution Scheme for Shell Free Vibration Problems

Although the general shell equations can be regarded as known since 1898, and the specific procedure for obtaining the complete solution of the free vibration problem of a finite cylindrical shell was contained in Love's work (Ref. 47) in 1927, numerical solutions of the complete free vibration problem began to appear only in the mid to late 1930's (Ref. 38). The complete boundary value problem was solved in detail by Arnold and Warburton (Ref. 5) and the effect of edge conditions on the natural

frequency of free vibration of a finite cylindrical shell was examined by Forsberg (Ref. 22). However, the free vibration problems treated in the aforementioned case studies were intended to reveal general behavior of a vibrating shell and the methods of analysis employed do not lend themselves favorably to practical applications. For certain classes of shell geometries, however, specialized methods (other than the finite element method) are available. One such method developed by Kalnins (Ref. 33) is employed in this investigation.

The Kalnins method used a computer-oriented procedure that ca n be applied to the free vibration problem of an arbitrary shell of revolution. The method is applicable to general boundary value problems governed by any number of ordinary first order differential equations. In the absence of any external loads, the fundamental equations can be written in matrix form:

$$\frac{d\{y(x)\}}{dx} = [A(x)]\ \{y(x)\} \tag{2.24}$$

where x is an independent variable, $\{y(x)\}$ is a column matrix whose elements represent m fundamental variables, and $[A(x)]$ is an (m, m) coefficient matrix whose elements are piecewise in an interval of x denoted by (a, b), where $a \leq x \leq b$. The system of Eqs. (2.24) together with m/2 homogeneous boundary conditions at each end point of the interval (x = a and x = b), form an eigenvalue problem.

The variables of the classical theory of shells used in this analysis are assumed to be separable in the form

$$\begin{Bmatrix} w \\ u_{\phi} \\ B_{\phi} \\ Q_{\phi} \\ N_{\phi} \\ N_{\theta} \\ M_{\phi} \\ M_{\theta} \end{Bmatrix} = \begin{Bmatrix} w_n \\ u_{\phi n} \\ B_{\phi n} \\ Q_{\phi n} \\ N_{\phi n} \\ N_{\theta n} \\ M_{\phi n} \\ M_{\theta n} \end{Bmatrix} \begin{Bmatrix} \cos(n\theta) \\ \sin(n\theta) \end{Bmatrix} \qquad (2.25)$$

$$\begin{Bmatrix} u_{\theta} \\ B_{\theta} \\ N_{\phi\theta} \\ M_{\phi\theta} \\ Q_{\theta} \end{Bmatrix} = \begin{Bmatrix} u_{\theta n} \\ B_{\theta n} \\ N_{\phi\theta n} \\ M_{\phi\theta n} \\ Q_{\theta n} \end{Bmatrix} \begin{Bmatrix} \sin(n\theta) \\ \cos(n\theta) \end{Bmatrix} \qquad (2.26)$$

where n = any integer. The independent variable x can be regarded as either the angle ϕ between the normal and the axis of symmetry of the shell, or the distance s, as shown in Fig. 12.

The (8,1) matrix of fundamental variables, $\{y(x)\}$ is defined as

$$\{y(x)\} = \begin{Bmatrix} w_n(x) \\ u_{\phi n}(x) \\ u_{\theta n}(x) \\ B_{\phi n}(x) \\ Q_n(x) \\ N_{\phi n}(x) \\ N_n(x) \\ M_{\phi n}(x) \end{Bmatrix} \tag{2.27}$$

The non-zero elements $A_{i,j}$ of the (8,8) coefficient matrix [A (x)] can be written in the form (when x is defined as s)

$$A_{1,2} = \frac{1}{R_\phi} \quad , \quad A_{1,4} = 1,$$

$$A_{2,1} = -P, \; A_{2,2} = -\nu\cos\phi, \; A_{2,3} = -\frac{n}{r},$$

$$A_{2,6} = \frac{1}{K}, \quad A_{3,1} = nGD\,\frac{\sin 2\phi}{Kr^3},$$

$$A_{3,2} = n\left(1 - GDJ\,\frac{\sin\phi}{Kr}\right)/r,$$

$$A_{3,3} = \left(1 - GDH\,\frac{\sin\phi}{Kr}\right)\frac{\cos\phi}{r}, \; A_{3,4} = 2n\,GD\,\frac{\sin\phi}{Kr^2},$$

$$A_{3,7} = 2\left(1 - GD\,\frac{\sin^2\phi}{Kr^2}\right)(1 - \nu)\,k,$$

$$A_{4,1} = -\frac{\nu n^2}{r^2}, \qquad A_{4,3} = -\frac{\nu n \sin\phi}{r^2},$$

$$A_{4,4} = -\frac{\nu \cos\phi}{r}, \qquad A_{4,8} = \frac{1}{D},$$

$$A_{5,1} = 2n^2 GD (1 - \nu) \frac{\cos^2\phi}{r^4} + n^4 D \left(\frac{1 - \nu^2}{r^4}\right)$$

$$+ K (1 - \nu^2) \frac{\sin^2\phi}{r^2} - {}^2 Eh \left(1 + \frac{h^2 n^2}{12 r^2}\right) L^2,$$

$$A_{5,2} = K (1 - \nu^2) \frac{\sin 2\phi}{2r^2} - n^2 GDJ (1 - \nu) \frac{\cos\phi}{r^3},$$

$$A_{5,3} = n (1 - \nu^2) \left(K + \frac{n^2 D}{r^2}\right) \frac{\sin\phi}{r^2}$$

$$- n GDH (1 - \nu) \cos^2\phi\, r^3 - n^{3} Eh^3 \frac{\sin\phi}{12 r^2 L^2},$$

$$A_{5,4} = n^2 D (1 - \nu) (1 + \nu + 2G) \frac{\cos\phi}{r^3}$$

$$A_{5,5} = -\frac{\cos\phi}{r}, \quad A_{5,6} = P, \quad A_{5,7} = -A_{3,1}, \quad A_{5,8}$$

$$A_{5,8} = -A_{4,1},$$

$$A_{6,1} = K (1 - \nu^2) \frac{\sin 2\phi}{2r^2} - n^2 GDJ (1 - \nu) \frac{\cos\phi}{2r^2},$$

$$A_{6,2} = K (1 - \nu^2) \frac{\cos^2\phi}{r^2} + n^2 GDJH (1 - \nu) \frac{\cos\phi}{2r^2},$$

$$A_{6,3} = nK (1 - \nu^2) \frac{\cos^2\phi}{r^2} + nGDJH (1 - \nu) \frac{\cos\phi}{2r^2},$$

$$A_{6,4} = - n GDJ \frac{(1 - \nu)}{r^2}, \qquad A_{6,5} = -\frac{1}{R\phi},$$

$$A_{6,6} = - (1 - \nu) \frac{\cos\phi}{r}, \qquad A_{6,7} = - n \left(1 - GDJ \frac{\sin\phi}{Kr}\right)$$

$$A_{7,1} = A_{5,3}, \qquad A_{7,2} = A_{6,3},$$

$$A_{7,3} = n^2 \left(\mathbb{K} + D \frac{\sin^2\phi}{r^2}\right) \frac{(1 - \nu^2)}{r^2}$$

$$+ GDH^2 (1 - \nu) \frac{\cos^2\phi}{2r^2} - \Omega^2 Eh \left(1 + h^2 \frac{\sin^2\phi}{12r^2}\right)/L^2,$$

$$A_{7,4} = - nD (1 - \nu) \left[GH - (1 + \nu) \frac{\sin\phi}{r}\right] \frac{\cos\phi}{r^2},$$

$$A_{7,6} = - A_{2,3}, \qquad A_{7,7} = - \left(2 - GDH \frac{\sin\phi}{kr}\right) \frac{\cos\phi}{r},$$

$$A_{7,8} = - A_{4,3},$$

$$A_{8,1} = A_{5,4}, \qquad A_{8,2} = A_{6,4}, \qquad A_{8,3} = A_{7,4},$$

$$A_{8,4} = D (1 - \nu)[(1 + \nu) \cos^2\phi + 2n^2 G] - \Omega^2 \frac{Eh^3}{12L^2},$$

$$A_{8,5} = 1, \qquad A_{8,7} = - A_{3,4}, \qquad A_{8,8} = - (1 - \nu) \frac{\cos\phi}{r}.$$

where

E = Young's Modulus

$G = 1/(1 + D \sin^2\phi/\mathbb{K}r^2)$

$H = 1/R_\phi - \frac{\sin\phi}{r}$

$J = \frac{1}{R_\phi} + \frac{\sin\phi}{r}$

L = some characteristic length of shell

$P = \frac{1}{R_\phi} + \frac{\nu \sin\phi}{r}$

$D = \frac{Eh^3}{12(1 - \nu^2)}$

$K = \frac{Eh}{(1 - \nu^2)}$ and

Ω = a non-dimensional frequency parameter, which is defined as the ratio of the product of the natural frequency and some length characteristic, L, of the shell to the speed of sound $(\frac{\omega L}{c})$

where

c = the speed of sound.

The solution of the boundary value problem governed by the system of Eqs. 2.24 is outlined as follows. At the ends of interval (a,b) the boundary conditions are

$$[T_a] \{y(a)\} + [T_b] \{y(b)\} = \{g\} \tag{2.28}$$

where $[T_a]$, $[T_b]$ are given (m,m) matrices and $\{g\}$ is a given (m,1) matrix. The solution of Eqs. 2.24 is

$$\{y(x)\} + [W(x)] \{c\} = \{d(x)\} \tag{2.29}$$

where $[W(x)]$ is an (m,m) matrix whose columns represent m linearly independent solutions of the homogeneous governing equations, $\{d(x)\}$ is a particular solution of Eqs. 2.24; and $\{c\}$ denotes a column matrix of m arbitrary constants.

Since the only requirment of the columns of $[W(x)]$ is that they be linerarly independent solutions of the system of Eqs. 2.24, in place of $[W(x)]$ in the interval (a,b) a matrix of linear combinations of the solutions of Eqs. 2.24 may be employed, which at x = a

reduces to a unit matrix [I]. This is done by evaluating Eqs. (2.29) at x = a

$$\{y(a)\} = [W(a)\ \{c\} + d(a)\} \tag{2.30}$$

solving for {c}

$$\{c\} = [W(a)]^{-1}\ \{y(a)\} - [W(a)]^{-1}\ \{d(a)\} \tag{2.31}$$

and replacing c in Eqs. (2.29) by Eqs. (2.31) to give

$$\{y(x)\} = [Y(x)]\ \{y(a)\} + \{z(x)\} \tag{2.32}$$

where

$$[Y(x)] = [W(x)][W(a)]^{-1} \tag{2.33}$$

$$\{z(x)\} = \{d(x)\} - [W(x)][W(a)]^{-1}\ \{d(a)\} \tag{2.34}.$$

The columns of [Y(x)] and {z(x)} are solutions of the m initial value problems given by

$$\frac{d\ [Y(a)]}{dx} = [A(x)][Y(x)],\ [\ (a)] = [I] \tag{2.35}$$

$$\frac{d\ \{z(x)\}}{dx} = [A(x)]\{z(x)\},\ \{z(a)\} = 0 \tag{2.36}.$$

Evaluating Eqs. (2.32) at x = b and substituting into Eqs. (2.28), then solving for {y(a)}, the result is

$$\{y(a)\} = ([T_a] + [T_b]\ [y(b)]^{-1}\ (\{g\} - [T_b]\ \{z(b)\}) \tag{2.37}.$$

At this point all unknowns at the beginning of the interval have been determined. The solutions can be regarded as determined throughout the interval from one more solution of initial value problem.

For free vibration problems, Eqs. (2.32) constitutes a linear homogeneous system of $\frac{m}{2}$ equations with $\frac{m}{2}$ unknown elements of $\{y(a)\}$. Requiring the vanishing of the determinant of the coefficient matrix of this system of equations gives the frequency equation and natural frequencies of the systems and a solution for $\{y(a)\}$. Once all elements of $\{y(a)\}$ are known, the mode shapes corresponding to a particular frequency can be obtained from Eqs. (2.32). Details of this procedure can be found in Ref. 33.

2.6 Free Vibration of Open-Top Cylindrical Tanks

In this section of the investigation, simplified expressions for the determination of natural frequencies and mode shapes for open-top cylindrical storage tanks, similar to the one shown in Fig. 8, are developed. The frequencies and mode shapes of concern are those associated with a circumferential wave number n = 1, and an axial wave number m = 1. These simplified expressions are applicable to a class of tanks whose height (H_o) to diameter (D_o) ratio (H_o/D_o) falls within the range 0.1 - 1.5 inclusive. This range encompasses the categories of both shallow ($H_o/D_o \leq 0.5$) and tall ($H_o/D_o \geq 0.75$) tanks, and includes all tanks within the practically important range of $0.1 \leq H_o/D_o \leq 0.7$.

To develop a data base for the fundamental frequencies and mode shapes for the aforementioned class of cylindrical tanks, a detailed parametric study was conducted. The prototype tanks (Fig. 9) had the following dimensions and material properties:

D_o (diameter) = 30.48 m (100.0 ft)

h (shell wall thickness) = 6.35 mm (0.25 in)

E_s (Young's Modulus) = 206900 MN/m^2 (30,000 ksi)

ρ_s (mass density of shell) = 20.3 (Kg/m^3) (.000733 lb

(.000733 lb-sec.^{2}/in^4)

ν (Poisson's ratio) = 0.3

The tank height, H_o, was varied from 3.048 m (10 ft) to 45.72 m (150 ft) at 3.048 m increments to accommodate the aspect ratio (H_o/D_o) range of 0.1 to 1.5. Since the shell natural frequency corresponding to an axial wave number m = 1 and a circumferential wave number n = 1 is not affected by the wall thickness, h (refer to Section 2.4) a constant value for the wall thickness for all prototype tanks is justified.

In this phase of the study, the tank model did not include any roof structure. It was assumed that the tank was fixed to a non-yielding support, with uniform boundary conditions at its base defined by the shell displacement constraints

$$u = 0, \quad v = 0, \quad w = 0, \quad \beta_\phi = 0$$

The analytical technique employed for the free vibration analysis was that described in Section 2.5, which was implemented through computer program KSHEL (Ref. 34).

The results of the free vibration analysis for the natural frequencies are represented in Fig. 13. The values of the natural frequency, ω, are non-dimensionalized with respect to the maximum

frequency in the group (52.52 cycles/sec), that correspond to a (H_o/D_o) ratio = 0.1, and are plotted against the tank height to diameter ratio (H_o/D_o).

A regression analysis was conducted on the frequency data generated in the parametric study for the purpose of attaining a simple expression to delineate the relationship between the non-dimensionalized frequencies (Fig. 13) and tank aspect ratio (H_o/D_o). The resulting expression, a cubic polynominal, is given by

$$\bar{f}\left(\frac{H_o}{D_o}\right) = C_1 + C_2\,(H_o/D_o) + C_3\,(H_o/D_o)^2 + C_4\,(H_o/D_o)^3 \tag{2.38}$$

where $\bar{f}\,(H_o/D_o)$ is the non-dimensionalized frequency function for any particular (H_o/D_o) ratio, and C_1, C_2, C_3 and C_4 are the cubic polynomial coefficients. To guarantee the greatest possible accuracy of the polynomial approximation, two sets of coefficients were extracted from the regression analysis; one set applicable to the range $0.1 \leq H_o/D_o \leq .65$, and the other set for the range $0.65 < \frac{H_o}{D_o} \leq 1.5$. This arrangement also facilitates the transition from shallow to tall tanks without appreciable error. The coefficients to be used in conjunction with Eq. 2.38 are presented in Table 1. In Fig. 14 the comparison of the analytical results for ω/ω_{max} versus H_o/D_o with those obtained from Eq. 2.38 is illustrated; excellent correlation is noted.

As was explained in Section 2.4, since the natural frequency of a cylindrical shell associated with a circumferential wave number n = 1 and an axial wave number m = 1, is primarily extensional in

nature, the natural frequencies of the class of cylindrical tanks under consideration are independent of their thickness. Therefore, the natural frequency of any cylindrical tank having an (H_o/D_o) ratio within the range 0.1 to 1.5 inclusive, may be determined from Eq. 2.38, used in conjunction with certain characteristics of the height and diameter of the tank only. The simplified expression relating the natural frequency (n = 1, m = 1) to the (H_o/D_o) ratio of the cylindrical tank is given by

$$f = \frac{[\bar{f}(H_o/D_o)]}{D_o} C_f \qquad (2.39)$$

where f is the natural frequency of the tank in cycles per second, $\bar{f}(H_o/D_o)$ is the non-dimensionalized frequency function determined by Eq. 2.38, C_f = 1600.2 m/sec (5252.0 ft/sec) is the frequency constant, and D_o is the diameter of the tank in meters (feet).

To test the accuracy of Eq. 2.39, numerical comparisons were made with the findings of several other investigators. The bench mark case is a cylindrical tank first analyzed by Edwards (Ref. 20). The empty cylindrical tank had the following dimensions and material properties:

H_o = 25.92 m (40 ft) $\quad E_s$ = 206,900 MN/m^2 (30,000 ksi)

D_o = 36.58 m (120 ft)

ρ_s = 20.3 kg/m^3 (.000733 lb-sec.^{2}/in^4)

h = 25.4 mm (1 in) $\quad \nu$ = 0.3

The natural frequency (corresponding to the n = 1, m = 1 mode) determined from Eq. 2.39 was 34.08 cycles/sec. This result is compared with those obtained by Shaaban and Nash (Ref. 60), Haroun (Ref. 26), and Edwards (Ref. 30), and values are presented in Table 2. The validity and accuracy of Eq. 2.39 are verified by this comparison.

Although the data base for the formulation of Eqs. 2.33 and 2.34 was compiled from the analytical results for a steel structure having material properties E_s = 206,900 MN/m^2 (30,000 ksi) and ρ_s = 20.3 kg/m^3 (.000733 lb-sec.^{2}/in^4), Eq. 2.39 may be modified to accommodate tanks fabricated from any linearly elastic material. The modified expression is given by

$$f = \frac{[\bar{f}(H_o/D_o)]\ C_f}{D_o} \sqrt{\frac{E\rho_s}{E_s\rho}} \qquad (2.40)$$

where E and ρ are Young's Modulus and the mass density, respectively, of the material used for fabrication of the tank.

The mode shape (m = 1, n = 1) for a cylindrical shell can be completely defined by the three displacement components v, u and w the circumferential, axial, and radial displacements respectively. For all three components, the variation along the length or height of the shell is similar; zero at the fixed base of the shell, increasing to their maximum value at the top. The magnitudes of u, v and w are normalized with respect to the largest value of displacement in the field so that the maximum value is 1.0. The maximum normalized values of u, v and w which occur at the top of the

shell are summarized in Table 3 for fifteen values of (H_o/D_o) in the range 0.1 - 1.5. From Table 3 it can be observed that the axial displacement component u is relatively insignificant for the entire range 0.1 - 1.5. It can also be observed that for values of (H_o/D_o) < 0.4, the circumferential displacement v is also relatively insignificant. However for larger values of H_o/D_o the circumferential displacement becomes more significant and is approximately equivalent in magnitude to the radial displacement at $H_o/D_o = 1.5$. This suggests that for tanks with an $(H_o/D_o) < 0.4$, the $m = 1$, $n = 1$ mode shape is accompanied by very little distortion of the cross-section, that is, the shell cross-section remains circular during vibration. However, for larger values of H_o/D_o, significant circumferential displacements occur, thus causing the cross-section to deviate from its circular shape and assume more of an eliptical form.

Therefore, allowing for varying degrees of distortion in the cross-section, due to circumferential displacements, the mode shape of the tank may be essentially described by the radial displacement component $\bar{w}$. The variation of $\bar{w}$ along the height of the tank is illustrated in Fig. 15 for several cases of (H_o/D_o). The maximum displacement occurs at the top of the tank and all other values are non-dimensionalized with respect to that quantity, so that the maximum value is always equal to 1.0. For each of the free vibration analyses conducted in the parametric study, a regression analysis was performed on the radial displacement component data, in a manner similar to that done for the natural frequencies. The resulting

expression, also a cubic polynomial, describes the relationship between the radial displacement, w, and the tank height parameter (z/H_o). This expression is given by

$$\bar{\bar{w}}\ (z/H_o) = C_1 + C_2\ (z/H_o) + C_3\ (z/H_o)^2 + C_4\ (z/H_o)^3 \tag{2.41}$$

where $\bar{\bar{w}}\ (z/H_o)$ is the radial displacement function, (z/H_o) is the height parameter such that $0 < (z/H_o) \leq 1.0$, and C_1, C_2, C_3 and C_4 are cubic polynomial coefficients. These coefficients, which are a function of the (H_o/D_o) ratio, must in turn be determined from the expression

$$C_i = A_{1i} + A_{2i}\ (H_o/D_o) + A_{3i}\ (H_o/D_o)^2 + A_{4i}\ (H_o/D_o)^3,$$

$$i = 1, 2, 3, 4 \tag{2.42}$$

where A_{1i}, A_{2i}, A_{3i} and A_{4i} are also cubic polynomial coefficients, which themselves were determined from a regression analysis of the C_i coefficients, and are listed in Table 4. Finally, to minimize the error in determining the coefficients C_i of Eq. 2.41, and to ensure that the maximum radial displacement component is equal to 1.0, the corrected expression relating radial displacement versus tank height becomes

$$\bar{w}\ (z/H_o) = \bar{\bar{w}}\ (z/H_o)\ C_w \tag{2.43}$$

where $\bar{\bar{w}}\,(z/H_o)$ is the radial displacement parameter determined from Eq. 2.41 and

$$C_w = \frac{1.0}{\sum_{i=1}^{4} C_i} .$$

To test the accuracy of the simplified expressions of Eqs. 2.41, 2.42 and 2.43 numerical comparisons with the results of other investigators were made. For the bench mark case referred to previously in this section, the fundamental mode of vibration of the radial displacement w was computed and is presented in Table 5 along with the results of Ref. 26. Once again, excellent correlations are noted.

2.7 Effect of Roof Structure on the Free Vibration of Empty Tanks

In practice, very rarely are cylindrical storage tanks constructed without some sort of roof structure. The American Petroleum Institute (Refs. 3 and 4) defines two basic categories of roof systems: (1) self-supporting roof and (2) supported roof; an example of the former which is supported only at its periphery is illustrated in Fig. 10. An example of the latter, supported by rafters and trusses, is illustrated in Fig. 16. In either case, the mass of the roof system can represent an appreciable portion of the mass of the total structure, thus significantly influencing the overall vibrational characteristics of the tank.

The parametric study for open-top cylindrical shells discussed in Section 2.6 was extended to include tanks with roof structures. In this phase of the investigation a circular plate attached at its periphery to the top of the shell was incorporated into the cylindrical tank model (Fig. 17). The roof mass was then related to the mass of the tank cylinder via the tank wall thickness in the following manner.

Realizing that

$$m_r \alpha \frac{D_o^2}{4} h_r \tag{2.44}$$

and

$$m_c \alpha \pi D_o H_o h \tag{2.45}$$

it follows, that

$$\frac{m_r}{m_c} = \frac{D_o h_r}{4 H_o h} \tag{2.46}$$

and

$$h_r = K_r h \tag{2.47}$$

where

$$K_r = \frac{4 m_r}{m_c} \frac{H_o}{D_o} \tag{2.48}$$

Therefore, through the use of Eq. 2.47 any roof structure may be represented by an equivalent circular plate of thickness h_r (Eq. 2.47); where m_r is the mass of the roof and its supporting rafters and trusses, and m_c is the mass of the tank cylinder. It should be noted here that since the roofs of typical cylindrical storage tanks have a very small pitch, the approximation of a circular plate at the top of the cylinder is not unreasonable for most instances.

The free vibration analysis was conducted over the same (H_o/D_o) range specified for the open-top tanks, 0.1 to 1.5 inclusive, and for values of roof mass coefficient, K_r = 1.0, 2.0 and 3.0. The results of the free vibration analysis for the natural frequencies for the cases corresponding to K_r = 1.0, 2.0 and 3.0 and K_r = 0 (open-top case) are plotted in Fig. 18. The values of the frequencies are normalized with respect to that of an open-top tank with (H_o/D_o) ratio = 0.1 (52.52 cycles/sec). From these results it can be concluded that the net effect of the roof mass is to lower the natural frequency of the structure. The reduction in frequency is more critical in the lower H_o/D_o range, or shallow tanks, where the roof mass represents a greater portion of the total mass of the structure, than it is in the higher H_o/D_o range (tall tanks). The increase in stiffness provided the structure due to the addition of roof structure is negligible, since the vibrational mode of the shell is primarily extensional in nature.

A regression analysis was conducted on the frequency data obtained in the free vibration analysis of tanks with roof structure. The relationship of non-dimensionalized frequency versus tank aspect ratio (H_o/D_o), for values of roof mass coefficient K_r = 1.0, 2.0 and 3.0 was modeled with a cubic polynomial in a manner similar to that done for the case of the open-top tanks. Thus the natural frequencies of cylindrical tanks with roof structures may also be determined from Eqs. 2.38 and 2.39. The cubic polynomial coefficients to be used in Eq. 2.38 for the cases K_r = 1.0, 2.0 and 3.0 appear in Table 6.

To determine the frequency of tanks whose roof mass parameter K_r is not exactly equal to 1.0, 2.0 or 3.0, linear interpolation is recommended.

A regression analysis was also performed on the radial displacement component data obtained from the free vibration analysis of cylindrical tanks with roof structures. Once again, a cubic polynomial was selected to represent the relationship between the radial displacement, w, and the tank height parameter (z/H_o). The expressions given by Eqs. 2.41, 2.42 and 2.43 to be used for the analysis of open-top tanks are also applicable to the analysis of tanks with roof structures. The coefficients A_{1i}, A_{2i}, A_{3i} and A_{4i} to be used in Eq. 2.42 to determine the C_i coefficients for use in Eq. 2.41 are listed in Table 7, (a), (b) and (c) for roof mass parameters K_r = 1.0, 2.0 or 3.0, respectively. To determine the mode shape of cylindrical tanks whose roof mass parameter K_r is not exactly equal to 1.0, 2.0 or 3.0, linear interpolation is recommended once again.

To summarize, the roof structure of cylindrical storage tanks has been modeled by an equivalent circular plate attached at its periphery to the top of the cylinder. The roof structure contributes very little to the overall stiffness of the structure, yet can increase the total mass of the system appreciably, such that the net effect is a lowering of the natural frequency of the tank. The same expressions used for the determination of natural frequency and mode shape for the open-top tanks, are applicable to the free vibration analysis of tanks with roof structures as well, merely by implementing the appropriate coefficients into these expressions.

2.8 Effect of Support Conditions on the Vibrational Characteristics of Cylindrical Tanks

In the analyses conducted up to this point, it has been assumed that the shell base is uniformly supported along its perimeter. In practice however this is rarely, if ever, the situation. Usually the tank is connected at its base to a foundation by anchor bolts located at discrete locations along the periphery. A typical anchorage detail for the cylindrical storage tank of Fig. 10 is illustrated in Fig. 11 (a) and (b).

The object of this phase of the investigation is to determine whether the vibrational characteristics (i.e. frequency and mode shape) of cylindrical storage tanks are significantly influenced by the manner in which the shells are attached to their foundation. For this study, the finite element method of analysis was employed. Because of the flexibility of the finite element method in defining different structural configurations with minimal changes in the basic analytical procedure, it offers great advantages. However, the major shortcoming of the method is the possible need to employ a large number of degrees of freedom to accurately describe the vibrational characteristics of the structural system. Therefore, in order to define the optimal finite element discretization, a pilot investigation was undertaken, the findings of which are summarized in Refs. 41 and 42.

The shell was discretized as a combination of rectangular flat shell elements with flexural and membrane stiffness capability

using the general purpose finite element program SAPIV (Ref. 7). The membrane action is defined by a combination of four constant strain triangles. Even with a coarse finite element discretization, this type of representation would yield fully acceptable results provided that there will not be a very steep gradient of membrane stresses within the shell element (Ref. 6). The flexural behavior of the element is defined by combining four linear-curvature-compatible (LCCT9) triangular plate bending elements (Refs. 15, 21). Past experience with this plate bending element in simulating the earthquake response of circular chimneys has been fully satisfactory (Ref. 40).

The finite element investigation included a family of tanks with aspect ratios, (H_o/D_o), of 0.1, 0.3, 0.5, 0.75, 1.0, 1.3, 1.5 and 2.0. The results of the analysis for the case of $H_o/D_o = 1.0$ typify the general trends observed in the investigation. Therefore, only the findings pertaining to this single case are examined here.

The structure under consideration ($H_o/D_o = 1.0$) had the following dimensions and material properties:

H_o = 9.14 m (30 ft) E_s = 206,900 MN/m^2 (30,000 ksi)

D_o = 9.14 m (30 ft) ρ_s = 20.3 Kg/m^3 (0.000733 lb-sec^2/in^4)

h = 4.76 mm (0.1875 in) ν= 0.3

The circular cross-section of the shell was modeled as a polygon due to the use of the flat shell elements. A massless bottom plate, having the same thickness as the shell wall, h, connected at its

periphery to the base of the cylinder was incorporated into the model to simulate any circumferential and radial constraint which may exist in practical situations. The complete finite element model consisted of 164 flat plate elements and 174 nodal points (approximately 1000 degrees of freedom). An isometric view of the discretization is shown in Fig. 19.

A horizontal cross-section of the finite element discretization is illustrated in Fig. 20. From this figure it can be seen that the nodal points are symmetrically located around the perimeter of the tank at increments of twenty degrees. The boundary conditions at the base of the tank are determined from the constraint of the displacement field assigned to these nodes along the perimeter of the tank bottom. Four cases of anchorage conditions were investigated

1. Supports at 20^{o} (assumed full fixity)
2. Supports at 40^{o}
3. Supports at 60^{o}
4. Supports at 120^{o}

The specified boundary conditions for each case are as follows:

Case 1: u, v, w, β_{ϕ} = 0 at each nodal point

Case 2: u, v, w, β_{ϕ} = 0 at every other nodal point
u = 0 elsewhere

Case 3: u, v, w, β_{ϕ} = 0 at every third nodal point,
u = 0 elsewhere

Case 4: u, v, w, β_{ϕ} = 0 at every sixth nodal point,
u = 0 elsewhere.

An illustration of these four support conditions is also represented in Fig. 20.

The natural frequency for the tank (H_o/D_o = 1.0) under the condition of full base fixity (Case 1) was determined to be 51.58 cps, with the mode shape exhibiting the familar characteristics of the m = 1, n = 1 configuration. Frequencies for this tank corresponding to higher circumferential modes, n = 2 through n = 10, are listed in Table 8. These frequencies were non-dimensionalized with respect to that value of frequency corresponding to n = 1 (51.58 cps), and the relation $\omega/\omega_{n=1}$ versus n is presented in Fig. 21; where ω is the natural frequency corresponding to any circumferential wave number n, and $\omega_{n=1}$ is the natural frequency corresponding to circumferential wave number n = 1. From this relationship it is observed that the natural frequency of the tank decreases as the number of circumferential waves increase, until the minimum value is attained at n = 7; from that point on, a very gradual increase in frequency is cited with increasing number of circumferential waves. This trend is typical of all cylindrical shells.

The circumferential mode shapes corresponding to the axial mode m = 1, for boundary condition cases 2, 3 and 4, are presented in Figs. 22, 23 and 24 respectively. The circumferential mode shapes appearing in these figures do not resemble the n = 1 wave, but exhibit a form influenced by higher circumferential wave numbers, n = 4 and n = 5 specifically. The natural frequencies associated with these modes are listed in Table 9. These results tend to

indicate that the non-uniform boundary conditions of cases 2, 3 and 4 promote participation of higher circumferential wave forms resulting in a lowering of the natural frequency of the tank.

It must be understood that the circumferential modes resulting in the non-uniform boundary condition cases are not the pure n = 4 or n = 5 modes, but rather are a consequence of a blending or coupling of the n = 1 mode with the n = 4 or n = 5 modes. The extent of this "mode coupling" can be assessed quantitatively by an examination of the pertinent mode shapes (Figs. 22, 23 and 24) and frequencies (Table 9). The obvious general conclusion is that for a decreasing number of support points, the participation of the higher circumferential modes is more prominent during vibration. Stated in another manner, as the boundary conditions at the base of the tank deviate from the ideal uniformly fixed condition, the "mode coupling" phenomenon becomes increasingly stronger.

The sensitivity of the shell vibrations to increased thickness of the bottom plate was also examined, however, no significant contribution could be ascertained.

In summary, the dynamic characteristics of the shell are affected by the manner in which it is attached to its foundation. The basic consequence of non-uniformity of boundary conditions at the base of the tank upon free vibration is the coupling of the n = 1 circumferential mode with higher circumferential modes, such as n = 4 and n = 5. The greater the deviation from the fully fixed base condition (or for fewer connection points), the greater is the

"mode coupling" or influence of higher circumferential modes upon the free vibration of the shell. This mixed-mode response is not disadvantageous provided it is realized that the associated frequency can be materially less than that corresponding to the $n = 1$ mode.

To be sure, these findings, based on 64 finite element case studies, are by no means conclusive. Yet to be determined is the relationship between mode coupling and natural frequency with the number of discrete support locations for any particular shell. Further insight into this complicated phenomenon warrants additional research.

3. VIBRATIONAL CHARACTERISTICS OF LIQUID FILLED CYLINDRICAL TANKS

3.1 Introduction

The results of the investigation of the horizontal free vibration of liquid-filled cylindrical storage tanks are presented in this chapter. The system considered is shown in Fig. 25. It is a circular cylindrical tank of diameter D_o (radius a) and height H_o fixed to a rigid base. The tank is presumed to be filled with a liquid of mass density, ρ_L, to a level h_L (Fig. 25). The upper surface of the liquid is considered to be free.

There are two major cases of vibration associated with the system under consideration, for which the circumferential variation of the response is described by $\cos(n\theta)$ (n is called the circumferential wave number and θ is the circumferential coordinate angle; refer to Section 2.1 for a detailed explanation). Case (1) corresponds to solutions with n = 1 (Fig. 1) and is often called lateral sloshing. Case (2) is often called breathing vibration, and it corresponds to all vibrations where n does not equal one (Fig. 1). This investigation is concerned with Case (1) only, that is lateral sloshing modes with n = 1.

The liquid and the shell structure are two separate systems that are coupled. Each system, acting alone, has an infinite number of modes of free vibration. If the coupled system is excited with

some forcing frequency Ω, then the response will also have the frequency Ω. The magnitude of the response will depend on the location of the forcing frequency, Ω, with respect to the natural frequencies of the coupled system (Ref. 34).

In this chapter the simulation of the coupling of the shell with the liquid is described and simplified expressions which accurately determine the fundamental natural frequencies of the liquid-shell system are developed.

3.2 Basic Concepts and Theory

The general behavior of fluid vibrating in a tank can be described based upon the experimental and analytical results presented in Refs. 1, 27, 28 and 37. The fluid contained in the tank is essentially divided into two zones (Fig. 25). The lower zone of fluid represents a mass which is constrained and tends to move as a rigid body with the motion of the vessel. The upper zone of fluid represents a mass which tends to move in a sloshing mode.

The exact mathematical procedure for describing fluid oscillations in a moving container is extremely complex. Therefore, the following simplifying assumptions are generally employed (Ref. 1):

1. Nonviscous fluid
2. Incompressible fluid
3. Small displacements, velocities and slopes of the liquid free surface

4. Irrotational flow field

5. Homogeneous fluid

The assumption of irrotational flow insures the existence of a fluid velocity potential, Φ, which must satisfy the Laplace equation (Ref. 1)

$$\nabla^2 \Phi = 0 \tag{3.1}$$

Referring to the cylindrical coordinate system (r, z, θ) shown in Fig. 25, the Laplace equation of motion for the fluid can be written as

$$\nabla^2 \Phi = \frac{\partial^2 \Phi}{\partial r^2} + \frac{1}{r}\frac{\partial \Phi}{\partial r} + \frac{1}{r^2}\frac{\partial^2 \Phi}{\partial \theta^2} + \frac{\partial^2 \Phi}{\partial z^2} = 0 \tag{3.2}$$

The mathematical boundary conditions for the solution for Φ are as follows (Ref. 1):

1. At the tank walls (@ r = a, refer to Fig. 25)

$$\frac{\partial \Phi}{\partial r} = \frac{\partial w}{\partial t} \tag{3.3}$$

where $\frac{\partial w}{\partial t}$ is the normal component of the tank wall velocity.

2. At the tank bottom (@ z = 0), the axial component of the liquid velocity must equal zero, therefore

$$\frac{\partial \Phi}{\partial z} = 0 \tag{3.4}$$

3. At the liquid free surface (@ z = h_L), imposing the condition that the fluid particles must stay on the surface, it follows that

$$\frac{\partial^2 \Phi}{\partial t^2} + g \frac{\partial \Phi}{\partial z} = 0 \tag{3.5}$$

where g is the acceleration of gravity.

The dynamic pressure can be determined by imposing Bernoulli's law and is given by

$$p_d = - \rho_L \frac{\partial \Phi}{\partial t} \tag{3.6}$$

where ρ_L is the mass density of the fluid. The total pressure p is the sum of the dynamic pressure p_d and the hydrostatic pressure p_s and is expressed by

$$p = p_d + p_s = - \rho_L \frac{\partial \Phi}{\partial t} + \rho_L g \, (h_L - z) \tag{3.7}.$$

Conceptually, it is advantageous to replace a fluid whose behavior is governed by Eqs. 3.2 through 3.5 with a system of lumped masses and springs. Such mechanical models have been formulated (Refs. 1, 28 and 63) by introducing the assumption that the tank can be considered as rigid. One of the objectives of this chapter will be to describe a procedure for determining natural frequencies of a flexible shell-fluid system from modified concepts of the mechanical analogs devised for rigid container systems.

3.3 Mechanical Analogs for Liquids Sloshing in Rigid Cylindrical Containers

According to the theoretical developments of Ref. 1, a complete mechanical analog for transverse sloshing must include an infinite number of oscillating masses, one for each of the normal sloshing modes. Such a system, referred to us a complex mechanical analog, is depicted in Fig. 26. It consists of one mass, m_o, rigidly attached to the container at elevation h_o and an infinite number of masses m_n ($n = 1, 2, 3, \ldots\infty$) attached to the container with springs at elevations h_n. The mass m_o represents the "constrained" fluid which tends to move as a rigid body with the motion of the vessel, and the masses m_n represent the fluid which tends to move in a sloshing mode. The springs which attach the sloshing masses to the walls of the tank have a stiffness K_n.

The equation of motion of the n^{th} sloshing mass for free vibration is

$$m_n \frac{d^2u_n}{dt^2} + K_n u_n = 0 \tag{3.8}$$

where u_n is the displacement of the n^{th} mass relative to the tank. Then the natural frequency of the n^{th} sloshing mass is determined from

$$\omega_n^2 = \frac{K_n}{m_n} \tag{3.9}$$

Physically, each mass in the mechanical system corresponds to the effective mass of the liquid that oscillates in each particular slosh mode, and, from its relative size, it is possible to assess how significant that mode is. A detailed analysis conducted in Chapter 6 of Ref. 1 indicates that the size of these spring-mass elements decreases rapidly with increasing mode number (i.e. as n increases). Thus it is generally acceptable to include in the mechanical model only the spring-mass corresponding to the fundamental mode, without appreciably affecting the dynamic response of the system.

A simple mechanical model for cylindrical tanks is shown in Fig. 27. An analytical derivation of the model parameters m_1, K_1, h_1 and h_o is included in Ref. 1, where

m_1 = equivalent mass of fundamental sloshing mode

K_1 = spring constant for fundamental sloshing mass

h_1 = height of sloshing mass m_1 measured from base of tank

h_o = height of stationary mass m_o measured from base of tank

The analytical expressions for the determination of these model parameters are presented in Table 10. The fixed or stationary mass m_o can be calculated by the equation

$$m_o = m_T - m_1 \tag{3.10}$$

where m_T is the total mass of fluid in the tank.

In the development of some simple mechanical models (Refs. 28 and 63), the stationary fluid mass, m_o, is given the value it would have if all the modal sloshing masses m_n ($n = 1, 2, \ldots \infty$) were included in the model. Thus, since only one of the modal masses is actually included, the total fluid mass of the real system, m_T, is slightly larger than the fluid mass of the simple mechanical model ($m_o + m_1$), that is

$$(m_T)_{\text{real system}} > m_o + m_1 \tag{3.11}$$

However, experimental evidence has shown that this mass total discrepancy is very minor (Ref. 1). Nevertheless, regardless of the model employed, the fundamental sloshing frequency, ω_1, is always determined from the expression given by

$$\omega_1 = \sqrt{\frac{K_1}{m_1}} \tag{3.12}$$

3.4 Free Vibration of Flexible Shell Fluid Systems

As was stated in Section 3.2 it is assumed that the fluid can be separated into two distinct layers. The mass in the lower layer, referred to as the stationary mass does not participate in sloshing, it simply moves with the walls of the shell. The mass in the upper layer, referred to as the sloshing mass, participates in sloshing. Therefore the coupled shell-fluid system is considered to consist of two separate systems:

1. The shell together with the stationary mass

2. The sloshing mass

Under this assumption, the coupled fluid-shell system can be represented by a two-degree-of-freedom system as shown in Fig. 28, where m_1 is the mass of the fluid that participates in sloshing, K_1 is the equivalent spring constant of the sloshing mass, M is the equivalent mass of the shell, which includes both the mass of the shell material and the stationary mass of fluid m_o, and K is the equivalent shell stiffness, calculated under the same conditions as M. The vibration of the coupled systems is then modeled by the simple mechanical analog shown in Fig. 27. The values of the model parameters m_1, m_o, K_1 and h_1 are determined from the appropriate expressions presented in Table 10. A procedure for determining values for K and M is detailed in subsection 3.4.1.

Once the values of m_1, K_1, M and K have been determined, the natural frequencies of the coupled systems of Fig. 28 can be computed from classical methods of mechanical vibrations (Refs. 24, 61 and 62). The natural frequencies of the two-mass, two-degree-of-freedom systems of Fig. 28 are then given by the expression

$$\omega^2 = A + \sqrt{A^2 - B} \tag{3.13}$$

where

$$A = \left(\frac{K}{M} + \frac{K_1}{M} + \frac{K_1}{m_1}\right)/2$$

and

$$B = \left(\frac{K_1}{m_1}\right)\left(\frac{K}{M}\right)$$

Indeed, the most difficult part of the analysis is the calculation of the equivalent mass M, and equivalent stiffness K for the shell together with the stationary fluid mass, m_o. Kalnins (Ref. 37) has developed a procedure to calculate M and K, which is employed in this investigation and is summarized in the following subsection.

3.4.1 Equivalent Mass and Stiffness of Shell-Fluid System

The equation of motion of the mass M (Fig. 28) which represents the shell and the stationary fluid mass m_o when vibrating in the lowest mode, is

$$M \frac{d^2x}{dt^2} + Kx - K_1 (x_1 - x) = 0 \tag{3.14}$$

where x is the displacement of mass M and x_1 is the displacement of mass m_1. The equivalent equation of motion for a shell is obtained from a paper by Kraus and Kalnins (Ref. 44). When the shell vibrates in the lowest mode (i.e. the mode corresponding to a circumferential wave number n = 1, and axial number m = 1), then from Ref. 44 its displacement vector can be written as

$$\vec{u} = \vec{u}_1 \, q(t) \tag{3.15}$$

where $\vec{u}_1$ is the displacement vector of the lowest mode of free vibration and q(t) denotes the generalized coordinate of the system. The equation of motion of the coupled shell-fluid system then becomes

$$M_1 \frac{d^2q}{dt^2} + M_1 \omega^2_M \, q = F_1 \tag{3.16}$$

where ω_M is the natural frequency of the lowest mode, M_1 and F_1 are the generalized mass and generalized force respectively where,

$$M_1 = \int_S \rho h \, \vec{u}_1 \cdot \vec{u}_1 \, dS \tag{3.17}$$

$$F_1 = \int_S \vec{p} \cdot \vec{u}_1 \, dS \tag{3.18}$$

and ρ is the mass density, h is the shell wall thickness, S is the reference surface of the shell, and $\vec{p}$ is the shell surface load vector (Ref. 44) that is causing the vibration of the shell. (A detailed discussion of generalized force and generalized mass is presented in Chapter 4).

It is assumed that the spring-mass system of the sloshing fluid m_1 is attached to the shell at one latitude circle which is located at a height h_1 above the base of the tank as shown in Fig. 27. Thus the spring must exert a horizontal force to the shell at that location of magnitude

$$F = K_1 \, (x_1 - x) \tag{3.19}$$

The shell surface load vector, $\vec{p}$, which appears in Eq. 3.18, must be determined in such a way that it represents the applied load F in Eq. 3.19. Since F is applied to one value of x, where x is the meridional arclength of the shell, then its distribution with x must be the Dirac Delta function (Ref. 61). It is also assumed that the force F is acting horizontally and parallel to the x_1 axis, as shown

in Fig. 29. Thus it follows that

$$\vec{p} = \left(\frac{F}{2\pi R_o}\right) \delta(x - x_o)\, \vec{i} \tag{3.20}$$

where R_o is the radius of the latitude circle at the location where the spring is attached, $\delta(x)$ is the Dirac Delta function, and $\vec{i}$ is a unit vector parallel to the x_1 axis (Fig. 29). Substitution of $\vec{p}$ from Eq. 3.20 into Eq. 2.18 for the generalized force yields

$$F_1 = \int_0^{2\pi} \int_a^b \left(\frac{F}{2\pi R_o}\right) \delta(x - x_o)\, \vec{i} \cdot \vec{u}_1\, dx\, r\, d\theta \tag{3.21}$$

where a and b are the end points of the meridian of the shell and x_o is the value of x where the spring is attached. Applying the property of the Dirac Delta function (Ref. 56) that

$$\int_a^b \delta(x - x_o)\, f(x)\, dx = f(x_o) \tag{3.22}$$

Then F_1 becomes

$$F_1 = F\, U_1 \tag{3.23}$$

where U_1 is the displacement of the shell parallel to the x_1 axis at the height, h_1, where the spring is attached (Fig. 27). U_1 is obtained from the free vibration mode shape of the shell and the stationary fluid mass m_o vibrating in the lowest mode (m = 1, n = 1).

For an axisymmetric shell U_1 is expressed by the usual shell displacements as

$$U_1 = (u_1 - u_\theta)/2 \tag{3.24}$$

where

$$u_1 = w \sin\phi + u_\phi \cos\phi \tag{3.25}$$

and w, u_ϕ, and u_θ are the normal, meridional, and circumferential displacements of the reference surface of the shell. The direction of u_1 is shown in Figs. 30a and 30b. The circumferential variation of these displacements is $\cos\theta$; all other θ variations vanish when integrated with respect to θ when going from Eq. 3.21 to Eq. 3.23. This is a direct consequence of the assumption that F, exerted by the attached spring, is uniformly distributed around the circumference. For the special case of a cylindrical shell, ϕ, the angle between the axis of the shell and the shell normal, is equal to 90°. Therefore Eq. 3.25 is reduced to

$$u_1 = w \tag{3.26}$$

and Eq. 3.24 becomes

$$U_1 = (w - u_\theta)/2 \tag{3.27}$$

Substituting F from Eq. 3.19 into Eq. 3.23 yields

$$F_1 = K_1 (x_1 - x) U_1 \tag{3.28}.$$

Then, substituting F_1 from Eq. 3.28 into Eq. 3.16 gives

$$M_1 \frac{d^2q}{dt^2} + M_1 \omega^2_M q = K_1 (x_1 - x) U_1 \tag{3.29}$$

The relationship between x and U_1 is given from Eq. 3.15 as

$$x = U_1 q(t) \tag{3.30}$$

which gives Eq. 3.29 the form

$$\left(\frac{M_1}{U_1^2}\right) \frac{d^2x}{dt^2} + \left(\frac{M_1}{U_1^2}\right) \omega_M^2 x = K_1 (x_1 - x) \qquad (3.31).$$

This equation reveals the equivalence of the vibration of the shell with that of the two-degree-of-freedom system shown in Fig. 28. Equation 3.31 becomes identical to Eq. 3.14 by relationships

$$M = \frac{M_1}{U_1^2} \qquad (3.32a)$$

and

$$K = \omega_M^2 \left(\frac{M_1}{U_1^2}\right) \qquad (3.32b)$$

These expressions give the equivalent parameters for representation of the shell and the stationary fluid mass, m_o, by a spring mass system. The calculation of the lowest mode of free vibration for the shell-fluid system is obtained by implementation of program KSHEL (Ref. 34). From the results of the KSHEL free vibration analysis, the parameters ω_M, M_1 and U_1 are obtained. M and K can then be determined from Eqs. 3.32a and 3.32b, respectively, and the natural frequencies of the coupled system (shell plus stationary fluid mass m_o with sloshing fluid mass m_1) can be calculated from Eq. 3.13.

3.4.2 Implementation of Free Vibration Procedure

This subsection contains the implementation of the free vibration procedure for flexible shell-fluid systems described in

the preceding subsections. The most critical aspect of the procedure is the joining of the shell with the stationary and sloshing fluid masses. For the case of a rigid shell it makes no difference whether the stationary fluid mass m_o and the sloshing fluid mass m_1 are attached to the shell at single points (as is illustrated by Fig. 27) or are distributed over portions of the shell wall; for an elastic shell, the manner of shell-fluid joining does make a difference (Ref. 37).

It is not reasonable to attach the stationary fluid mass m_o to a single point on the shell wall, since this practice will result in a gross misrepresentation of the mode shape. The precise distribution of the stationary mass along the shell wall can be determined from the fluid mechanics problem, a very time consuming and different process. A simple and reasonable solution, suggested by Kalnins (Ref. 37), is to distribute the stationary fluid mass m_o, as calculated from the formulas of Ref. 1, uniformly along the shell wall from the base of the shell to the point where the spring of the sloshing fluid mass m_1 is attached, at elevation h_1 (Fig. 27). The addition of the stationary fluid mass m_o can then be effected by increasing the mass density of the shell material by the amount of m_o/V, where V is the volume of the shell wall from the bottom of the shell to the point where the sloshing spring K_1 is attached (Fig. 27), that is

$$V = \pi D_o h h_1 \tag{3.33}$$

where D_o is the diameter of the shell, h is the shell wall thickness

and h_1 is the distance from the bottom of the shell to the point where the sloshing spring is attached. Such a procedure will result in better approximations of M_1, U_1 and ω_M of the lowest mode of free vibration (m = 1, n = 1) since the mode shape will not be distorted as it would by attaching the stationary fluid mass m_o at one point on the shell wall.

Attaching the sloshing mass m_1 at one point as located by the distance h_1 (Fig. 27) seems reasonable, because that location is needed only for the determination of U_1 in the shell-m_o free vibration problem (Ref. 37), and the sloshing fluid mass does not affect the mode shape of the shell-fluid system. Although the spring of the sloshing mass in reality should be distributed over a vertical portion of the shell wall, it is reasonable to assume that its effect on the shell will not change appreciably when that portion is narrowed, since natural frequencies are overall characteristics of systems, and are not significantly affected by local redistributions of mass or stiffness properties.

3.4.3 Practical Application

As a practical application of the procedure detailed in subsection 3.4.2, a shell-liquid system analyzed by Haroun (Ref. 26) is considered. The shell-liquid system has the following dimensions and physical properties:

H_o = 21.946 m (72.0 ft) E = 206900.0 MN/m^2 (30,000 ksi)

D_o = 14.63 m (48.0 ft) ρ_s = 20.3 kg/m^3 (0.000733 lb-sec^2/in^4)

h = 10.92 mm (0.43 in.) ν = 0.3

It is completely filled with water (ρ_L = 2.6 kg/m^3). The following model parameters are calculated from the relationship presented in Table 10:

m_T = 9599.4 kg (21163.1 lb-sec^2/in)

m_1 = 1454.4 kg (3206.4 lb-sec^2/in)

m_o = 8144.9 kg (17956.6 lb-sec^2/in)

K_1 = 1391330.0 N/m (7944.7 lb/in)

h_1 = 17.94 m (707.5 in)

The volume of the shell wall, from the base of the tank to the point where the sloshing fluid mass, M_1, is attached, is calculated by Eq. 3.33 as

$$\rho_{m_o} = \frac{m_o}{V} = 902.89 \text{ kg/m}^3 \ (0.032619 \text{ lb-sec}^2/\text{in}^4)$$

Thus the equivalent mass density of the shell wall, ρ_E from the base to elevation h_1 is

$$\rho_E = \rho_s + \rho_{m_o} = 923.18 \text{ kg/m}^3 \ (0.032619).$$

A free vibration analysis for the lowest mode (m = 1, n = 1) was conducted on the shell-m_o system, modified as prescribed in the foregoing, by employment of program KSHEL (Ref. 34). The values of natural frequency, ω_M, and generalized mass, M_1, for the shell-m_o system resulting from the analysis were given as

$$\omega_M = 23.1849 \text{ rad/sec}$$

$$M_1 = 2701.8 \text{ kg } (5956.5 \text{ lb-sec}^2/\text{in})$$

The dimensionless shell wall displacements, u_1 and u_θ, at the point where the sloshing fluid mass m_1 was attached were given as

$$u_1 = w = 0.896$$

$$u_\theta = - 0.873$$

from which the horizontal displacement, U_1, as calculated by Eq. 3.27 is

$$U_1 = 0.8846.$$

The equivalent mass, M, and the stiffness, K, of the shell-m_o system, that are needed to represent it as a spring mass system similar to that illustrated in Fig. 28, are given by Eqs. 3.22a and 3.22b, respectively, as

$$M = 3452.5 \text{ kg } (7611.4 \text{ lb-sec}^2/\text{in})$$

$$K = 7.17 \times 10^8 \text{ N/m } (4.09 \times 10^6 \text{ lb/in}).$$

Finally, the two natural frequencies of the coupled shell-m_o system and the sloshing mass, m_1, when regarded as a two-degree-of freedom system, are obtained from Eq. 3.31 as

$$\omega^I = 1.57 \text{ rad/sec } (0.2503 \text{ cps}) - \text{sloshing fluid frequency}$$

$$\omega^{II} = 23.208 \text{ rad/sec } (3.69 \text{ cps}) - \text{shell-}m_o \text{ frequency.}$$

These results are compared with those obtained by Haroun (Ref. 26) in Table II where excellent correlation is noted.

Examination of the resulting frequencies ω^{I} and ω^{II} indicates that the sloshing of the fluid is much too weak to affect the free vibration of the shell-m_o system. This fact is immediately evident by comparing the frequency of the shell-m_o system alone (ω_M = 23.185 rad/sec), with the frequency of the coupled shell-m_o component in the two-degree-of-freedom system (ω^{II} = 23.208 rad/sec). The difference between ω_M and ω^{II} is negligible. Thus it is reasonable to assume that the sloshing mass frequency, ω^{I}, and the frequency of the shell m_o system, ω_M or ω^{II}, are independent of one another. This vibrational independence of sloshing fluid mass and stationary fluid mass plays a key role in simplifying the dynamic analysis of liquid storage tanks (Chapter 5).

Although the sloshing fluid mass, m_1, has virtually no effect upon the frequency of the shell-m_o system, the natural frequency of the shell system alone is significantly affected by the stationary fluid mass, m_o. The frequency of the empty shell was calculated to be 120.5 rad/sec, versus 23.208 rad/sec for the coupled shell-m_o system (refer to Table 12 for summary and comparison of pertinent shell and shell fluid frequencies).

3.5 Simplified Free Vibration Analysis of Flexible Fluid Filled Tanks

In this section simplified expressions for the determination of natural frequencies for fluid filled, open-top cylindrical tanks, similar to the one illustrated in Fig. 25, are developed.

The procedure for the free vibration analysis of flexible liquid storage tanks detailed in Section 3.4 was utilized to perform the parametric study.

Because the coupling effect of the sloshing mass, m_1, with the shell-m_o system is weak (refer to subsection 3.4.2), it is possible as well as convenient to consider the total problem as two uncoupled systems:

1. The shell-m_o system
2. Liquid sloshing, m_1, in a similar rigid container.

Therefore, only the shell-m_o (stationary fluid mass) system was considered in the free vibration analysis. The natural frequency of the sloshing fluid mass m_1 in a flexible tank system is determined from the appropriate model parameters for a similar rigid tank and is expressed by Eq. 3.12. A comparison of the fundamental sloshing frequency in a tall tank (Ref. 26) full of water as calculated by the procedure outlined in Section 3.4, with that obtained by Eq. 3.12 for a similar rigid tank is made in Table 13. The two values are practically indistinguishable.

The results of the free vibration analysis for the natural frequencies of the shell-m_o system are represented in Figs. 31 and 32 for completely full and half full tanks, respectively. In each case the values of the natural frequency, ω, are non-dimensionalized with respect to the maximum frequency occurring in the H_o/D_o range ratio of 0.1 to 1.5, which is that corresponding to an aspect ratio $(H_o/D_o) = 0.1$. Thus in Fig. 31 $(\omega_{100})_{max}$ (19.32 cps) refers to the

natural frequency of a tank completely full of water with an $(H_o/D_o) = 0.1$. Similarly, in Fig. 32, $(\omega_{50})_{max}$ (40.11 cps) refers to the natural frequency of a tank half full of water having aspect ratio $H_o/D_o = 0.1$.

A regression analysis, similar to that done for empty tanks in Section 2.8, was conducted on the frequency data generated in the parametric study for the purpose of attaining a simple expression to delineate the relationship between non-dimensionalized frequencies (Figs. 31 and 32) and tank aspect ratio. This relationship was modeled with a cubic polynomial.

For convenience sake, the same non-dimensionalizing frequency paramter was used for both the completely full and half full cases. That parameter, $(\omega_o)_{max}$ (52.52 cps), is the natural frequency of an empty tank with aspect ratio $(H_o/D_o) = 0.1$. Therefore, the frequency versus height to diameter ratio relationships for both the completely full and half full cases may be determined from the expression

$$\bar{f}\,(H_o/D_o) + C_1 + C_2\,(H_o/D_o) + C_3\,(H_o/D_o)^2 + C^4\,(H_o/D_o)^3 \tag{3.34}$$

where $\bar{f}\,(H_o/D_o)$ is the non-dimensionalized frequency function for any (H_o/D_o) within the range 0.1 to 1.5 and C_1, C_2, C_3 and C_4 are the cubic polynomial coefficients.

To guarantee the greatest possible accuracy of the polynomial approximation, two sets of coefficients, for both the completely full and half full cases, were extracted from the

regression analysis; one set applicable to the aspect ratio range $0.1 \leq H_o/D_o \leq 0.4$, and the other set for the aspect ratio range $0.4 < H_o/D_o \leq 1.5$. These coefficients, to be used in conjunction with Eq. 3.34, are presented in Tables 14 and 15 for the completely full case ($h_L/H_o = 1.0$) and half full case ($h_L/H_o = 0.5$) respectively. Comparisons of the analytical results for $\omega/(\omega_o)_{max}$ versus H_o/D_o with those obtained from Eq. 3.34 are made in Fig. 33 for the tank completely full of water and in Fig. 34 for the tanks half full of water. Excellent correlation is noted for both cases.

3.5.1 Features of Free Vibration

Similar to the (n = 1, m = 1) vibration form of empty shells, the fundamental vibration mode of fluid-filled tanks is primarily extensional in nature. However, unlike empty shells, the natural frequencies of fluid-filled shells are not independent of their wall thickness.

For an empty shell, both the shell mass (for open-top cylindrical tanks) and the shell stiffness are directly proportional to the shell wall thickness. Therefore, the ratio of shell stiffness to shell mass (which is in turn proportional to the square of the natural frequency) is constant for any shell wall thickness, and the natural frequency of the shell remains unchanged for any wall thickness. For a fluid-filled shell, the total mass of the system is increased by the added mass of the fluid, while the stiffness remains unchanged for any wall thickness. For a fluid-filled shell, the total mass of the system is increased by the added mass of the fluid

while the stiffness remains unchanged. Now considering two fluid-filled shells identical in every way except for shell wall thickness, the shell with the thinner wall has a smaller overall stiffness than the shell with the thicker wall, but at the same time the ratio of shell stiffness to shell mass is the same for both shells. Consequently, the total stiffness to mass ratio of the shell with the thinner wall is reduced comparatively more by the addition of the fluid mass than is that of the shell with the thicker wall. Thus the shell-fluid system with the thinner shell wall will evidence a natural frequency which is lower than that of the identical shell-fluid system with the thicker wall.

Therefore, in the development of an expression for the determination of natural frequencies for fluid filled cylindrical tanks, a term to account for shell wall thickness was incorporated. The equation for the fundamental natural frequency of a tank completely filled with fluid is given as

$$f = C_f \frac{\overline{f}\ (H_o/D_o)}{D_o} \sqrt{\frac{C_a\ h\ \rho_w}{\rho_L\ D_o}} \tag{3.35}$$

and the expression for the natural frequency of a tank half filled with fluid is given by

$$f = C_f \frac{\overline{f}\ (H_o/D_o)}{2D_o} \left[\sqrt{\frac{C_a\ h\ \rho_w}{\rho_L\ D_o}} + \sqrt{\frac{C_b\ \rho_w}{\rho_L\ D_o}} \right] \tag{3.36}$$

where,

f = natural frequency in cycles per second

C_f = 1600.8 m/sec (5252.0 ft/sec)

$\bar{f}\ (H_o/D_o)$ = non-dimensionalized frequency parameter determined from Eq. 3.34.

C_a = 1.2 for S.I. units (100 for English units)

C_b = 15.24 for S.I. units (50 for English units)

D_o = diameter of tank in meters (feet)

h = average thickness of tank wall in mm (inches)

ρ_w = mass density of water

ρ_L = mass density of fluid in tank

As was mentioned previously in this section, the data base for the formulations of Eqs. 3.35 and 3.36 was derived from the analysis of a steel shell structure having a modulus of elasticity E_s = 206900 MN/m^2 (30,000 ksi) and mass density ρ_s = 20.3 kg/m^3 (0.000733 lb-sec.^{2}/un.^{4}). Equations 3.35 and 3.36 may be modified to accommodate tanks fabricated of other linear elastic materials in the following manner. To make the corrections for the stiffness properties, or modulus of elasticity, multiply the frequency, f, as determined from Eqs. 3.35 or 3.36 by $\sqrt{E/E_s}$, where E is the elastic modulus of the tank wall material. To account for difference in mass density, replace h in Eqs. 3.35 and 3.36 by an equivalent thickness, h_e, where

$$h_e = \frac{h\,\rho_s}{\rho} \tag{3.37}$$

and ρ is the mass density of the tank wall material.

The effect of liquid depth in cylindrical storage tanks upon the natural frequency of the shell-fluid system is illustrated in Fig. 35. In this comparative study, three cases of liquid depth are considered:

1. Empty tank ($\frac{h_L}{H_o} = 0.0$)

2. Tank 50% full of water ($\frac{h_L}{H_o} = 0.5$)

3. Tank 100% full of water ($\frac{h_L}{H_o} = 1.0$)

All frequencies are normalized with respect to the frequency ($(\omega_o)_{max} = 52.52$ cps) of an empty tank having height to diameter ratio $H_o/D_o = 0.1$. From this figure it is observed that as the level of fluid in the tank increases, the natural frequency decreases. This is the obvious result since the mass of the shell-fluid system increases with the level of fluid, while the structure stiffness properties remain unchanged.

It is also noted, from a careful examination of Fig. 35, that the reduction in the tanks' natural frequencies, due to the increase in fluid level, is much more significant for the shallow or broad tanks ($H_o/D_o \leq 0.5$) than it is for tall tanks. This can be explained by the fact that the amount of fluid mass in the tank is directly proportional to the square of the tank diameter (D_o) and to the tank height (H_o). For a shallow tank, the largest dimension is the diameter, and for a tall tank the largest dimension is the height. Thus since the fluid mass is proportional to the product

($H_o D_o^2$), the increase in fluid mass is relatively more for a shallow tank than it is for a tall tank.

Another interesting aspect of the free vibration of liquid-filled tanks is illustrated by Fig. 36. This figure represents the relationship between the relative amount of fluid mass, m_1, participating in sloshing and the tank aspect ratio, H_o/D_o, for both completely full and half full tanks. For shallow tanks, the greater portion of the total fluid mass participates in sloshing, while for tall tanks the major portion of the fluid mass vibrates with the shell. Obviously, this relationship is significant in assessing the dynamic response of fluid-shell systems.

In Figs. 37 and 38 the mode shapes for some selected aspect ratios (H_o/D_o) are shown. In Fig. 38 the radial displacement mode w is presented for a shallow tank ($H_o/D_o = 0.333$) for the cases of completely full and half full with water. The radial displacement mode for a tall fluid filled tank ($H_o/D_o = 1.5$) is represented in Fig. 37. Examination of these figures reveals that the radial displacement mode, w, is of the same order of magnitude and similar to the fundamental mode of vibration of an empty shell, Fig. 15, for the case of the tall tank, Fig. 37. For small aspect ratios (shallow tanks, Fig. 38) the radial displacement becomes comparatively much larger at the lower portion of the tank than at the top, and does not resemble the vibration mode of an empty tank. This is also an important factor in the assessment of the seismic response of liquid-filled tanks presented in Chapter 5.

3.5.2 Numerical Comparisons

To verify the accuracy of the frequency approximations developed for liquid-filled tanks (specifically, Eqs. 3.35 and 3.36) which were presented in the previous subsection, several numerical examples are considered. The results obtained by the present analysis are compared with those of other investigators. Examples of both shallow and tall tanks are analyzed for each of two cases:

1. Completely full with water $(\frac{h_L}{H_o} = 1.0)$
2. Half full with water $(\frac{h_L}{H_o} = 0.5)$

The shell dimensions and material properties, as well as the essential fluid properties are as follows:

a. Tall Tank $(H_o/D_o = 1.5)$

H_o = 21.946 m (72.0 ft)

D_o = 14.63 m (48.0 ft)

E = 206900.0 MN/m^2 (30,000 ksi)

ν = 0.3

ρ_s = 20.3 kg/m^3 (0.000733 lb-sec^2/in^4)

ρ_L = 2.6 kg/m^3 (0.000094 lb-$sec.^2/in^4$)

h = 25.4 mm (1.0 in), 10.92 mm (0.43 in), 7.315 mm (0.288 in)

h_L = 21.946 m (72.0 ft), 10.973 in (36.0 ft)

b. Shallow Tank ($H_o/D_o = 0.333$)

$H_o = 12.192$ m (40.0 ft)

$D_o = 36.576$ m (120.0 ft)

$E = 206900.0$ MN/m^2 (30,000 ksi)

$\nu = 0.3$

$\rho_s = 20.3$ kg/m^3 (0.000733 lb-sec^2/in^4)

$\rho_L = 2.6$ kg/m^3 (0.000094 lb-sec^2/in^4)

$h = 25.4$ mm (1.0 in)

$h_L = 12.192$ m (40.0 ft), 6.096 m (20.0 ft)

In Table 16 the numerical results obtained by the present analysis for the natural frequencies of a shallow liquid filled tank are summarized, and compared with the numerical results obtained by Haroun (Ref. 26) and Edwards (Ref. 20). In no instance is the discrepency greater than 2%. The numerical results for the natural frequencies of a tall liquid filled tank, obtained in the present analysis, are compared with the results obtained in the investigation of Ref. 26, and are presented in Table 17. In this comparative study, the effect of shell wall thickness upon the natural frequency of the shell-liquid system can be observed. Excellent correlation is also cited in these comparisons.

This comparative study clearly indicates that the simple expressions developed in this investigation can determine the natural frequencies of liquid filled cylindrical tanks without appreciable error. Moreover, the numerical results obtained in the present

analysis involve only the evaluation of a few simple analytical expressions.

4. SEISMIC ANALYSIS OF EMPTY CYLINDRICAL TANKS

4.1 Introduction

Simplified expressions for conducting seismic analyses of empty cylindrical storage tanks are developed in this chapter. These expressions form the basis of accurate, yet easy-to-apply procedures for determining shell stresses, base shears, overturning moments, and shell displacements induced in cylindrical tanks by horizontal earthquake ground motion.

The seismic analysis of thin walled cylindrical shells described in this chapter is based upon the response spectrum concept, which has been pioneered by Biot (Ref. 11) and Housner et al (Ref. 29), and the classical approach of normal mode vibration (Refs. 24, 61 and 62). The pertinent parameters entering into the normal mode analysis (i.e. generalized force, generalized mass, and mode participation factor) are defined and calculated with the use of shell theory, rather than from equivalent lumped-mass or beam models, thus ensuring the accuracy of the procedures described herein.

In the present investigation, only one mode of free vibration is considered, that corresponding to an axial wave number $m = 1$ and a circumferential wave number $n = 1$ (refer to Section 2.1 for a detailed explanation). The contribution of higher axial modes has previously been determined to be negligible (Ref. 39), and it will

be shown (Subsection 4.2.2) that horizontal vibration excludes all but the n = 1 circumferential mode. The natural frequency of the shell structure is determined from the appropriate simplified expressions developed in Chapter 2, and the corresponding mode participation factor is determined from expressions developed in Subsection 4.4.1.

The analytical derivation of the mode participation factor for axisymmetrical shells presented in Refs. 36 and 39, is summarized in Section 4.2. In Subsection 4.2.2, the solution for mode participation for a general axisymmetric shell is condensed for application to the special case of a cylindrical shell.

4.2 Dynamic Response of an Axisymmetric Shell

4.2.1 Systems and Assumptions

The shell under consideration is a structure which is symmetric about a straight axis oriented vertically with respect to a horizontal foundation which is capable of moving only horizontally (Ref. 39). The main objective of this phase of the investigation is to find the response of the shell to a given horizontal motion of the foundation. Mathematically, the problem consists of finding the stresses and displacements of the shell when it is subjected to time dependent boundary conditions at one end, the rest of the shell being free of any constraints.

It is assumed that a continuous axisymmetric boundary surface of the shell has been chosen and that a thickness has been assigned at every point of the reference surface. The locations of the material points within the thickness are given by the two axisymmetric shell coordinates ϕ and θ, on the reference surface, and by the distance ζ, which is measured from the reference surface along its positive normal $\vec{t}_\zeta$ (Fig. 39).

A general mathematical model for the deformation of a thin shell is based on the hypothesis that the displacement field $\vec{v}$ is linear in ζ in the form (Ref. 39)

$$\vec{v}\,(\phi,\ \theta,\ \zeta) = \vec{u}\,(\phi,\ \theta) + \zeta\,\vec{\beta}(\phi,\ \theta) \tag{4.1}$$

Since the reference surface is defined by $\zeta = 0$, then $\vec{u}$ is the displacement vector of the material points lying on the reference surface. Thus it is resolved

$$\vec{u} = u_\phi\,\vec{t}_\phi + u_\theta\,\vec{t}_\theta + w\,\vec{t} \tag{4.2}$$

$$\vec{\beta} = \beta_\phi\,\vec{t}_\theta + \beta_\theta\,\vec{t}_\theta + \beta_\zeta\,\vec{t}_\zeta \tag{4.3}$$

where $\vec{t}_\phi$, $\vec{t}_\theta$, and $\vec{t}_\zeta$ is a triad of unit vectors, tangent to the ϕ, θ and ζ coordinate curves, respectively (Refer to Fig. 39). For infinitesimal deformations, β_ϕ and β_θ, are the angles of rotation of the normal in the directions of $\vec{t}_\phi$ and $\vec{t}_\theta$, respectively, while β_ζ times the thickness gives the change in thickness of the shell.

To obtain the conditions that the foundation imposes on the six shell displacements u_ϕ, u_θ, β_ϕ, β_θ, w and β_ζ, at the points where the shell is in contact with the foundation, it is assumed that the

base of the shell is continuously and rigidly attached to a rigid foundation (Fig. 39). It is further assumed that the foundation experiences a horizontal time dependent displacement given by

$$\overline{U}_x = U_x f_x (t) \tag{4.4}$$

where U_x is some amplitude factor and f_x is the time variation. (It is also assumed that the foundation displacement $\overline{U}_x$ is the same as the ground motion x(t)). The displacements of the foundation are transferred to the shell by the following conditions at its base:

$$\begin{aligned} u_r &= U_x \cos\theta\, f_x (t) && \text{(a)} \\ u_\theta &= - U_x \sin\theta\, f_x (t) && \text{(b)} \\ \beta_\phi &= \beta_\theta = \beta_\zeta = 0 && \text{(c)} \end{aligned} \tag{4.5}$$

where u_r is the displacement perpendicular to the axis of symmetry. To express the displacements of the foundation in terms of the shell displacements, the following transformation is employed

$$\begin{aligned} u_\phi &= u_r \cos\phi && \text{(a)} \\ w &= u_r \sin\phi && \text{(b)} \end{aligned} \tag{4.6}$$

Finally, the problem becomes to find the response of the shell when the displacements

$$\begin{aligned} u_\phi &= U_x f_x (t) \cos\phi \cos\theta && \text{(a)} \\ u_\theta &= - U_x f_x (t) \sin\theta && \text{(b)} \\ w &= U_x f_x (t) \sin\phi\cos\theta && \text{(c)} \\ \beta_\phi &= \beta_\theta = \beta_\zeta = 0 && \text{(d)} \end{aligned} \tag{4.7}$$

are prescribed at the circle of contact between the reference surface of the shell and the foundation, the rest of the shell being free of any constraint.

4.2.2 Mode Participation Factor

The displacement response to time dependent boundary conditions is constructed in the form (Ref. 36)

$$\vec{u}\ (\phi,\ \theta,\ t) = \vec{u}^{s}\ (\phi,\ \theta) + \vec{u}\ (\phi,\ \theta)\ \Gamma\ F(t) \quad \text{(a)}$$

$$\vec{\beta}\ (\phi,\ \theta,\ t) = \vec{\beta}^{s}\ (\phi,\ \theta) + \vec{\beta}(\phi,\ \theta)\ \Gamma\ F(t) \quad \text{(b)}$$

(4.8)

The terms with the superscript s identify variables of a static solution for the shell when it is subjected to the boundary conditions given by Eqs. 4.7 with the time functions omitted; $\vec{u}$ and $\vec{\beta}$ give the displacement field in the fundamental mode (m = 1) of free vibration; Γ is the mode participation factor (Ref. 39) given by

$$\Gamma = J/(\omega M) \tag{4.9}$$

where

$$J = \int_{s} \{\rho_0 \vec{u}^{s} \cdot \vec{u}\} ds \tag{4.10}$$

$$M = \int_{s} \{\rho_0 \vec{u} \cdot \vec{u}\} ds \tag{4.11}$$

and F(t) denotes the Duhamel integral (Refs. 24, 61, 62) defined as

$$F(t) = \int_{0}^{t} \ddot{x}(\tau)\ \sin\ \omega(t - \tau) d\tau \tag{4.12}$$

where $\ddot{x}(t)$ is the horizontal ground acceleration. Thus we can have

$$\ddot{x}(t) = U_x \ddot{f}_x(t) \tag{4.13}$$

where the dots denote time derivatives.

The integrals J and M can be interpreted as the generalized force and generalized mass (Ref. 14), respectively, in the fundamental mode (m = 1) of vibration. They must be evaluated over the entire reference surface, S, of the shell, with shell density measures given by

$$\rho_0 = \int_{\zeta_1}^{\zeta_2} \rho(\phi, \theta)\, d\zeta = \rho h \tag{4.14}$$

where ζ_1 and ζ_2 denote the distances of the boundary surfaces of the shell from the reference surface, ρ denotes the mass density of the shell material, and h denotes the shell thickness.

For an axisymmetric shell (Fig. 39), excited horizontally through its foundation, the static solution (with superscript s) is represented by a rigid body movement of the whole shell through a horizontal distance U_x (Ref. 39). With reference to Eqs. (4.7), such a rigid body solution throughout the shell is given by

$$\vec{u}^s = U_x \cos\phi \cos\theta\, \vec{t}_\phi - U_x \sin\theta\, \vec{t}_\phi + U_x \sin\phi \cos\phi\, \vec{t}_\zeta \tag{4.15}$$

and

$$\vec{\beta}^s = 0 \tag{4.16}$$

while all other (stress) variables are identically zero. Using Eqs. 4.15 and 4.16 from the static solution, and expressing for a shell of revolution the surface integral for J as an integrated integral, J from Eq. 4.10 can be written as

$$J = \int_{s_1}^{s_2} \int_{0}^{2\pi} \vec{u}^s \cdot (\rho_0 \ddot{\vec{u}})\, r\, d\theta\, ds \qquad (4.17)$$

where s is the arclength along the meridian (curve of intersection of reference surface and a plane through the axis of symmetry; refer to Fig. 6), s_1 and s_2 are the endpoints of the meridian, θ is the circumferential angular coordinate, and r is the distance to a point on the reference surface from the axis of symmetry (Fig. 39).

The free vibration solutions are separable in the ϕ and θ coordinates in the form (Ref. 39).

$$u_\phi (\phi, \theta) = u_{\phi n} (\phi) \cos n\theta \qquad (4.18)$$

with similar expressions for all other variables. Theoretically there is an infinite number of resonant modes of the shell for each given value of the circumferential wave number n, and all the modes, for all wave numbers, must be used in the integrand of Eq. 4.17. However, when the terms of the scalar products of Eq. 4.17 are integrated with respect to θ, only the modes for n = 0 and n = 1 survive. This can be illustrated by considering the first term of the first scalar product in the integrand of Eq. 4.17 in the form

$$J = \int_{s_1}^{s_2} \int_{0}^{2\pi} \{(\rho_0 U_x \cos\phi \cos\theta)\, u_{\phi n}\, u_{\phi n} \cos n\theta\}\, r\, d\theta\, ds \tag{4.19}$$

where $n = 0, 1, 2, 3 \ldots \infty$

Noting that

$$\int_{0}^{2\pi} \cos n\theta\, d\theta = \begin{cases} 2\pi, & \text{for } n = 0 \\ 0, & \text{for } n \geq 1 \end{cases} \tag{4.20}$$

and

$$\int_{0}^{2\pi} \cos\theta \cos n\theta\, d\theta = \begin{cases} \pi, & \text{for } n = 1 \\ 0, & \text{for } n \geq 2 \end{cases} \tag{4.21}$$

It is obvious that out of all the modes of free vibration, as given by Eq. 4.18 with n = 0, 1, 2, ..., only those with n = 0 and n = 1 participate in the general solution of the problem. Moreover, since this investigation is concerned with horizontal excitation of the shell only, the solution corresponding to n = 0 also does not participate.

Thus, for the problem at hand, the expression for J can be simplified to

$$J = U_x\, j \tag{4.22}$$

where

$$j = \int_{s_1}^{s_2} \int_{0}^{2\pi} \{\rho_o\, (u_\phi \cos\phi - u_\theta + w \sin\theta)\}\, r\, d\theta\, ds \tag{4.23}$$

Therefore, it is obvious that the participation factor for horizontal motion involves only the n = 1 circumferential mode, with modal displacements u_ϕ, u_θ and w. No modes with circumferential wave numbers other than n = 1 enter into the general solution. Similarly, the generalized mass for the n = 1 mode is given by

$$M = \int_{s_1}^{s_2} \int_{0}^{2\pi} \rho_0 \{(u_\phi)^2 + (u_\theta)^2 + (w)^2\} r \, d\theta \, ds \qquad (4.24)$$

For the special case of a cylindrical shell (where the angle ϕ between the axis of symmetry and the shell normal at the reference surface (Fig. 39) is 90^o), Eqs. 4.23 and 4.24 can be simplified to

$$j = \int_{s_1}^{s_2} \int_{0}^{2\pi} \rho_0 (u_\theta + w) \, r \, d\theta \, ds \qquad (4.25)$$

and

$$M = \int_{s_1}^{s_2} \int_{0}^{2\pi} \rho_0 \{(u_\phi)^2 + (u_\theta)^2 + (w)^2\} \, r \, d\theta \, ds \qquad (4.26)$$

The static solution, represented by $\vec{u}^s$ and $\vec{\beta}^s$ in Eq. 4.8, is given by Eqs. 4.15 and 4.16. Since the $\vec{u}^s$ terms represent a rigid body motion of the shell (which is the same as that of the foundation), the $\vec{u}^s$ terms in the response can be omitted if the

displacements u_ϕ, u_θ and w are measured with respect to the foundation. No change is needed for $\vec{\beta}^s$, because according to Eq. 4.16, $\vec{\beta}_s = 0$.

Finally, the response of the shell may be expressed by (Ref. 39)

$$A = U_x \; B \; \Gamma \; F(t) \tag{4.27}$$

where the symbol A represents any desired variable of the solution (such as displacement or stress) and B represents the same variable taken from the solution of the fundamental mode (m = 1, n = 1) of free vibration. The mode participation factor, Γ, is given by (Ref. 39)

$$\Gamma = j/(\omega M) \tag{4.28}.$$

The Duhamel integral in Eq. 4.27, F(t), contains the acceleration of the horizontal motion, $\ddot{x}(t)$. The complete response of the shell, as given by Eq. 4.8 is determined once the time variation F(t) is known. The following section is concerned with finding the peak value of F(t) from the response spectrum.

4.3 Response Spectrum

If a deterministic response to a known ground motion is desired, the Duhamel integral, given in Eq. 4.12, must be evaluated at various times t, which then provides the time dependence of the response in the solution, Eq. 4.27 (Ref. 39). However, seismic design is concerned with a ground motion that is expected to occur

in the future, so that its deterministic record cannot be anticipated. The use of an acceleration record of a previous earthquake in Eq. 4.12 is possible, but often proves to be not very judicious. A more logical, commonly employed procedure for seismic design is the Response Spectrum approach (Refs. 12, 16, 50, 51, 52, 53 and 58).

The response spectrum is defined as a graphical relationship of a single degree of freedom system with damping to dynamic motion or forces (Ref. 58). The most usual measures of responses are maximum displacement, S_d, which is a measure of strain in the spring element of the system, maximum pseudo relative velocity, S_v, which is a measure of energy absorption in the spring of the system, and maximum pseudo acceleration, S_a, which is a measure of the maximum force in the spring of the system.

More specifically, if it is assumed that horizontal ground acceleration records of some past earthquake are available (i.e. in Eq. 4.12 $\ddot{x}(t)$ is known for a sufficient range of t), then it is possible to evaluate the function

$$F(t) = \int_0^t \ddot{x}(\tau) \sin \omega(t - \tau) \, d\tau \qquad (4.29)$$

for a given value of ω, and record only the maximum value of F(t), denoted by

$$V = \max [F(t)] \qquad (4.30)$$

over all times t (note that V is equal to the maximum pseudo relative velocity of the system S_v). Repeating this calculation for a wide range

of frequencies, a plot of the relationship between V (or S_v) and ω, for a single earthquake can be produced. Such a plot is called the velocity response spectrum of an earthquake. An example of a velocity response spectrum obtained from the ground accelerations recorded at El Centro, California, 18 May 1940 (N - S component) is presented in Fig. 40 (reproduced from Ref. 52).

Although actual response spectra for earthquake motions are quite irregular, they have the general shape of a trapezoid (Ref. 58). A generalized spectrum is shown in Fig. 41, plotted on a logarithmic tripartite graph, and modified so that the various regions of the spectrum are smoothed to straight line portions. On the same graph are shown the maximum values of ground acceleration, velocity, and displacement. The figure therefore indicates that the spectral values of acceleration, velocity, and displacement (i.e. S_a, S_v and S_d, respectively) may be interpreted as the ground motion maxima multiplied by amplification factors. Details for constructing such spectra are described in Refs. 2, 49, 50, 51 and 53.

Regardless of the nature of the response spectrum, the relationship between spectral displacement, S_d, psuedo spectral velocity, S_v, and pseudo spectral acceleration S_a, at any specific frequency, ω, are defined by the expressions

$$S_a = \omega S_v \tag{4.31}$$

and

$$S_d = \frac{S_v}{\omega} \tag{4.32}.$$

4.3.1 Application of Response Spectrum Technique

A design estimate of the response of a cylindrical tank to horizontal earthquake motion, can be obtained from a revised form of Eq. 4.27, given as

$$A = B \Gamma S_v \tag{4.33}$$

where the symbol A represents any desired variable of the response (such as displacement or stress), B represents the same variable taken from the solution of the fundamental mode of free vibration ($m = 1$, $n = 1$), Γ is the mode participation factor defined by Eq. 4.28, and S_v is the pseudo spectral velocity which is determined from an appropriate design spectrum, such as that illustrated in Fig. 41. The determination, from simplified expressions, of pertinent values for B and Γ, to be used in Eq. 4.33, is one of the concerns of the following section.

4.4 Procedure for Seismic Analysis

The pertinent stress variables necessary for evaluating the seismic response of thin walled, cylindrical tanks are the axial membrane stress resultant, N_ϕ (or N_z) and the circumferential stress resultant (hoop stress), N_θ (refer to Fig. 7). The most significant shell displacement component describing the general vibratory form of the shell is the radial displacement, w. The variables representing N_z, N_θ and w, which correspond to the parameter B in Eq. 4.33, as well as the variable representing the mode participation factor,

Γ, can be determined from the results of the free vibration analysis of empty cylindrical tanks described in Chapter 2.

The development of simple expressions, from the free vibration data previously mentioned, for the shell stress and displacement variables, and mode participation factor are detailed in the following subsections. Simplified expressions for base shear and overturning moment are also developed in this section.

4.4.1 Mode Participation Factor

The result of the free vibration analysis conducted in Chapter 2, for the class of tanks exhibiting an aspect ratio (H_o/D_o) range of 0.1 to 1.5, for the mode participation factor, Γ (as determined by numerical integration (Ref. 34) of Eqs. 4.25, 4.26 and 4.28) is represented in Fig. 42. The values of Γ are normalized with respect to the maximum factor in the group, Γ_{max} (0.02437 sec.), which corresponds to $H_o/D_o = 0.1$, and are plotted against tank aspect ratio (Fig. 42).

A regression analysis was conducted on the mode participation data generated in the parametric study for the purpose of attaining a simple expression to delineate the relationship between the non-dimensional participation function and tank aspect ratio. The resulting expression, a cubic polynomial, is given by

$$\overline{\Gamma}\left(\frac{H_o}{D_o}\right) = C_1 + C_2\left(\frac{H_o}{D_o}\right) + C_3\left(\frac{H_o}{D_o}\right)^2 + C_4\left(\frac{H_o}{D_o}\right)^3 \tag{4.34}$$

where $\overline{\Gamma}(H_o/D_o)$ is the non-dimensional mode participation function for any particular H_o/D_o ratio in the range 0.1 - 1.5, inclusive; and C_1, C_2, C_3 and C_4 are the cubic polynomial coefficients extracted from the regression analysis, which are presented in Table 18. The comparison of the analytical results for Γ/Γ_{max} versus H_o/D_o, with those obtained from Eq. 4.34 is illustrated in Fig. 43. Excellent correlation is noted.

From examination of Eqs. 4.25, 4.26 and 4.28, it is observed that the mode participation factor is independent of the shell thickness, and is conditional only to the modal displacement components u_θ, u_ϕ and w, and the natural frequency, ω. Therefore, the mode participation factor, Γ, for any cylindrical tank having an H_o/D_o ratio within the range 0.1 to 1.5, may be determined from Eq. 4.34 used in conjunction with certain characteristics of the height and diameter of the tank. The simple expression relating the mode participation factor to the aspect ratio of the tank is given by:

$$\Gamma = C_m D_o \overline{\Gamma} \left(\frac{H_o}{D_o}\right) \tag{4.35}$$

where $\overline{\Gamma}(H_o/D_o)$ is the non-dimensional mode participation function determined by Eq. 4.34, C_m = 0.0017952 sec/m (0.0005472 sec/ft) is a constant and D_o is the diameter of the tank in meters (feet).

Although the data base used for the formulation of Eqs. 4.34 and 4.35 was generated from the analysis of a steel structure having a modulus of elasticity E_s = 206700 MN/m^2 (30,000 ksi), and mass density ρ_s = 20.3 kg/m^3 (0.000733 $lb\text{-}sec^2/in^4$), Eq. 4.35 may be

modified to accommodate tanks fabricated of materials with different properties, resulting in the expression given as

$$\Gamma = \frac{C_m D_o \Gamma \left(\frac{H_o}{D_o}\right)}{\sqrt{\frac{E\rho_s}{E_s\rho}}} \qquad (4.36)$$

where E and ρ are the elastic modulus and mass density, respectively, of the shell material.

Equations 4.34, 4.35 and 4.36 are also applicable to cylindrical storage tanks having a roof structure. The values of the cubic polynomial coefficients, C_1, C_2, C_3 and C_4, to be used in Eq. 4.34, are presented in Table 19 for roof mass coefficients $K_r = 1.0$, $K_r = 2.0$ and $K_r = 3.0$ (refer to Section 2.7 for an explanation of the roof mass coefficient).

4.4.2 Shell Displacement and Stress Variables

Having established a procedure for approximating the mode participation factor for empty cylindrical tanks, both with and without a roof structure, the evaluation of the shell displacement and stress variables (that is, the parameter B) to be used in Eq. 4.33 is considered.

As was previously stated in this section, the relevant displacement variable is the radial displacement component, w. The critical stress variables are the circumferential stress component, N_θ, and the axial stress component, N_z (Fig. 44). Simplified expressions for evaluating the radial displacement variable,

$\overline{w}$ (z/H_o), have been developed in Section 2.6, and are represented by Eqs. 2.41, 2.42 and 2.43. The remainder of this subsection is devoted to the development of similar expressions for the membrane stress variables N_θ and N_z.

From the results of the free vibration analyses of empty tanks conducted in Chapter 2, data pertaining to the variation of the circumferential stress resultant, N_θ, and the axial stress resultant, N_z, along the height of the tank were recorded and plotted for each case in the parametric study. Typical stress distributions are illustrated in Figs. 45 and 46 for N_z and N_θ, respectively. To define the relationship of membrane stress resultant (N_θ and N_z) versus tank height, with a simple analytical expression, a regression analysis was performed on the accumulated stress resultant data for each case in the free vibration study. The resulting expression, a quadratic polynomial, is given by

$$\overline{\overline{N}}\ (z/H_o) = C_1 + C_2\ (z/H_o) + C_3\ (z/H_o)^2 \qquad (4.37)$$

where $\overline{\overline{N}}\ (z/H_o)$ is the non-dimensionalized stress function representing either N_θ or N_z, z/H_o is the height parameter such that

$$0 < \frac{z}{H_o} \leq 1.0, \text{ for } N_z$$

and

$$0.2 \leq \frac{z}{H_o} \leq 1.0, \text{ for } N_\theta$$

For values of $z/H_o < 0.2$, the N_θ versus z/H_o relationship becomes discontinuous; however, N_θ can be conservatively estimated as νN_z in this range, where ν is Poisson's ratio.

The quadratic polynomial coefficients, C_1, C_2 and C_3, of Eq. 4.37 are a function of the tank aspect ratio (H_o/D_o), and must in turn be determined from the quadratic expression given by

$$C_i = A_{1i} + A_{2i} \left(\frac{H_o}{D_o}\right) + A_{3i} \left(\frac{H_o}{D_o}\right)^2, \quad i = 1, 2, 3 \qquad (4.38)$$

where A_{1i}, A_{2i} and A_{3i} are quadratic polynomial coefficients also. The "A" coefficients pertinent to $\overline{N}_z$ are listed in Table 20, and those pertaining to N_θ are listed in Table 21.

The stress variables $\overline{N}_z$ and $\overline{N}_\theta$ (determined from $\overline{\overline{N}}_z$ or $\overline{\overline{N}}_\theta$) are expressed as

$$\overline{N}\left(\frac{z}{H_o}\right) = C_N \, h \, \overline{\overline{N}}\left(\frac{z}{H_o}\right) \qquad (4.39)$$

where $\overline{N}\ (z/H_o)$ is the stress variable for N_z or N_θ; $\overline{\overline{N}}\ (z/H_o)$ is the non-dimensionalized stress function for N_z or N_θ (determined from Eq. 4.39); h is the shell thickness in meters (inches); C_N is a constant such that

$$C_{N_z} = \frac{2933.7}{D_o} \frac{MN}{m^3} \quad \left(C_{N_z} = \frac{1396000.0}{D_o} \frac{lb}{in^3}\right)$$

and

$$C_{N_\theta} = \frac{10675.7}{D_o} \frac{MN}{m^3} \quad \left(C_{N_\theta} = \frac{5080000.0}{D_o} \frac{lb}{in^3}\right.$$

where D_o is the diamter of the tank in meters (feet).

Equations 4.37, 4.38 and 4.39 are also valid for determining the membrane stress resultants in tanks having a roof structure. The quadratic coefficients A_{1i}, A_{2i}, etc. to be used in conjunction with Eq. 4.38 for the determination of $\bar{\bar{N}}_z$ are listed in Tables 22(a), (b) and (c), respectively, for roof mass coefficients $K_r = 1.0$, $K_r = 2.0$ and $K_r = 3.0$ (refer to Section 2.7 for explanation of roof mass coefficients). For the determination of $\bar{\bar{N}}_\theta$, the appropriate A_i coefficients to be used in Eq. 4.38 are listed in Tables 23(a), (b) and (c) for roof mass coefficients $K_r = 1.0$, $K_r = 2.0$ and $K_r = 3.0$, respectively.

In summary, a design estimate of the response of an empty cylindrical tank subjected to horizontal earthquake motion, can be obtained from the expression

$$A = B \Gamma S_v \tag{4.33}$$

where the symbol A may represent either the radial displacement w, or the axial stress resultant N_z, or the circumferential stress resultant N_θ. B represents the corresponding variable of the free vibration response $\bar{w}$, $\bar{N}_z$ or $\bar{N}_\theta$ (determined from Eq. 2.43 for $\bar{w}$, and Eq. 4.39 for N_z or N_θ). Γ is the mode participation factor determined from Eq. 4.35, and S_v is the pseudo spectral velocity in m/sec (inches/sec) determined from an appropriate design spectrum.

As a specific illustration, the distribution of the axial membrane stress resultant, N_z, along the height of the tank at a circumferential coordinate angle θ equal to zero degrees, as determined from Eq. 4.33 has the form

$$N_z \left(\frac{z}{H_o}\right) = \bar{N}_z \left(\frac{z}{H_o}\right) \Gamma S_v \qquad (4.40)$$

The circumferential variation of any displacement or stress variable determined in this fashion is given as $\cos\theta$.

For tanks constructed of materials other than steel (E_s = 206900 MN/m^2; 30,000 ksi) the displacement variable, $\bar{w}$, and the stress variables, N, obtained from Eq. 4.33, must be multiplied by the ratios E_s/E and E/E_s, respectively; where E is the elastic modulus of the shell material.

4.4.3 Base Shear and Overturning Moment

In addition to the displacement and stress variables, the subject of the previous subsection, the shear force developed at the base of the tank and the overturning moment of the structure, induced by earthquake motion, are also of particular importance in assessing the response of the system. This subsection is concerned with the development of simple expressions to estimate the base shear and overturning moment of empty cylindrical tanks subject to horizontal earthquake ground motion.

The base shear and overturning moment cannot be determined directly from the results of the free vibration analyses conducted in Chapter 2. Therefore, to accommodate a simple derivation of expressions for base shear and overturning moment, the cylindrical tank is idealized as a cantilever column (Fig. 47). The forces developed in the structure during an earthquake may be found most

reliably in terms of the effective inertia forces, which depend upon the effective (spectral) acceleration, S_a (Ref. 14). The effective inertia force per unit length, q(z), along the structure is given by (refer to Fig. 47)

$$q(z) = \mu(z)\ \psi(z)\ \Gamma\omega\ S_a \tag{4.41}$$

where $\mu(z)$ is the mass per unit length, $\psi(z)$ is the shape function (which may be reasonably approximated by $\bar{w}(z)$, Eq. 2.43), Γ is the mode participation factor determined from Eq. 4.35, ω is the natural frequency of the system in radians per second, and S_a is the spectral acceleration.

The maximum base shear force, Q_{max}, is given by the integral of all the effective inertia forces acting over the height of the structure:

$$Q_{max} = \int_0^{H_o} q(z)\ dz = \Gamma\ \omega\ S_a \int_0^{H_o} \psi(z)\ \mu(z)\ dz \tag{4.42}$$

The overturning moment, M_{OTM}, is defined as the sum of the moments of the effective inertia forces about the base of the tank. Thus the overturning moment is expressed by the itegral

$$M_{OTM} = \int_0^{H_o} q(z)\ z\ dz = \Gamma\ \omega\ S_a \int_0^{H_o} \psi(z)\ \mu(z)\ z\ dz \tag{4.43}$$

For tanks with roof structure, the expressions for base shear and overturning moment, respectively, are given by

$$Q_{max} = \Gamma \omega S_a \left[\int_0^{H_o} \psi(z) \mu(z) \, dz + m_r \right] \tag{4.44}$$

and

$$M_{OTM} = \Gamma \omega S_a \left[\int_0^{H_o} \psi(z) \mu(z) \, z \, dz + m_r H_o \right] \tag{4.45}$$

where m_r is the mass of the roof structure.

4.4.4 Flow Diagram

To facilitate application of the seismic design procedures presented in this section, a flow diagram is provided (Table 24). It is envisioned that this flow diagram will grant the investigator the contingency to quickly identify, and properly implement the pertinent expressions for the analysis at hand. At the investigator's discretion, one or more of the steps outlined in the flow diagram may be omitted.

5. SEISMIC ANALYSIS OF LIQUID-FILLED CYLINDRICAL TANKS

5.1 Introduction

In this phase of the investigation the seismic response of open-top, liquid-filled cylindrical storage tanks is considered. Simple expressions for evaluating the seismic response of the flexible shell-liquid system are presented in this chapter. These expressions provide for an uncomplicated, but accurate procedure for determining the hydrodynamic pressures induced in cylindrical liquid storage tanks subject to horizontal earthquake motion. Expressions for calculating the resulting shell stresses, base shears and overturning moments are also presented.

The more exact analyses show that the hydrodynamic pressures can be separated into impulsive and convective parts (Ref. 27). The impulsive pressures are those associated with inertial forces produced by accelerations of the walls of the container and are directly proportional to these accelerations. The convective pressures are those produced by the oscillations of the fluid and are therefore the consequences of the impulsive pressures (Ref. 63). In this investigation the impulsive and convective pressures are treated separately. The fluid is assumed to be incompressible and the fluid displacements are assumed to be small.

The shell-fluid system investigated is illustrated in Fig. 48. It is a circular cylindrical tank of diameter, D_o (radius a) and

height, H_o. The tank is filled to a height, h_L, with a liquid of mass density ρ_L. It is assumed that the base of the tank is continuously fixed to a rigid foundation which is excited by a horizontal component of earthquake ground motion of acceleration $\ddot{x}(t)$. The location of points within the shell-fluid system are specified by the cylindrical coordinate system r, θ and z (Fig. 48).

The shell-fluid system is analyzed by implementation of a modified version of the procedure for rigid containers, first presented by Housner (Ref. 27) and later amplified by the Atomic Energy Commission (Ref. 63). Both the impulsive and convective effects in a rigid shell-fluid system subject to lateral ground motion are investigated. However, only the impulsive effects in flexible shell-fluid systems are considered, the reason being that the convective effects are insensitive to shell flexibility and therefore can be determined from the procedures developed for the analysis of rigid containers (Refs. 20, 26, 68; also refer to Section 3.4).

5.2 Hydrodynamic Pressures in Rigid Containers

5.2.1 Impulsive Pressures

The maximum impulsive hydrodynamic pressures, p_i, exerted against the wall of a rigid tank (refer to Fig. 48) may be expressed in the form (Refs. 63, 65)

$$p_i(z, \theta) = \rho_L \ddot{x} h_L \left[\left(1 - \frac{z}{h_L}\right) - \frac{1}{2} \left(1 - \frac{z}{h_L}\right)^2 \sqrt{3} \tanh \left(\frac{\sqrt{3} D_o}{2h_L}\right) \right] \tag{5.1}$$

where $\ddot{x}$ is the maximum horizontal ground acceleration, z is the elevation measured from the base of the tank, and θ is the circumferential coordinate angle.

If the tank is slender, having an aspect ratio (H_o/D_o) and liquid depth ratio (h_L/D_o) greater than 0.75 (Ref. 63), the entire mass of fluid below a depth of 0.75 D_o tends to respond as a rigid body as far as the impulsive pressures are concerned. Therefore, for purposes of evaluating the impulsive pressures, $p_i(z, \theta)$, the container can be regarded as a tank with a fictitious bottom at a datum 0.75 D_o below the liquid surface, and supported on a solid mass extending from the fictitious bottom to the actual bottom (Fig. 49). Equation 5.1 is applicable to the portion above the datum, but the pressure at depths below the fictitious bottom are given by (Ref. 63)

$$p_i(z, \theta) = \rho_L \ddot{x} \frac{D_o}{2} \cos\theta \qquad (5.2)$$

5.2.2 Convective Pressures

When the walls of a fluid container are subjected to accelerations, the fluid itself is excited into oscillations, and this motion produces pressures on the walls of the container. The convective hydrodynamic pressure, $p_c(z, \theta)$, exerted against the wall of a rigid tank (refer to Fig. 48) may be expressed in the form (Ref. 63)

$$p_c(z, \theta) = \sqrt{\frac{3}{8}}\ \rho_L \frac{D_o^2}{4}\ \theta_h\ \left(1 - \frac{\cos^2\theta}{3} - \frac{\sin^2\theta}{2}\right)$$

$$\cos\theta\ \frac{\cosh\left(2\sqrt{\frac{27}{8}}\ \frac{h_L - z}{D_o}\right)}{\sinh\left(2\sqrt{\frac{27}{8}}\ \frac{h_L}{D_o}\right)}\ \omega_1^2 \qquad (5.3)$$

where θ is the circumferential coordinate angle, ω_1 is the natural frequency of the fundamental sloshing fluid mass (refer to Chapter 3 for a detailed explanation), and θ_h is the angular amplitude of free oscillation at the liquid surface (Ref. 63). The quantities ω_1 and θ_h, respectively, are expressed by

$$\omega_1^2 = \frac{3.68\ g}{D_o} \tanh\left(3.68\ \frac{h_L}{D_o}\right) \qquad (5.4)$$

and

$$\theta_h = \frac{3.068\ (S_d)_1}{D_o} \tanh\left(3.68\ \frac{h_L}{D_o}\right) \qquad (5.5)$$

where g is the acceleration of gravity and $(S_d)_1$ is the spectral displacement, determined from an appropriate response spectrum (refer to Section 4.3), of the fundamental sloshing fluid mass.

Finally, the maximum water-surface displacement (height of sloshing) d_{max} (Fig. 25), induced in a cylindrical tank subject to horizontal earthquake motion is given by

$$d_{max} = \frac{0.204\ D_o \coth\left(3.68\ \frac{h_L}{D_o}\right)}{\frac{2g}{\omega_1^2\ \theta_h\ D_o} - 1.0} \qquad (5.6)$$

5.2.3 Base Shear and Overturning Moment

The hydrodynamic base shear for the structure, representing the total dynamic force (impulsive and convective) exerted by the liquid on the tank, may be determined by consideration of the simple mechanical analog illustrated in Fig. 27, and expressed by

$$(Q_i)_{max} = m_o \ddot{x} \tag{5.7}$$

and

$$(Q_c)_{max} = m_1 (S_a)_1 \tag{5.8}$$

where Q_i and Q_c represent the impulsive and convective components of base shear, respectively, m_o is the impulsive mass of liquid, m_1 is the convective mass of the liquid that participates in the first sloshing mode (analytical expressions for the model parameters m_o and m_1 are presented in table 25), $(S_a)_1$ is the spectral acceleration of the fundamental sloshing mass, and $\ddot{x}$ is the maximum ground acceleration.

The hydrodynamic overturning moment for the structure, representing the total dynamic force exerted by the liquid on the tank, may also be determined by consideration of the simple mechanical analog (Fig. 27). The impulsive $(M_{OTM})_i$ and convective $(M_{OTM})_c$ components of overturning moment, respectively, are given by

$$(M_{OTM})_i = m_o h_o \ddot{x} \tag{5.9}$$

and

$$(M_{OTM})_c = m_1 h_1 (S_a)_1 \tag{5.10}$$

where h_o and h_1 are the vertical distances measured from the tank bottom to the impulsive mass, m_o, and the mass of the first sloshing mode, m_1, respectively. In Table 25, where the analytical expressions for the various model parameters are presented, two expressions for h_o exist; h_o(IBP) and h_o(EBP), where the abbreviations IBP and EBP designate "including bottom pressure" and "excluding bottom pressure", respectively. For calculation of the impulsive hydrodynamic overturning moment, $(M_{OTM})_i$, by application of Eq. 5.9, h_o (IBP) must be used. Use of h_o(EBP) in Eq. 5.9 will result in the calculation of the maximum impulsive bending moment on a cross-section of the tank just above the base.

A conservative estimate of the absolute maximum value of the total hydrodynamic (impulsive and convective components) base shear and overturning moment may be obtained by taking the numerical sum calculated from Eqs. 5.7 and 5.8 for base shear, and Eqs. 5.9 and 5.10 for overturning moment. Using this approach it is assumed that the spectral acceleration of the sloshing fluid mass, $(S_a)_1$, and the maximum ground acceleration, $\ddot{x}$, occur simultaneously. More judicious methods for combining the modal maxima are prescribed in Ref. 17.

5.3 Impulsive Effects in Flexible Shell-Liquid Systems

In this section a simple procedure for determining the magnitude and distribution of hydrodynamic forces, and the subsequent shell stresses, induced in a flexible shell-liquid system subjected to horizontal earthquake ground motion is presented. The effects of

tank flexibility on impulsive base shear and overturning moment are also considered. The scope of the investigation is limited to tanks completely filled ($h_L/H_o = 1.0$) and partly filled ($h_L/H_o = 0.5$) with liquid.

Because the oscillations of the convective effects are dominated by natural frequencies much lower than those characterizing the impulsive effects (refer to Section 3.4), they cannot be appreciably affected by tank flexibility (Ref. 65). Therefore, it is anticipated that the convective effects in flexible tanks can be accurately assessed by the procedures applicable to rigid tanks (Refs. 27, 63 and 70).

5.3.1 Hydrodynamic Pressures

From the results of the present study, an expression governing the impulsive component of the hydrodynamic pressure exerted on the walls of a flexible tank is proposed. That expression is given by

$$p_i(z, \theta) = \{\rho_L \ddot{x} h_L[(1 - \frac{z}{h_L}) - \frac{1}{2}(1 - \frac{z}{h_L})^2] \sqrt{3} \tanh (\frac{\sqrt{3} D_o}{2hL}) + \rho_L [\psi(\frac{z}{H_o})] (S_a - \ddot{x}) h_L [1 - (\frac{z}{h_L})^2]\} \cos\theta \quad (5.11)$$

The first portion of the expression is recognized as Eq. 5.1, which governs the distribution of the impulsive wall pressure in a rigid tank. The second portion of the expression, developed in this study, represents the contribution of shell flexibility to the generation of hydrodynamic wall pressures.

Both the "rigid tank" and "flexible tank" components of Eq. 4.51 are functions of the dimensionless height parameter, z/h_L. The term $[1 - (z/h_L)^2]$, determined from the results of the free vibration analysis of liquid-filled tanks conducted in Chapter 3, governs the variation of the hydrodynamic pressure along the height of the tank. The term $\psi(z/H_o)$, which represents the tank defection configuration, determined fron an analytical examination of the mode shapes associated with the free vibration analyses conducted in Chapter 3, governs the variation of the wall acceleration along the height of the tank. The deflection configuration, $\psi(z/H_o)$ is given by

$$\psi(\frac{z}{H_o}) = \sin\ (\frac{\pi z}{2z_m}) \tag{5.12}$$

for $0 < \frac{z}{H_o} \leq \frac{z_m}{H_o}$, and

$$\psi(\frac{z}{H_o}) = \sin\ [\frac{\pi}{2}\ (\frac{1.0 - \frac{z}{H_o}}{1.0 - \frac{z_m}{H_o}})] \tag{5.13}$$

for $\frac{z_m}{H_o} < \frac{z}{H_o} \leq 1.0$.

The dimensionless parameter z_m/H_o represents the relative height of the tank at which the wall acceleration attains its maximum value. Values of z_m/H_o for tanks having an aspect ratio within the range 0.1 to 1.5, inclusive, and for liquid levels corresponding to h_L/H_o = 0.5 and h_L/H_o = 1.0 are presented in Table 26.

From a careful examination of Eq. 5.11, it is noted that the most significant distinction between the "flexible tank" contribution and the "rigid tank" contribution to hydrodynamic wall pressures

involves the nature of the acceleration component employed. In the "rigid tank" portion of Eq. 5.11 the hydrodynamic pressures are proportional to the maximum ground acceleration, $\ddot{x}$. In the "flexible tank" portion of Eq. 5.11 the hydrodynamic pressures are proportional to the maximum spectral acceleration, S_a. The spectral acceleration, S_a, is evaluated for the natural frequency of the flexible shell-fluid system, which may be determined from the appropriate expressions (Eqs. 3.34, 3.56 and 3.36) presented in Chapter 3. Depending on the value of this frequency and the design spectrum employed in the analysis, the spectral acceleration, S_a, may be substantially greater than the maximum ground acceleration, $\ddot{x}$, the value applicable to rigid tanks. It follows that the tank flexibility may increase significantly the impulsive component of the hydrodynamic effects (Ref. 65).

5.3.2 Shell Stresses in a Flexible Tank-Fluid System

As was previously stated in Section 4.4, the pertinent stress variables necessary for evaluating the seismic response of thin walled, cylindrical tanks subject to horizontal earthquake ground motion are the circumferential membrane stress resultant, N_θ, and the axial membrane stress resultant, N_z (refer to Fig. 44). The circumferential component of stress can be determined directly from the hydrodynamic impulsive wall pressure (which is governed by Eq. 5.11), and is expressed by the equation

$$N_\theta(z, \theta) = \frac{p_i(z, \theta)\, D_o}{2} \tag{5.14}$$

A typical distribution of the axial membrane stress resultant, N_z, along the height of the tank is represented in Fig. 50. A reasonable approximation of the maximum value of axial stress, which occurs at the base of the tank, can be obtained from the bending moment computed about a cross section at the base of the tank (Ref. 20). This bending moment at the tank base, M_{BM}, is given by

$$M_{BM} = m_o S_a h_o + m_s S_a \frac{H_o}{2} \tag{5.15}$$

where m_o is the impulsive fluid mass, m_s is the mass of the shell, h_o is the vertical distance from the bottom of the tank to the impulsive mass, H_o is the height of the tank, and S_a is the spectral acceleration of the flexible shell-fluid system. The model parameters m_o and h_o can be determined from the appropriate expressions presented in Table 25. When calculating M_{BM} from Eq. 5.15, h_o(EBP) must be used.

The maximum axial stress resultant, $(N_z)_{max}$, which occurs at the tank base (or at z = 0), can be determined from the relation given by

$$(N_z)_{max} = \frac{M_{BM} D_o h}{2I} \tag{5.16}$$

where I is the moment of inertia of the tank cross section about the diameter, and is equal to $\frac{\pi D_o^3 h}{8}$. Substitution of this value for I into Eq. 5.16 results in

$$(N_z)_{max} = \frac{4 M_{BM}}{\pi D_o^2} \tag{5.17}$$

The heightwise variation of the circumferential membrane stress, N_z, which is illustrated in Fig. 50, can be reasonably approximated in a conservative manner by the linear function $(1 - z/H_o)$. Therefore, the axial membrane stress resultant variable, $N_z(z)$, may be expressed as

$$N_z(z) = \frac{4\, M_{BM}\, (1 - \frac{z}{H_o})}{\pi D_o^{\,2}} \qquad (5.18).$$

A comparison of the N_z stress distribution described by Eq. 5.18 with the actual stress distribution is also illustrated in Fig. 50. It is noted that Eq. 5.18 will always yield a slightly conservative value for N_z.

5.3.3 Impulsive Base Shear and Overturning Moment

For liquid filled cylindrical tanks having an aspect ratio, H_o/D_o, within the range 0.1 to 1.5, a reasonable upper bound estimate of the absolute maximum hydrodynamic base shear due to horizontal earthquake ground motion may be obtained from the corresponding solution for a rigid tank. This is accomplished merely by replacing the maximum ground acceleration, $\ddot{x}$, in Eq. 5.7 with the spectral acceleration, S_a, corresponding to the fundamental natural frequency of the flexible shell-liquid system. The resulting expression for the total impulsive base shear (including the mass of the tank) in a flexible tank is given by

$$(Q_i)_{max} = (m_o + m_s)\, S_a \qquad (5.19)$$

where m_o is the mass of the impulsive liquid (refer to Table 24 for analytical expression for m_o) and m_s is the mass of the shell.

For values of H_o/D_o much greater than 0.5, this approach for calculating the maximum impulsive base shear (Eq. 5.19) is generally too conservative. This is so because the analytical expression for m_o (Table 25) tends to overestimate the impulsive fluid mass participating in the fundamental mode of vibration in that aspect ratio range. A more plausible estimate of the impulsive base shear for tanks having an aspect ratio and liquid depth ratio (h_L/D_o) greater than 0.5 can be made by effectively reducing the impulsive fluid mass, m_o. Based on the results of a study concerning the participation of the impulsive fluid mass in the first mode of vibration of the shell-liquid system (Ref. 65), a modified version of Eq. 5.19 is proposed. It is expected that more accurate results for impulsive base shear for liquid filled cylindrical tanks (where $h_L/H_o = 1.0$) having aspect ratios within the range $0.5 < H_o/D_o \leq 1.5$ can be attained by the expression given by

$$(Q_i)_{max} = m_o \left[1.1 - 0.2 \left(\frac{H_o}{D_o}\right)\right] S_a + m_s S_a \qquad (5.20)$$

Finally, a conservative estimate of the impulsive overturning moment for a flexible tank may also be obtained from the corresponding solution for a rigid tank. This may be accomplished simply by replacing the maximum ground acceleration, $\ddot{x}$, which appears in the expression applicable to rigid tanks (Eq. 5.9), by the spectral acceleration, S_a, corresponding to the flexible shell-liquid system.

Thus the expression governing the impulsive overturning moment in a flexible, cylindrical liquid storage tank is given by

$$(M_{OTM})_i = (m_o h_o + \frac{m_s H_o}{2}) S_a \qquad (5.21)$$

The model parameters m_o and h_o can be determined from the appropriate expressions presented in Table 25. In the calculation of $(M_{OTM})_i$ by Eq. 5.21, h_o(IBP) must be used.

5.3.4 Flow Diagram

To facilitate application of the procedures for the seismic analysis (impulsive effects) of cylindrical liquid storage tanks detailed in this chapter, a flow diagram is presented (Table 27). It is envisioned that expedient identification and implementation of the appropriate expressions developed in this chapter will be enhanced by it. One or more of the steps outlined in the flow chart may be omitted at the investigator's discretion.

5.3.5 Numerical Comparisons

To verify the accuracy of the expressions for seismic analysis developed in this section, numerical comparisons were made with the results of another investigation (Ref. 26). An example of both a tall tank and a shallow tank are analyzed. The physical characteristics of the open-top, shell-fluid systems under considerations are as follows:

(a) Tall Tank ($H_o/D_o = 1.5$)

H_o = 21.95 m (72 ft)

D_o = 14.63 m (48 ft)

h = 25.4 mm (1.0 in)

E_s = 206900.0 MN/m^2 (30,000 ksi)

ρ_s = 20.3 kg/m^3 (0.000733 $lb\text{-}sec^2/in^4$)

ν = 0.3

ρ_L = 2.6 kg/m^3 (0.000094 $lb\text{-}sec^2/in^4$)

h_L = 21.95 m (72 ft)

(b) Shallow Tank ($H_o/D_o = 0.333$)

H_o = 12.19 m (40 ft)

D_o = 36.58 m (120 ft)

E_s = 206900.0 MN/m^2 (30,000 ksi)

h = 25.4 mm (1.0 in)

ρ_s = 20.3 kg/m^3 (0.000733 $lb\text{-}sec^2/in^4$)

ν = 0.3

ρ_L = 2.6 kg/m^3 (0.000094 $lb\text{-}sec^2/in^4$)

h_L = 12.19 m (40 ft)

The input ground motion was the N-S component of the 1940 El Centro Earthquake. The maximum horizontal ground acceleration for this case was 0.348 g. The spectral acceleration, S_a, for the flexible shell-fluid systems were determined to be 0.858 g and 0.813 g, for the tall tank (f = 5.5 cps) and shallow tank (f = 6.23 cps), respectively (where g is the acceleration of gravity). The modal damping ratio for the shell-liquid systems was assumed to be 2% (Ref. 18).

A comparison of the impulsive hydrodynamic pressure at three locations along the tank height (located on a vertical plane defined by circumferential coordinate angle θ equal to 0^{o}) is presented in Table 28 for the tall tank. The results obtained by the present analysis are in close agreement with those obtained by the finite element method (Ref. 26). However, the impulsive hydrodynamic pressures calculated by the "rigid tank" approach are substantially less than those obtained by either the present analysis or the finite element method. At the tank's midheight, the impulsive hydrodynamic pressure was calculated to be more than 3 times greater for a flexible tank than for a rigid tank.

In Table 29 a similar comparison of the axial stress resultant, N_z, in a tall tank is made. Once again, the results from the present analysis are in close agreement with the results of the finite element analysis (Ref. 26). The unconservativeness of the rigid tank analysis is also made evident by this comparison. The maximum axial stress in a flexible tank (occurring at the base, z/H_o = 0.0), as determined by the present analysis, is approximately 2.5 times greater than that calculated for a rigid tank.

Comparisons of impulsive base shears and overturning moments in the tall tank are made in Table 30. Excellent correlations of the results obtained by the present analysis with those obtained by the finite element analysis (Ref. 26) are noted. However, the results for base shear and overturning moment obtained by the rigid tank analysis are unconservative by factors of 2.1 and 2.5, respectively.

In Table 31, numerical comparisons of the impulsive hydrodynamic wall pressures in the shallow tank are made. Once again, excellent agreement of the results obtained in the present study with those of Ref. 26 is cited. The pressures calculated by the "rigid tank" theory are consistently unconservative by a factor of 2 or more.

Finally, the numerical results of maximum impulsive axial stress, base shear, and overturning moment for the case of the shallow tank are presented in Table 32. Excellent correlation with the results of the present study and the finite element investigation (Ref. 26) is again noted. However, the values for axial stress, base shear and overturning moment calculated by the methods developed in the present study exceed those obtained by the "rigid tank" procedure by factors of 2.3, 2.4 and 2.5 respectively.

The numerical comparisons described in the foregoing validate the accuracy of the simplified procedures for the seismic analysis of liquid-filled cylindrical tanks developed in this investigation. These comparisons also illustrate the unconservativeness of the "rigid tank" analysis procedures which are currently employed by many practicing engineers.

6. SUMMARY AND CONCLUSIONS

6.1 Summary and Conclusions

The reported investigation, dealing with the dynamic behavior of cylindrical liquid storage tanks, was conducted in four separate, but related phases:

1. Vibrational Characteristics of Empty Cylindrical Storage Tanks.
2. Vibrational Characteristics of Liquid-filled Cylindrical Storage Tanks.
3. Seismic Analysis of Empty Cylindrical Storage Tanks.
4. Seismic Analysis of Liquid-filled Cylindrical Storage Tanks.

The results of the study pertaining to the vibrational characteristics of empty cylindrical tanks were presented in Chapter 2. Special emphasis was assigned to the tank free vibration aspects asssociated with a circumferential wave number, n, equal to one and an axial wave number, m, also equal to one. Simple analytical expressions, in the form of cubic polynomials, which accurately predict the natural frequencies and radial mode shapes affiliated with the n = 1, m = 1 mode were developed. Since the nature of the vibration of this mode (n = 1, m = 1) is primarily extensional,

it was concluded that the natural frequency of the system is independent of the shell wall thickness.

The free vibration study concerning empty tanks was extended to include tanks having a roof structure. The roof system was represented in the shell model by an equivalent circular plate continuously connected at its periphery to the top of the cylinder. The results of this aspect of the study indicated that the primary effect of the roof structure upon the vibrational characteristics of the shell system was a reduction in natural frequency. The obvious explanation for this phenomenon is that the addition of a roof structure increases the total mass of the system but at the same time contributes negligibly to the stiffness of the system. Moreover, the reduction in frequency due to the addition of a roof structure was more substantial for shallow tanks than for tall tanks. The reason for this response was attributed to the fact that the roof structure in a shallow tank represents a relatively greater portion of the total mass of the tank than does a similar roof structure in a tall tank. Finally, simple analytical expressions were also developed which accurately predict the natural frequency ($n = 1$, $m = 1$) and mode shape of tanks having a roof structure.

The effect of boundary conditions upon the vibrational characteristics of empty cylindrical storage tanks was also examined in Chapter 2. The results of a finite element study indicated that the basic consequence of noncontinuous (i.e. discrete support points) boundary conditions at the base of the tank upon the free vibration

of the system is a coupling of the n = 1 mode with higher order (i.e. n > 1) circumferential modes. The greater the deviation from the ideal, continuous boundary conditions at the base of the tank, the more prevalent was the mode coupling phenomenon (or the influence of higher circumferential modes upon the free vibration of the shell).

In Chapter 3 the results of the investigation concerning the free vibration of liquid-filled cylindrical storage tanks were presented. The shell-liquid system was considered to consist of two separate systems:

1. The shell structure together with a stationary fluid mass
2. The sloshing fluid mass

From the results of the free vibration study it was concluded that the vibration of the sloshing fluid mass was unaffected by the vibration of the shell and stationary mass, and vice versa. It was also concluded that the vibration of the sloshing fluid mass was insensitive to shell flexibility.

Simple analytical expressions, in the form of cubic polynomials, which accurately determine the natural frequency (corresponding to the m = 1, n = 1 mode) of the flexible shell together with the stationary fluid mass were developed in Chapter 3. The fundamental natural frequency of the sloshing fluid mass (in flexible containers), it was concluded, can be accurately determined from the existing expressions applicable to rigid containers.

In Chapter 4 simplified procedures for conducting a seismic analysis (by the response spectrum technique) of empty cylindrical storage tanks were presented. The results of the free vibration studies of empty tanks, described in Chapter 2, form the basis of these seismic analysis procedures. For the simplified analysis, the empty tanks were idealized as continuous, single-degree-of-freedom systems. However, the pertinent vibrational parameters (such as generalized force, generalized mass, and mode participation factor) were defined and calculated with the use of shell theory, rather than from equivalent lumped-mass or beam models, thus assuring the accuracy of the procedures. Simple analytical expressions, in the form of cubic and quadratic polynomials, were developed which accurately predict shell stresses, shell displacements, base shears and overturning moments induced in empty cylindrical storage tanks (both with and without a roof structure) by horizontal earthquake ground motion.

Simplified procedures for conducting a seismic (response spectrum) analysis of flexible, liquid-filled cylindrical storage tanks were presented in Chapter 5. Both totally full and half full liquid storage tanks were considered. The hydrodynamic pressures developed when a fluid container is subjected to horizontal accelerations were separated into impulsive and convective parts, and were treated independently. The convective pressures, which are those produced by the oscillations of the sloshing fluid mass, can be

accurately determined from the existing expressions applicable to rigid containers.

Simple analytical expressions, applicable to both completely full and half full tanks, which accurately determine impulsive hydrodynamic wall pressures, shell stresses, base shear, and overturning moment were developed for cylindrical tanks subjected to horizontal earthquake ground motion. Favorable numerical comparisons for several case studies of the results obtained from the present study with those obtained in other investigations were made, thus verifying the accuracy of the simplified procedures. These numerical comparisons also illustrated the unconservativeness of the "rigid tank" procedures currently employed by many practicing engineers.

6.2 Recommendations for Future Research

The results of the investigations into the vibrational characteristics and seismic analysis of cylindrical liquid storage tanks presented in this dissertation are by no means final or complete. To the contrary, the findings of the investigation reported herein indicate several aspects of the subject area which warrant further study. It is recommended that research be continued or initiated on the following topics:

1. The effect of roof structure on the vibration of shallow, liquid-filled cylindrical tanks. Since the greater portion of the liquid mass in shallow tanks participates in sloshing, the mass of the roof

structure may have significant impact on the natural frequency of the shell-liquid system.

2. The effect of roof structure on the higher order ($n > 1$) circumferential modes of vibration which have been found to be excited when the boundary conditions at the base of the tank deviate from the ideal, continuous condition.
3. Additional studies on the effect of base boundary conditions on the vibrational characteristics of cylindrical tanks is needed. The relationship between mode coupling and natural frequency with the number of discrete support locations for any particular cylindrical tank is yet to be determined.
4. The performance of anchor bolts on cylindrical tanks during past earthquakes has been poor. The localized stress conditions which develop in the tank wall in the vicinity of anchors, which attach the tank to its foundation, of liquid storage tanks subject to horizontal ground motion is an area in which no research information exists to date. Obviously this is another area in need of future investigations.

5. The effect of the roof structure on the response of liquid filled tanks where the freeboard is less than the sloshing height warrants investigation. In this case the sloshing action of the convective fluid mass is restricted and thus could alter and complicate the overall response of the shell-fluid system. Also, significant hydrodynamic pressures against the roof structure would develop in this situation which would undoubtedly affect design recommendations for the tank roof.

Research into the aforementioned topics will undoubtedly result in a better understanding of the vibrational characteristics of cylindrical liquid storage tanks, and lead to the development of new and more realistic analysis and design procedures.

TABLE 1

CUBIC POLYNOMIAL COEFFICIENTS FOR NATURAL FREQUENCY

(OPEN TOP TANKS)

C_1	C_2	C_3	C_4	RANGE
1.01233	0.262992	- 4.10171	3.76038	$0.1 \leq \frac{H_o}{D_o} < 0.65$
1.08245	- 1.34536	0.686224	- 0.128323	$0.65 \leq \frac{H_o}{D_o} \leq 1.5$

$$\bar{f} = C_1 + C_2 \left(\frac{H_o}{D_o}\right) + C_3 \left(\frac{H_o}{D_o}\right)^2 + C_4 \left(\frac{H_o}{D_o}\right)^3 \qquad (2.38)$$

TABLE 2

NUMERICAL COMPARISONS - NATURAL FREQUENCY

(OPEN TOP TANK)

H_o = 25.92 m (40 ft) E_s = 206,900 MN/m^2 (30,000 ksi)

D_o = 36.58 m (120 ft) ρ_s = 20.3 Kg/m^3 (0.000733 $lb\text{-}sec^2/in^4$)

h = 25.4 mm (1.0 in) ν = 0.3

(NATURAL FREQUENCY IN CPS FOR n = 1, m = 1 MODE)

Present Analysis	Ref. 20	Ref. 67	Ref. 26	Ref. 68
34.29	34.03	34.08	34.04	34.66

TABLE 3

MAXIMUM NORMALIZED SHELL DISPLACEMENT COMPONENTS

OCCURRING AT $z/H_o = 1.0$

$\frac{H_o}{D_o}$	u	v	w
0.1	.036	.0428	1.0
0.2	.0713	.166	1.0
0.3	.109	.355	1.0
0.4	.140	.533	1.0
0.5	.164	.666	1.0
0.6	.185	.759	1.0
0.7	.202	.822	1.0
0.8	.215	.866	1.0
0.9	.226	.897	1.0
1.0	.233	.920	1.0
1.1	.238	.937	1.0
1.2	.242	.950	1.0
1.3	.243	.960	1.0
1.4	.243	.968	1.0
1.5	.242	.974	1.0

TABLE 4

CUBIC POLYNOMIAL COEFFICIENTS FOR FUNDAMENTAL VERTICAL MODE

RADIAL DISPLACEMENT VARIABLE $\bar{w}$ (OPEN TOP TANKS)

i	A_1	A_2	A_3	A_4	RANGE
1	-0.089975	0.798316	- 1.32103	0.725883	$0.1 \leq \frac{H_o}{D_o} \leq 0.7$
	0.139783	-0.149235	0.08672	- 0.020660	$0.7 < \frac{H_o}{D_o} \leq 1.5$
2	2.21298	-2.498860	3.75593	- 2.859850	$0.1 \leq \frac{H_o}{D_o} \leq 0.7$
	1.823820	-0.538976	- 0.314666	0.139689	$0.7 < \frac{H_o}{D_o} \leq 1.5$
3	-2.28703	5.258140	- 4.64918	1.79064	$0.1 \leq \frac{H_o}{D_o} \leq 0.9$
	-2.76497	4.58248	- 2.18674	0.405458	$0.9 < \frac{H_o}{D_o} \leq 1.5$
4	0.95334	0.260315	-13.5113	18.5019	$0.1 \leq \frac{H_o}{D_o} \leq 0.5$
	0.184601	-0.504041	0.0826718	0.003546	$0.5 < \frac{H_o}{D_o} \leq 1.5$

$$C_i = A_{1i} + A_{2i} \left(\frac{H_o}{D_o}\right) + A_{3i} \left(\frac{H_o}{D_o}\right)^2 + A_{4i} \left(\frac{H_o}{D_o}\right)^3, \quad i = 1, 2, 3, 4 \qquad (2.42)$$

$$\bar{\bar{w}} \left(\frac{z}{H_o}\right) = C_1 + C_2 \left(\frac{z}{H_o}\right) + C_3 \left(\frac{z}{H_o}\right)^2 + C_4 \left(\frac{z}{H_o}\right)^3, \quad 0 \quad \frac{z}{H_o} \leq 1.0 \qquad (2.41)$$

$$\bar{w} \left(\frac{z}{H_o}\right) = \bar{\bar{w}} \left(\frac{z}{H_o}\right) C_w \quad \text{where} \quad \left(C_w = 1.0 / \sum_{i=1}^{4} C_i\right) \qquad (2.43)$$

TABLE 5

NUMERICAL COMPARISONS - FUNDAMENTAL VERTICAL MODE SHAPE

(RADIAL DISPLACEMENT w)

$\frac{z}{H_o}$	Present Analysis	Ref. 26	Ref. 67
0.1	.2186	.2245	.2242
0.2	.3615	.3765	.3773
0.3	.4874	.4920	.4920
0.4	.5973	.6035	.6036
0.5	.6927	.7052	.7054
0.6	.7750	.7946	.7949
0.7	.8456	.8699	.8702
0.8	.9056	.9294	.9298
0.9	.9567	.9716	.9720
1.0	1.0000	1.0000	1.0000

TABLE 6

CUBIC POLYNOMIAL COEFFICIENTS FOR NATURAL FREQUENCY

(TANKS WITH ROOF STRUCTURE)

K_r = Roof Mass Coefficient

K_r	C_1	C_2	C_3	C_4	RANGE
1.0	0.786567	- 1.17223	1.07850	- 0.514795	$0.1 \leq \frac{H_o}{D_o} \leq 0.65$
	0.74771	- 0.90676	0.492937	- 0.104452	$0.65 < \frac{H_o}{D_o} \leq 1.5$
2.0	0.723751	- 1.34884	1.51371	- 0.751037	$0.1 \leq \frac{H_o}{D_o} \leq 0.65$
	0.60062	- 0.710395	0.388042	- 0.0841134	$0.65 \leq \frac{H_o}{D_o} \leq 1.5$
3.0	0.689968	- 1.54628	2.05999	- 1.12655	$0.1 \leq \frac{H_o}{D_o} \leq 0.65$
	0.513494	- 0.587046	0.307777	- 0.0632645	$0.65 < \frac{H_o}{D_o} \leq 1.5$

$$\overline{f} = C_1 + C_2 \left(\frac{H_o}{D_o}\right) + C_3 \left(\frac{H_o}{D_o}\right)^2 + C_4 \left(\frac{H_o}{D_o}\right)^3 \qquad (2.38)$$

$$K_r = 4 \frac{m_r}{m_c} \frac{H_o}{D_o} \qquad (2.48)$$

m_r = mass of tank roof and supporting structure

m_c = mass of tank cylinder

H_o = height of tank

D_o = diameter of tank

TABLE 7 (a)

CUBIC POLYNOMIAL COEFFICIENTS FOR FUNDAMENTAL VERTICAL MODE

RADIAL DISPLACEMENT VARIABLE $\bar{w}$

(Tanks with Roof Structure, $K_r = 1.0$)

i	A_1	A_2	A_3	A_4	RANGE
1	-0.0806288	- 0.305919	- 0.661456	0.734952	$0.1 \le \frac{H_o}{D_o} \le 0.5$
	-0.157613	0.496401	- 0.419872	0.113917	$0.5 \le \frac{H_o}{D_o} \le 1.5$
2	2.13641	- 9.80437	39.1597	-43.5108	$0.1 \le \frac{H_o}{D_o} \le 0.5$
	2.65479	- 2.9480	1.90195	- 0.515507	$0.5 \le \frac{H_o}{D_o} \le 1.5$
3	-4.43301	19.0397	-62.3857	69.3175	$0.1 \le \frac{H_o}{D_o} \le 0.5$
	-5.78996	10.8499	- 6.67043	1.36473	$0.5 \le \frac{H_o}{D_o} \le 1.5$
4	3.33493	- 8.75453	20.7375	-23.0417	$0.1 \le \frac{H_o}{D_o} \le 0.5$
	4.49493	- 9.47946	6.66519	- 1.56211	$0.5 \le \frac{H_o}{D_o} \le 1.5$

$$C_1 = A_{1i} + A_{2i} \left(\frac{H_o}{D_o}\right) + A_{3i} \left(\frac{H_o}{D_o}\right) + A_{4i} \left(\frac{H_o}{D_o}\right)^3, \quad i = 1, 2, 3, 4 \tag{2.42}$$

$$\bar{\bar{w}} \left(\frac{z}{H_o}\right) = C_1 + C_2 \left(\frac{z}{H_o}\right) + C_3 \left(\frac{z}{H_o}\right)^2 + C_4 \left(\frac{z}{H_o}\right)^3 \tag{2.41}$$

$$\bar{w} \left(\frac{z}{H_o}\right) = \bar{\bar{w}} \left(\frac{z}{H_o}\right) C_w \quad \text{where} \quad \left(C_w = 1.0 / \sum_{i=1}^{4} C_i\right) \tag{2.43}$$

TABLE 7 (b)

CUBIC POLYNOMIAL COEFFICIENTS FOR FUNDAMENTAL VERTICAL MODE

RADIAL DISPLACEMENT VARIABLE $\overline{w}$

(Tanks with Roof Structure, $K_r = 2.0$)

i	A_1	A_2	A_3	A_4	RANGE
1	0.0830497	- 1.314960	4.828940	5.255215	$0.1 \leq \frac{H_o}{D_o} \leq 0.5$
	-0.0794525	0.313819	0.320369	0.103063	$0.5 < \frac{H_o}{D_o} \leq 1.5$
2	-1.112680	20.352000	-48.378000	36.336700	$0.1 \leq \frac{H_o}{D_o} \leq 0.5$
	2.0787270	- 1.581730	1.018400	- 0.359951	$0.5 < \frac{H_o}{D_o} \leq 1.5$
3	3.7241200	-46.806300	117.415000	89.121700	$0.1 \leq \frac{H_o}{D_o} \leq 1.5$
	-2.7532500	2.7705	- 0.225263	- 0.258464	$0.5 < \frac{H_o}{D_o} \leq 1.5$
4	-1.2752700	24.1728	-63.738200	48.406300	$0.1 \leq \frac{H_o}{D_o} \leq 0.5$
	1.6724500	- 1.3582	- 0.521523	0.504622	$0.5 < \frac{H_o}{D_o} \leq 1.5$

$$C_i = A_{1i} + A_{2i} \left(\frac{H_o}{D_o}\right) + A_{3i} \left(\frac{H_o}{D_o}\right)^2 + A_{4i} \left(\frac{H_o}{D_o}\right)^3, \quad i = 1, 2, 3, 4 \qquad (2.42)$$

$$\overline{w}\left(\frac{z}{H_o}\right) = C_1 + C_2 \left(\frac{z}{H_o}\right) + C_3 \left(\frac{z}{H_o}\right)^2 = C_4 \left(\frac{z}{H_o}\right)^3, \quad 0 < \frac{z}{H_o} \leq 1.0 \qquad (2.41)$$

$$\overline{w}\left(\frac{z}{H_o}\right) = \overline{\overline{w}}\left(\frac{z}{H_o}\right) C_w \quad \text{where} \quad \left(C_w = 1.0 / \sum_{i=1}^{4} C_i\right) \qquad (2.43)$$

TABLE 7 (c)

CUBIC POLYNOMIAL COEFFICIENTS FOR FUNDAMENTAL VERTICAL MODE

RADIAL DISPLACEMENT VARIABLE $\overline{w}$

(Tanks with Roof Structure, $K_r = 3.0$)

i	A_1	A_2	A_3	A_4	RANGE
1	0.1019380	1.620500	6.297910	7.233600	$0.1 \leq \frac{H_o}{D_o} \leq 0.4$
	-0.0951424	0.388558	- 0.416326	0.139522	$0.4 < \frac{H_o}{D_o} \leq 1.5$
2	-0.39744	14.498500	-33.773500	24.543300	$0.1 \leq \frac{H_o}{D_o} \leq 0.5$
	2.09972	1.910130	1.477480	- 0.542978	$0.5 < \frac{H_o}{D_o} \leq 1.5$
3	2.52294	-34.172000	84.48100	-63.313300	$0.1 < \frac{H_o}{D_o} \leq 0.5$
	-5.90120	15.801400	-16.4294	5.992700	$0.5 < \frac{H_o}{D_o} \leq 1.5$
4	-0.928958	18.5036	-48.1153	36.512000	$0.1 \leq \frac{H_o}{D_o} \leq 0.5$
	3.13965	- 7.61006	7.32423	- 2.498780	$0.5 < \frac{H_o}{D_o} \leq 1.5$

$$C_i = A_{1i} + A_{2i} \left(\frac{H_o}{D_o}\right) + A_{3i} \left(\frac{H_o}{D_o}\right)^2 + A_{4i} \left(\frac{H_o}{D_o}\right)^3 \quad i = 1, 2, 3, 4 \tag{2.42}$$

$$\overline{w} \left(\frac{z}{H_o}\right) = C_1 + C_2 \left(\frac{z}{H_o}\right) + C_3 \left(\frac{z}{H_o}\right)^2 + C_4 \left(\frac{z}{H_o}\right)^3 \quad 0 < \frac{z}{H_o} \leq 1.0 \tag{2.41}$$

$$\overline{w} \left(\frac{z}{H_o}\right) = \overline{\overline{w}} \left(\frac{z}{H_o}\right) C_w \quad \text{where } \left(C_w = 1.0 / \sum_{i=1}^{4} C_i\right) \tag{2.43}$$

TABLE 8

NATURAL FREQUENCIES FOR COS nθ MODES (m = 1)

(Open Top Tank)

H_o = 9.14 m (30 ft) E_s = 206,900 MN/m^2 (30,000 ksi)

D_o = 9.14 m (30 ft) ρ_s = 20.3 kg/m^3 (0.000733 $lb\text{-}sec^2/in^4$)

h = 4.76 mm (0.1875 in) ν = 0.3

Circumferential Wave (n)	Natural Frequency (cps)
1	51.58
2	25.7
3	14.18
4	8.746
5	5.97
6	4.58
7	4.109
8	4.284
9	4.897
10	5.789

TABLE 9

EFFECT OF BOUNDARY CONDITIONS UPON NATURAL FREQUENCY OF CYLINDRICAL TANK (Axial Wave m = 1)

Boundary Case	Circumferential Wave	Frequency (cps)
1	1	51.47
2	4 - 5	39.90
3	5	31.00
4	5	16.40

TABLE 10

MODEL PARAMETERS FOR CYLINDRICAL TANK

(Simple Model - Refer to Fig. 27)

$$m_T = \frac{1}{4} \rho_L \pi D_o^2 h_L$$

$$m_1 = m_T \left(\frac{D_o}{4.4\ h_L}\right) \tanh\ (3.68 \frac{h_L}{D_o})$$

$$m_o = m_T - m_1$$

$$K_1 = m_T \left(\frac{g}{1.19\ h_L}\right) [\tanh\ (3.68 \frac{h_L}{D_o})]^2$$

$$\ell_1 = \frac{D_o}{3.68} \tanh\ (3.68 \frac{h_L}{D_o})$$

$$\ell_o = \frac{m_T}{m_o} \left[\frac{h_L}{2} - \frac{D_o^2}{8\ h_L}\right] - \ell_1 \frac{m_1}{m_o}$$

$$h_1 = h_L - \ell_1$$

$$h_o = h_L - \ell_o$$

where,

ρ_L = mass density of liquid in tank

g = acceleration of gravity

D_o = diameter of tank

h_L = height of liquid in tank

TABLE 11

NATURAL FREQUENCIES FOR A TALL FLUID FILLED TANK

	Present Analysis	(Ref. 26)
Coupled Shell-m_o System	3.69 cps	3.56 cps
Sloshing Fluid Mass m_1	0.2503 cps	0.2497 cps

where

H_o = 21.95 m (72 ft) $\quad$ E = 206900 MN/m^2 (30,000 ksi)

D_o = 14.63 m (48 ft) $\quad$ ρ_s = 20.3 kg/m^3

h = 10.92 mm (0.43 in) $\quad$ ρ_L = 2.6 kg/m^3

ν = 0.3 $\quad$ h_L = 14.63 m (48 ft)

TABLE 12

EFFECT OF STATIONARY AND SLOSHING FLUID MASSES ON NATURAL FREQUENCY OF A TALL CYLINDRICAL TANK

System	Frequency (rad/sec)
Sloshing mass m_1	1.57
Shell m_o (coupled)	23.208
Shell m_o (uncoupled)	23.1849
Empty Shell	120.5

TABLE 13

FUNDAMENTAL SLOSHING FREQUENCY IN A TALL CYLINDRICAL TANK

System	Frequency (cps)
Flexible Tank	0.2503
Rigid Tank	0.2505

TABLE 14

CUBIC POLYNOMIAL COEFFICIENTS FOR NATURAL FREQUENCY

(Tank Full with Liquid; $\frac{h_L}{H_o} = 1.0$)

$$\bar{f}\left(\frac{H_o}{D_o}\right) = C_1 + C_2\,(H_o/D_o) + C_3\,(H_o/D_o)^2 + C_4\,(H_o/D_o)^3$$

C_1	C_2	C_3	C_4	RANGE
0.801874	- 5.76702	17.4727	- 17.9596	$0.1 \leq \frac{H_o}{D} \leq 0.4$
0.256054	- 0.316141	0.148879	- 0.0242073	$0.4 < \frac{H_o}{D_o} \leq 1.5$

TABLE 15

CUBIC POLYNOMIAL COEFFICIENTS FOR NATURAL FREQUENCY

(Tank Half Full with Liquid; $\frac{h_L}{H_o} = 0.5$)

$$\bar{f}\left(\frac{H_o}{D_o}\right) = C_1 + C_2\,(H_o/D_o) + C_3\,(H_o/D_o)^2 + C_4\,(H_o/D_o)^3$$

C_1	C_2	C_3	C_4	RANGE
1.76195	- 14.0309	44.9335	- 48.4143	$0.1 \leq \frac{H_o}{D_o} \leq 0.4$
0.369341	- 0.401425	0.215224	- 0.049211	$0.4 < \frac{H_o}{D_o} \leq 1.5$

TABLE 16

NATURAL FREQUENCIES OF A WATER FILLED SHALLOW CYLINDRICAL TANK

H_o = 12.19 m (40 ft) $\quad \nu = 0.3$

D_o = 36.58 m (120 ft) $\quad E = 206900\ MN/m^2$ (30,000 ksi)

h = 25.4 mm (1 in) $\quad \rho = 203\ kg/m^3$ (0.000733 lb-sec^2/in^4)

Water Depth, h_L/H_o	Natural Frequency (cps)		
	Ref. (26)	(Ref. (20)	Present Analysis
1.0	6.18	6.20	6.23
0.5	9.88	---	9.70
0	34.04	34.03	34.29

TABLE 17

NATURAL FREQUENCIES OF A WATER FILLED TALL CYLINDRICAL TANK

H_o = 21.95 m (72 ft) $\quad E = 206900\ MN/m^2$ (30,000 ksi)

D_o = 14.63 m (48 ft) $\quad \rho = 20.3\ kg/m^3$ (0.000733 lb-sec^2/in^4)

Water Depth h_L/H_o	Shell Wall Thickness, h	Natural Frequency (cps)	
		Ref. (26)	Present Analysis
1.0	25.4 mm (1.0 in)	5.31	5.43
1.0	10.82 mm (0.43 in)	3.56	3.63
1.0	7.315 mm (0.288 in)	2.93	2.97
0.5	25.4 mm (1.0 in)	11.42	11.492
0.5	10.92 mm (0.43 in)	--	9.18
0.5	7.315 mm (0.288 in)	--	7.67
0	---	19.26	19.18

TABLE 18

CUBIC POLYNOMIAL COEFFICIENTS FOR MODAL PARTICIPATION FACTOR, $\overline{\Gamma}$

(OPEN-TOP TANKS)

C_1	C_2	C_3	C_4	RANGE
0.0684453	0.0896858	0.0994536	0.0055273	$0.1 \leq \frac{H_o}{D_o} \leq 1.5$

$$\overline{\Gamma} = C_1 + C_2 \left(\frac{H_o}{D_o}\right) + C_3 \left(\frac{H_o}{D_o}\right)^2 + C_4 \left(\frac{H_o}{D_o}\right)^3 \qquad (4.34)$$

TABLE 19

CUBIC POLYNOMIAL COEFFICIENTS FOR MODAL PARTICIPATION FACTOR

(TANKS WITH ROOF STRUCTURE)

K_r - Roof Mass Coefficient

K_r	C_1	C_2	C_3	C_4	RANGE
1.0	0.0339638	0.245286	- 0.0366713	0.0531889	$0.1 \leq \frac{H_o}{D_o} \leq 1.5$
2.0	0.040868	0.040868	- 0.0705786	0.05515	$0.1 \leq \frac{H_o}{D_o} \leq 1.5$
3.0	0.0558758	0.290178	- 0.0470643	0.0553761	$0.1 \leq \frac{H_o}{D_o} \leq 1.5$

$$\overline{\Gamma} = C_1 + C_2 \left(\frac{H_o}{D_o}\right) + C_3 \left(\frac{H_o}{D_o}\right)^2 + C_4 \left(\frac{H_o}{D_o}\right)^3 \qquad (4.34)$$

TABLE 20

QUADRATIC POLYNOMIAL COEFFICIENTS FOR AXIAL STRESS VARIABLE $\overline{\overline{N}}_z$

(OPEN-TOP TANKS)

i	A_1	A_2	A_3	RANGE
1	- 0.442257	4.18610	- 2.97839	$0.1 \leq \frac{H_o}{D_o} \leq 0.7$
	1.38914	- 0.453727	0.00377905	$0.7 < \frac{H_o}{D_o} \leq 1.5$
2	0.714654	- 6.60974	4.55015	$0.1 \leq \frac{H_o}{D_o} \leq 0.7$
	- 2.26655	0.740323	- 0.008797	$0.7 < \frac{H_o}{D_o} \leq 1.5$
3	- 0.266922	2.37431	- 1.55248	$0.1 \leq \frac{H_o}{D_o} \leq 0.7$
	0.858539	- 0.289564	0.00815617	$0.7 < \frac{H_o}{D_o} \leq 1.5$

$$C_i = A_{1i} + A_{2i} \left(\frac{H_o}{D_o}\right) + A_{3i} \left(\frac{H_o}{D_o}\right)^2, \quad i = 1, 2, 3 \qquad (4.38)$$

$$\overline{\overline{N}}_z \left(\frac{z}{H_o}\right) = C_1 + C_2 \left(\frac{z}{H_o}\right) + C_3 \left(\frac{z}{H_o}\right)^2, \quad 0 < \frac{z}{H_o} \leq 1.0 \qquad (4.37)$$

TABLE 21

QUADRATIC POLYNOMIAL COEFFICIENTS FOR CIRCUMFERENTIAL STRESS VARIABLE $\overline{\overline{N}}_\theta$

(OPEN-TOP TANKS)

i	A_1	A_2	A_3	RANGE
1	0.191939	- 0.547297	0.442259	$0.1 \leq \frac{H_o}{D_o} \leq 0.6$
	0.0511747	- 0.0731962	0.0261525	$0.6 < \frac{H_o}{D_o} \leq 1.5$
2	0.978298	0.12189	- 2.05627	$0.1 \leq \frac{H_o}{D_o} \leq 0.6$
	0.767036	- 0.938242	0.291029	$0.6 < \frac{H_o}{D_o} \leq 1.5$
3	0.0650312	- 1.86341	2.64265	$0.1 \leq \frac{H_o}{D_o} \leq 0.6$
	- 0.344946	0.499699	- 0.180198	$0.6 < \frac{H_o}{D_o} \leq 1.5$

$$C_i = A_{1i} + A_{2i} \left(\frac{H_o}{D_o}\right) + A_{3i} \left(\frac{H_o}{D_o}\right)^2, \quad i = 1, 2, 3 \qquad (4.38)$$

$$\overline{\overline{N}}_\theta \left(\frac{z}{H_o}\right) = C_1 + C_2 \left(\frac{z}{H_o}\right) + C_3 \left(\frac{z}{H_o}\right)^2, \quad 0.2 < \frac{z}{H_o} \leq 1.0 \qquad (4.37)$$

TABLE 22(a)

QUADRATIC POLYNOMIAL COEFFICIENTS FOR AXIAL STRESS VARIABLE $\overline{\overline{N}}_z$

TANKS WITH ROOF STRUCTURE, $K_r = 1.0$

i	A_1	A_2	A_3	RANGE
1	0.265048	2.6922	- 2.31527	$0.1 \leq \frac{H_o}{D_o} \leq 0.6$
	1.12862	0.0138629	- 0.21145	$0.6 < \frac{H_o}{D_o} \leq 1.5$
2	- 0.165426	- 3.43119	2.49912	$0.1 \leq \frac{H_o}{D_o} \leq 0.6$
	- 1.46742	0.0583485	0.173056	$0.6 < \frac{H_o}{D_o} \leq 1.5$
3	- 0.103181	0.847816	- 0.388429	$0.1 \leq \frac{H_o}{D_o} \leq 0.6$
	0.211874	0.159939	- 0.066615	$0.6 < \frac{H_o}{D_o} \leq 1.5$

$$C_i = A_{1i} + A_{2i} \left(\frac{H_o}{D_o}\right) + A_{3i} \left(\frac{H_o}{D_o}\right)^2, \quad i = 1, 2, 3 \qquad (4.38)$$

$$\overline{\overline{N}}_z \left(\frac{z}{H_o}\right) = C_1 + C_2 \left(\frac{z}{H_o}\right) + C_3 \left(\frac{z}{H_o}\right)^2, \quad 0 < \frac{z}{H_o} \leq 1.0 \qquad (4.37)$$

TABLE 22(b)

QUADRATIC POLYNOMIAL COEFFICIENTS FOR AXIAL STRESS VARIABLE $\overline{\overline{N}}_z$

TANK WITH ROOF STRUCTURE, $K_r = 2.0$

i	A_1	A_2	A_3	RANGE
1	0.478068	2.48205	- 2.37272	$0.1 \leq \frac{H_o}{D_o} \leq 0.6$
	1.29212	- 0.24022	- 0.12052	$0.6 < \frac{H_o}{D_o} \leq 1.5$
2	- 0.431494	- 2.98807	2.67065	$0.1 \leq \frac{H_o}{D_o} \leq 0.6$
	- 1.23845	- 0.190285	0.288065	$0.6 < \frac{H_o}{D_o} \leq 1.5$
3	- 0.019253	0.395888	- 0.130243	$0.1 \leq \frac{H_o}{D_o} \leq 0.6$
	0.0111039	0.346697	- 0.141286	$0.6 < \frac{H_o}{D_o} \leq 1.5$

$$C_i = A_{1i} + A_{2i} \left(\frac{H_o}{D_o}\right) + A_{3i} \left(\frac{H_o}{D_o}\right)^2, \quad i = 1, 2, 3 \qquad (4.38)$$

$$\overline{\overline{N}}_z = C_1 + C_2 \left(\frac{z}{H_o}\right) + C_3 \left(\frac{z}{H_o}\right)^2, \qquad 0 < \frac{z}{H_o} \leq 1.0 \qquad (4.37)$$

TABLE 22(c)

QUADRATIC POLYNOMIAL COEFFICIENTS FOR AXIAL STRESS VARIABLE $\bar{\bar{N}}_z$

TANKS WITH ROOF STRUCTURE, $K_r = 3.0$

i	A_1	A_2	A_3	RANGE
1	0.608212	2.57544	- 3.05494	$0.1 \leq \frac{H_o}{D_o} \leq 0.5$
	1.36414	- 0.370922	- 0.0642124	$0.5 < \frac{H_o}{D_o} \leq 1.5$
2	- 0.557884	- 3.1266	3.6894	$0.1 \leq \frac{H_o}{D_o} \leq 0.5$
	- 1.39594	0.198098	0.117251	$0.5 < \frac{H_o}{D_o} \leq 1.5$
3	- 0.033353	0.542025	- 0.618857	$0.1 \leq \frac{H_o}{D_o} \leq 1.5$
	- 0.00627	0.291839	- 0.119137	$0.5 < \frac{H_o}{D_o} \leq 1.5$

$$C_i = A_{1i} + A_{2i} \left(\frac{H_o}{D_o}\right) + A_{3i} \left(\frac{H_o}{D_o}\right)^2, \quad i = 1, 2, 3 \quad (4.38)$$

$$\bar{\bar{N}}_z\left(\frac{z}{H_o}\right) = C_1 + C_2 \left(\frac{z}{H_o}\right) + C_3 \left(\frac{z}{H_o}\right)^2, \quad 0 < \frac{z}{H_o} \leq 1.0 \quad (4.37)$$

TABLE 23(a)

QUADRATIC POLYNOMIAL COEFFICIENTS FOR CIRCUMFERENTIAL STRESS VARIABLE $\overline{\overline{N}}_\theta$

TANKS WITH ROOF STRUCTURE, $K_r = 1.0$

i	A_1	A_2	A_3	RANGE
1	0.0821146	- 0.121017	0.0352807	$0.1 \leq \frac{H_o}{D_o} \leq 0.8$
	0.0469199	- 0.0668164	0.0244768	$0.8 < \frac{H_o}{D_o} \leq 1.5$
2	- 0.0710643	0.339102	- 0.19281	$0.1 \leq \frac{H_o}{D_o} \leq 0.8$
	0.228774	- 0.260197	0.0783451	$0.8 < \frac{H_o}{D_o} \leq 1.5$
3	0.636397	- 1.51931	0.906262	$0.1 \leq \frac{H_o}{D_o} \leq 0.8$
	0.0325932	- 0.0537606	0.0237666	$0.8 < \frac{H_o}{D_o} \leq 1.5$

$$C_i = A_{1i} + A_{2i} \left(\frac{H_o}{D_o}\right) + A_{3i} \left(\frac{H_o}{D_o}\right)^2, \quad i = 1, 2, 3 \qquad (4.38)$$

$$\overline{\overline{N}}_\theta \left(\frac{z}{H_o}\right) = C_1 + C_2 \left(\frac{z}{H_o}\right) + C_3 \left(\frac{z}{H_o}\right)^2, \quad 0.2 \leq \frac{z}{H_o} \leq 1.0 \qquad (4.37)$$

TABLE 23(b)

QUADRATIC POLYNOMIAL COEFFICIENTS FOR CIRCUMFERENTIAL STRESS VARIABLE $\overline{\overline{N}}_\theta$

TANKS WITH ROOF STRUCTURE, $K_r = 2.0$

i	A_1	A_2	A_3	RANGE
1	0.352785	- 1.24997	1.11839	$0.1 \leq \frac{H_o}{D_o} \leq 0.7$
	0.0093189	- 0.0017308	- 0.003029	$0.7 < \frac{H_o}{D_o} \leq 1.5$
2	- 2.80075	14.5698	- 18.9509	$0.1 \leq \frac{H_o}{D_o} \leq 0.4$
	0.126277	- 0.1447742	0.0465587	$0.4 < \frac{H_o}{D_o} \leq 1.5$
3	1.33861	- 2.42524	- 1.54085	$0.1 \leq \frac{H_o}{D_o} \leq 0.4$
	0.0582763	- 0.0755686	0.0267977	$0.4 < \frac{H_o}{D_o} \leq 1.5$

$$C_i = A_{1i} + A_{2i} \left(\frac{H_o}{D_o}\right) + A_{3i} \left(\frac{H_o}{D_o}\right)^2, \quad i = 1, 2, 3 \qquad (4.38)$$

$$\overline{\overline{N}}_\theta\left(\frac{z}{H_o}\right) = C_1 = C_2 \left(\frac{z}{H_o}\right) + C_3 \left(\frac{z}{H_o}\right)^2, \quad 0.2 \leq \frac{z}{H_o} \leq 1.0 \qquad (4.37)$$

TABLE 23(c)

QUADATRIC POLYNOMIAL COEFFICIENTS FOR CIRCUMFERENTIAL STRESS VARIABLE

$\overline{\overline{N}}_\theta$

TANKS WITH ROOF STRUCTURE, $K_r = 3.0$

i	A_1	A_2	A_3	RANGE
1	0.148724	- 0.329932	0.149165	$0.1 \leq \frac{H_o}{D_o} \leq 0.5$
	0.0414211	- 0.062895	0.0244114	$0.5 < \frac{H_o}{D_o} \leq 1.5$
2	- 1.56127	8.25974	- 11.6807	$0.1 \leq \frac{H_o}{D_o} \leq 0.4$
	0.0275444	0.00954823	- 0.0170391	$0.4 < \frac{H_o}{D_o} \leq 1.5$
3	0.358804	2.51895	- 7.38195	$0.1 \leq \frac{H_o}{D_o} \leq 0.4$
	0.119292	- 0.198201	0.0834478	$0.4 < \frac{H_o}{D_o} \leq 1.5$

$$C_i = A_{1i} + A_{2i} \left(\frac{H_o}{D_o}\right) + A_{3i} \left(\frac{H_o}{D_o}\right)^2, \quad i = 1, 2, 3 \quad (4.38)$$

$$\overline{\overline{N}}_\theta \left(\frac{z}{H_o}\right) = C_1 + C_2 \left(\frac{H_o}{D_o}\right) + C_3 \left(\frac{H_o}{D_o}\right)^2, \quad 0.2 \leq \frac{z}{H_o} \leq 1.0 \quad (4.37)$$

TABLE 24

FLOW DIAGRAM - SEISMIC ANALYSIS OF EMPTY CYLINDRICAL TANKS

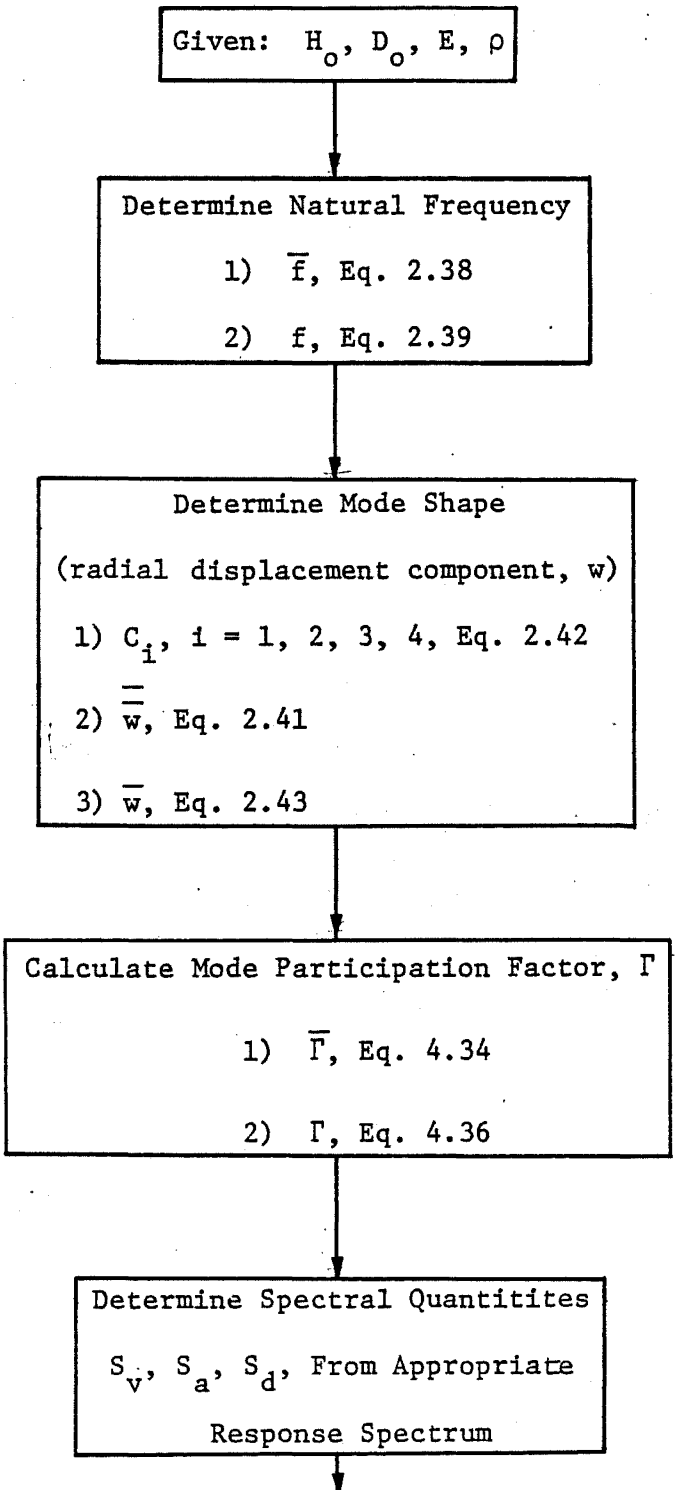

TABLE 24 (continued)

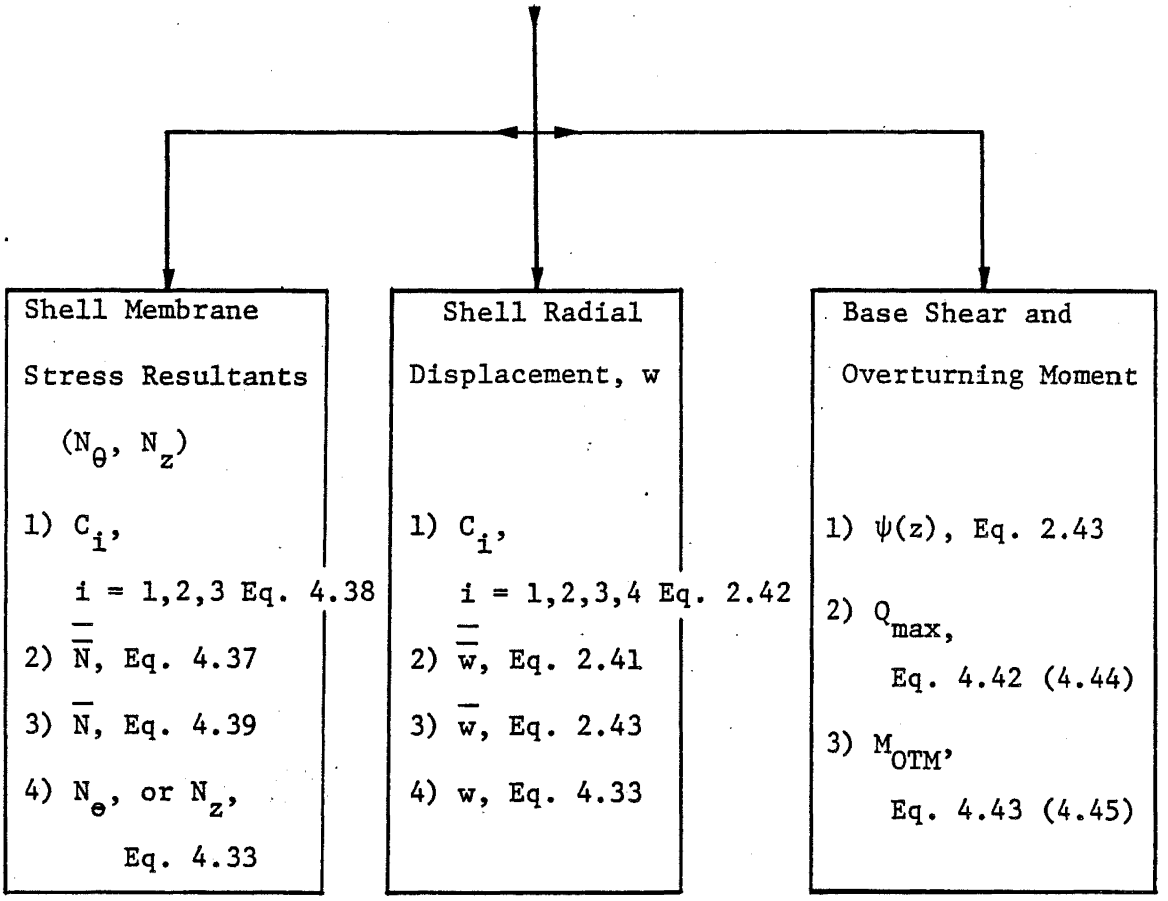

TABLE 25

MODEL PARAMETERS FOR CYLINDRICAL TANK

(SIMPLE MODEL - REFER TO FIG. 3.3)

$$m_T = \frac{1}{4} \rho_L \pi D_o^2 h_L$$

$$m_o = \frac{m_T \tanh \left(\sqrt{3} \frac{D_o}{2h_L}\right)}{\frac{\sqrt{3} D_o}{2h_L}}$$

$$m_1 = 0.159 \frac{D_o}{h_L} \tanh \left(3.68 \frac{h_L}{D_o}\right) m_T$$

$$h_o(\text{EBP}) = \frac{3}{8} h_L$$

$$h_o(\text{IBP}) = \frac{1}{8} \left[\frac{4.0}{\frac{\tanh \left(\sqrt{3} \frac{D_o}{2h_L}\right)}{\sqrt{3} \frac{D_o}{2h_L}}} - 1.0 \right] h_L$$

$$h_1(\text{EBP}) = \left[1.0 - \frac{\cosh \left(3.68 \frac{h_L}{D_o}\right) - 1.0}{3.68 \frac{h_L}{D_o} \sinh \left(3.68 \frac{h_L}{D_o}\right)} \right] h_L$$

$$h_1(\text{IBP}) = \left[1.0 - \frac{\cosh \left(3.68 \frac{h_L}{D_o}\right) - 2.01}{3.68 \frac{h_L}{D_o} \sinh \left(3.68 \frac{h_L}{D_o}\right)} \right] h_L$$

TABLE 25 (continued)

MODEL PARAMETERS FOR CYLINDRICAL TANK

(SIMPLE MODEL - REFER TO FIG. 3.3)

$$K_1 = \frac{0.585}{h_L} m_T \, g(\tanh 3.68 \frac{h_L}{D_o})^2$$

where,

ρ_L = mass density of liquid in tank

g = acceleration of gravity

D_o = diameter of tank

h_L = height of liquid in tank

TABLE 26

RELATIVE LOCATION OF MAXIMUM WALL ACCELERATIONS IN LIQUID-FILLED CYLINDRICAL TANKS

$\frac{H_o}{D_o}$	$\frac{z_m}{H_o}$	
	$\frac{h_L}{H_o} = 1.0$	$\frac{h_L}{H_o} = 0.5$
0.1	0.05	0.03
0.2	0.11	0.07
0.3	0.18	0.15
0.4	0.28	0.17
0.5	0.40	0.18
0.6	0.49	0.19
0.7	0.57	0.21
0.8	0.62	0.23
0.9	0.67	0.25
1.0	0.70	0.27
1.1	1.0	0.28
1.2	1.0	0.29
1.3	1.0	0.30
1.4	1.0	0.31
1.5	1.0	0.33

TABLE 27

FLOW DIAGRAM - SEISMIC ANALYSIS OF CYLINDRICAL LIQUID STORAGE TANKS (IMPULSIVE EFFECTS)

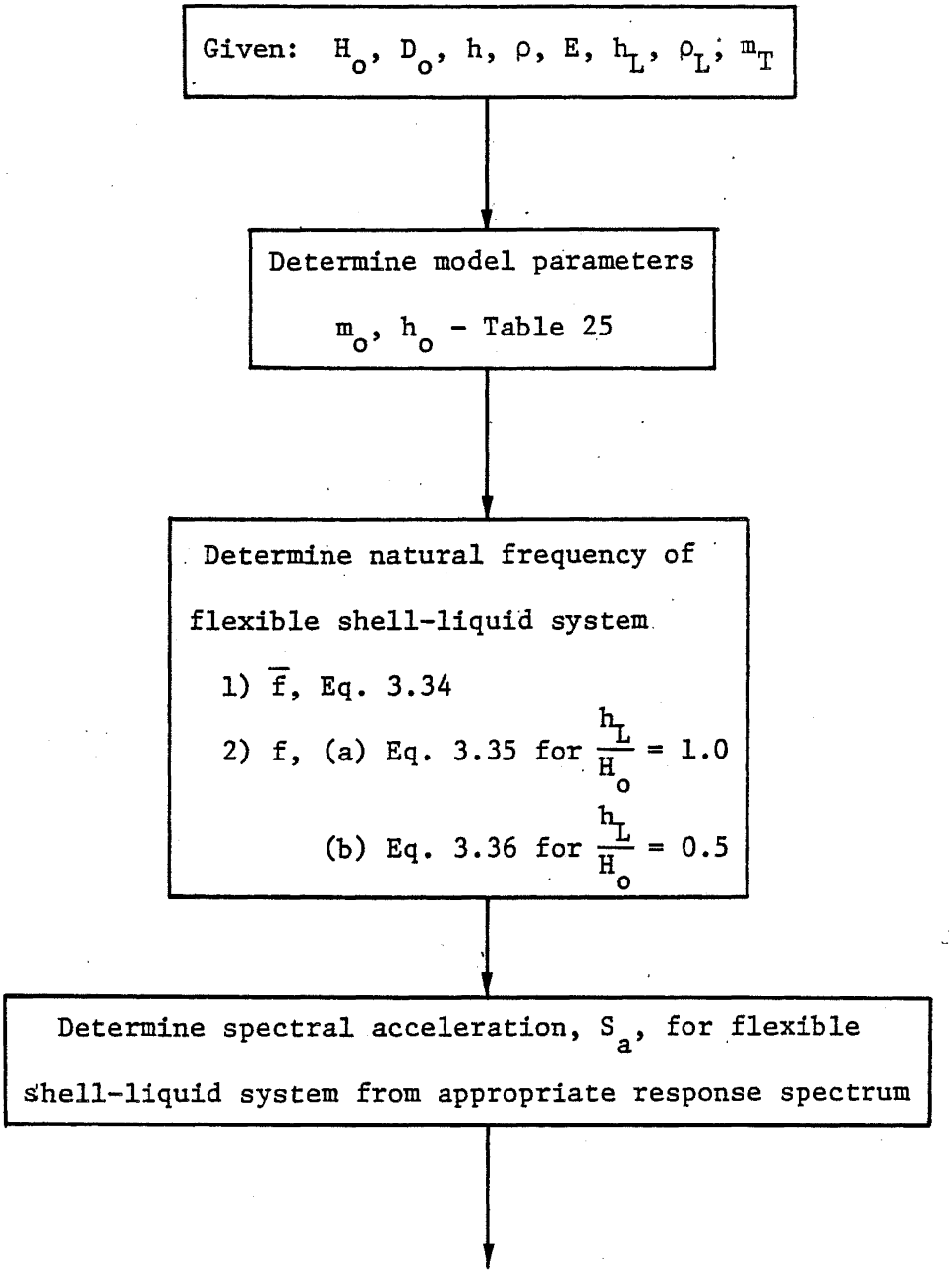

TABLE 27 (continued)

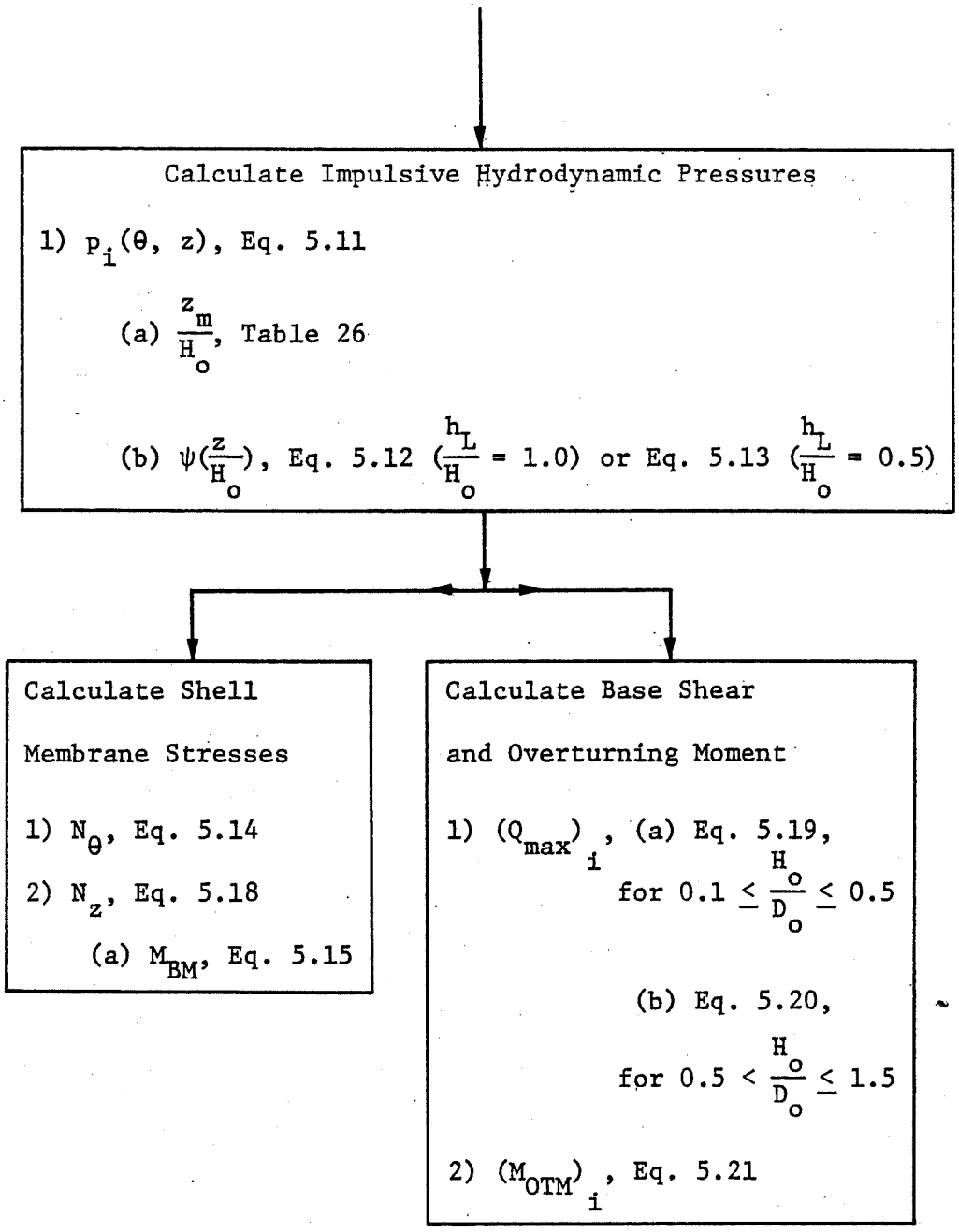

TABLE 28

NUMERICAL COMPARISONS OF IMPULSIVE HYDRODYNAMIC PRESSURES

FOR A TALL TANK

$\frac{z}{H_o}$	Present Analysis	Ref. 26	Rigid Tank
0.083	48125.4 Pa (6.98 psi)	51848.6 Pa (7.52 psi)	33853.2 Pa (4.91 psi)
0.1	51021.2 Pa (7.4 psi)	57916.0 Pa (8.4 psi)	33646.4 Pa (4.88 psi)
0.5	83978.1 Pa (12.18 psi)	81702.9 Pa (11.85 psi)	25510.6 Pa (3.7 psi)

TABLE 29

NUMERICAL COMPARISONS OF AXIAL STRESS RESULTANT, N_z

FOR A TALL TANK

$\frac{z}{H_o}$	Present Analysis	Ref. 26	Rigid Tank
0.0	1.48 MN/m (8.47 k/in)	--	0.602 MN/m (3.44 k/in)
0.0958	1.48 MN/m (8.46 k/in)	1.47 MN/m (8.38 k/in)	--
0.125	1.36 MN/m (7.76 k/in)	1.25 MN/m (7.12 k/in)	--

TABLE 30

NUMERICAL COMPARISONS OF IMPULSIVE HYDRODYNAMIC BASE SHEAR AND OVERTURNING MOMENT FOR A TALL TANK

	Present Analysis	Ref. 26	Rigid Tank
Base Shear	24.1 MN (54.2×10^2 kips)	22.7 MN (51.1×10^2 kips)	11.4 MN (25.6×10^2 kips)
Overturning Moment	232.7 MN-m (1.69×10^5 k-ft)	--	92.9 MN-m (6.86×10^4 k-ft)

TABLE 31

NUMERICAL COMPARISONS OF IMPULSIVE HYDRODYNAMIC PRESSURES FOR A SHALLOW TANK

$\frac{z}{H_o}$	Present Analysis	Ref. 26	Rigid Tank
0.1	72463.9 Pa (10.51 psi)	65707.0 Pa (9.53 psi)	35370.1 Pa (5.13 psi)
0.5	61914.9 Pa (8.98 psi)	58743.3 Pa (8.52 psi)	26820.6 Pa (3.89 psi)
0.9	8894.2 Pa (1.29 psi)	17788.5 Pa (2.58 psi)	6798.2 Pa (0.986 psi)

TABLE 32

NUMERICAL COMPARISONS OF MAXIMUM AXIAL STRESS RESULTANT, N_z IMPULSIVE HYDRODYNAMIC BASE SHEAR, AND IMPULSIVE HYDRODYNAMIC OVERTURNING MOMENT FOR A SHALLOW TANK

	Present Analysis	Ref. 26	Rigid Tank
$(N_z)_{max}$	0.182 MN/m (1.04 k/in)	0.190 MN/m (1.08 k/in)	0.078 MN/m (0.446 k/in)
Base Shear	41.1 MN (92.4×10^2 k)	39.7 MN (89.2×10^2 k)	17.4 MN (39.2×10^2 k)
Overturning Moment	572.8 MN-m (4.2×10^5 k-ft)	--	244.0 MN-m (1.8×10^5 k-ft)

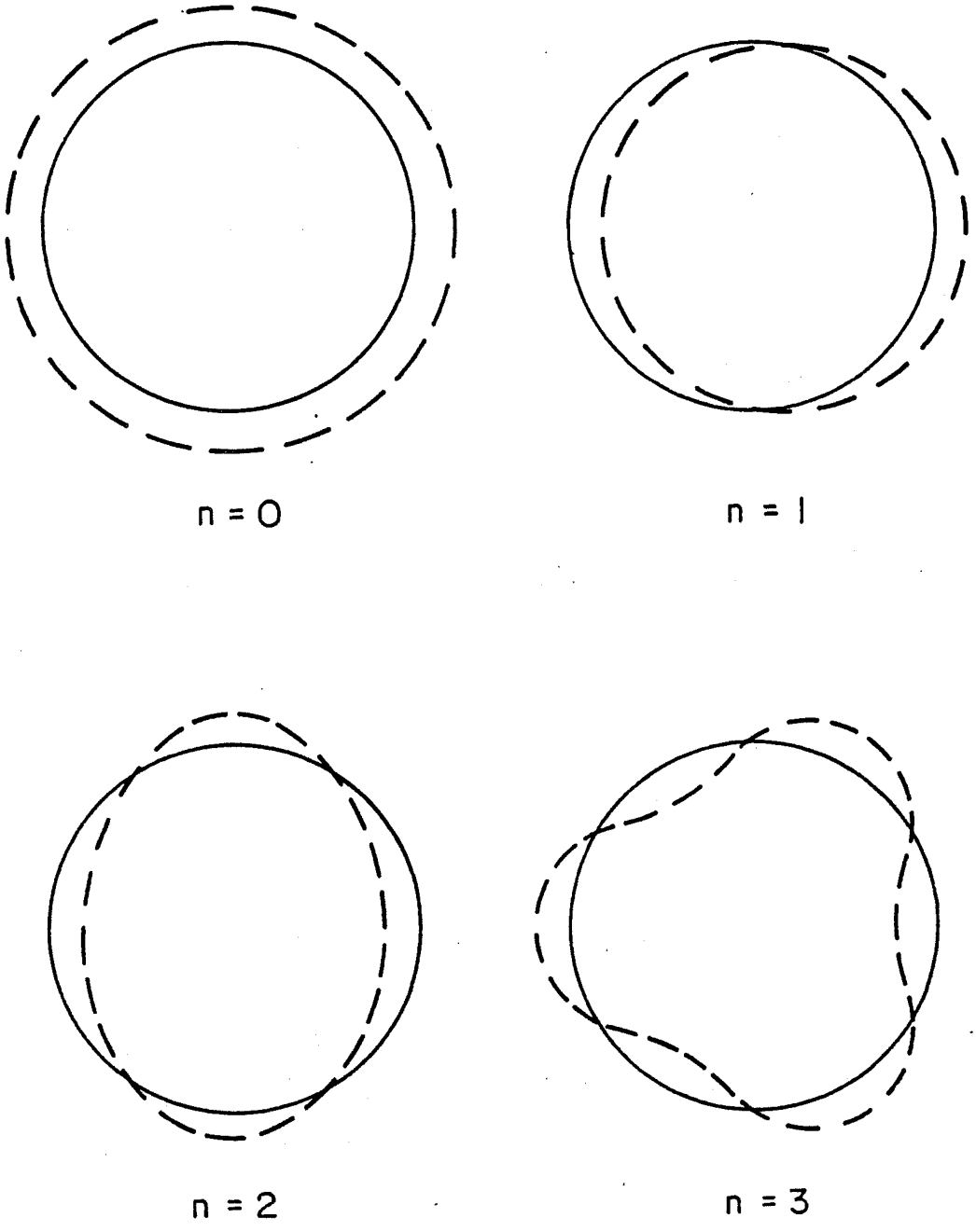

Fig. 1 Circumferential Vibration Mode Shapes

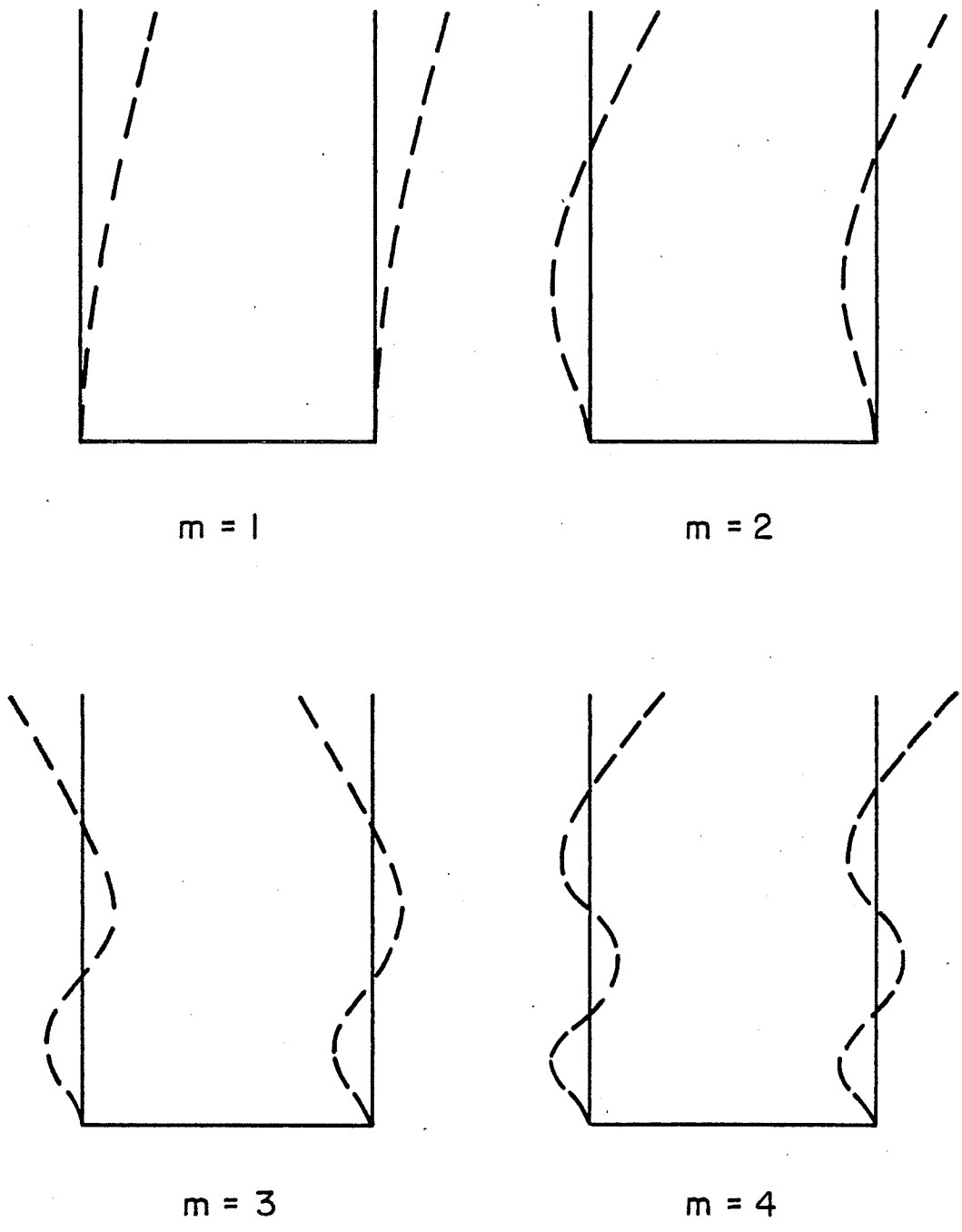

Fig. 2 Axial Vibration Mode Shapes

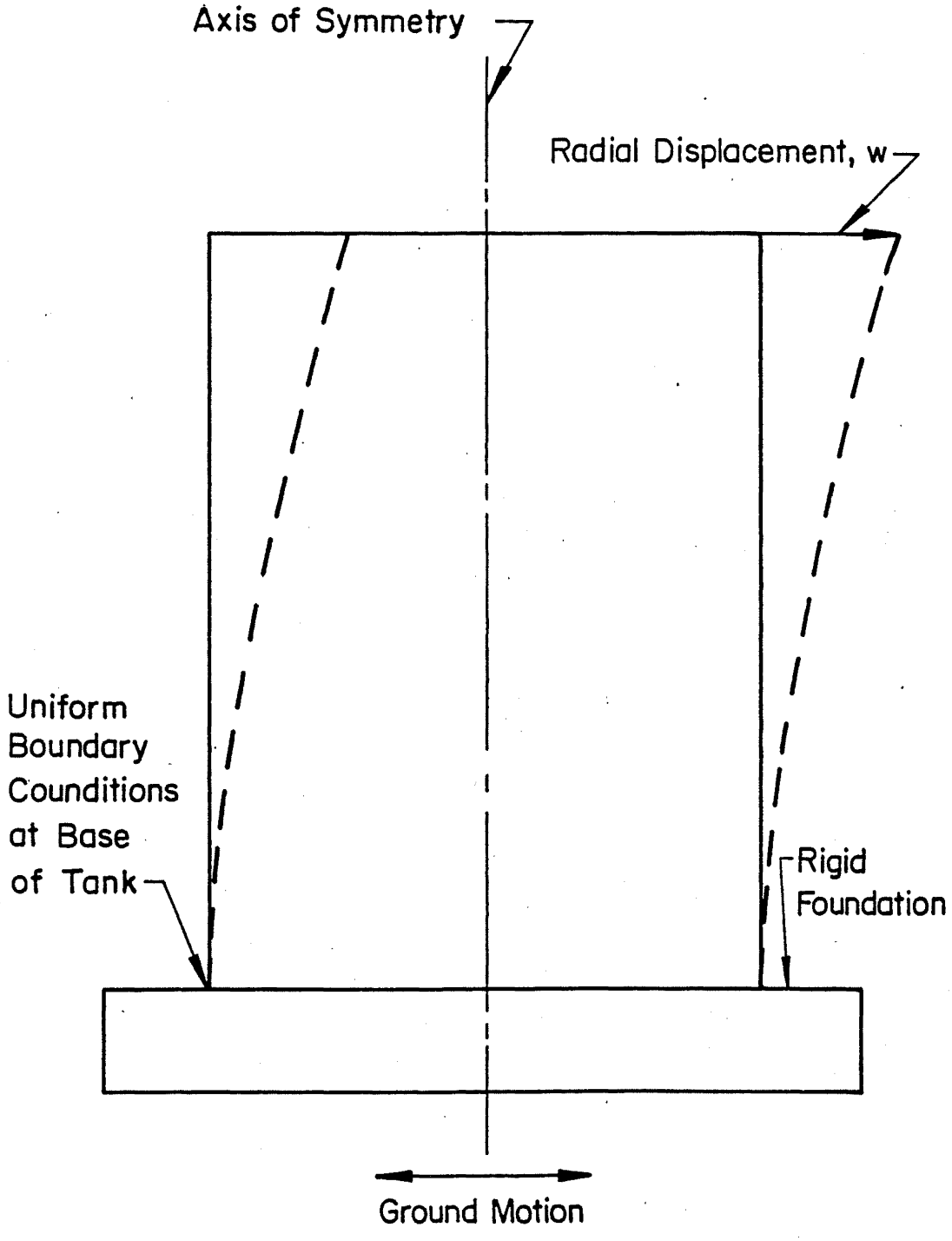

Fig. 3 Cylindrical Tank Uniformly Attached to a Rigid Foundation

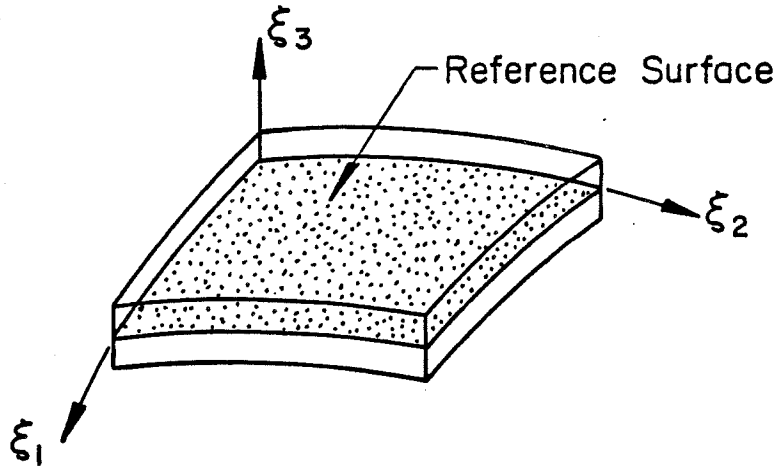

Fig. 4 Two-Dimensional Reference Surface

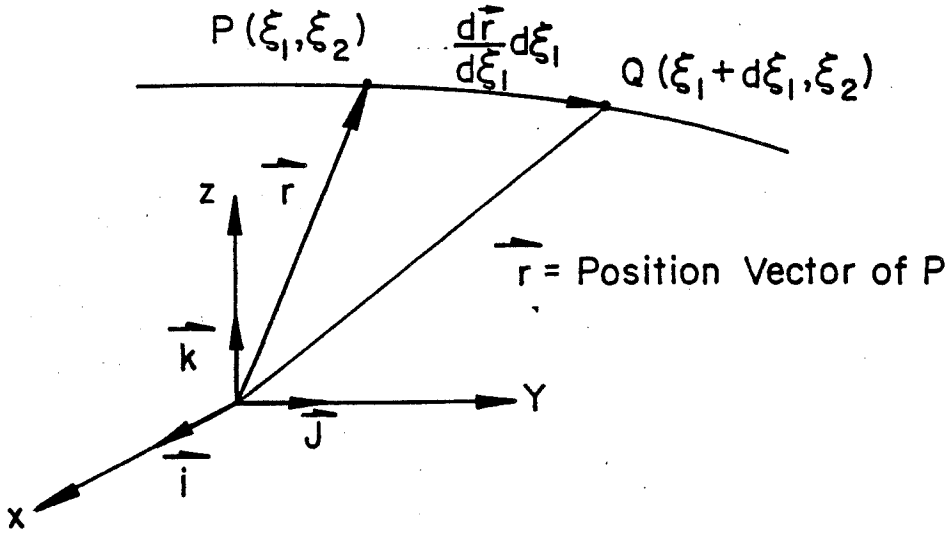

Fig. 5 Metric Components and Normal Vector

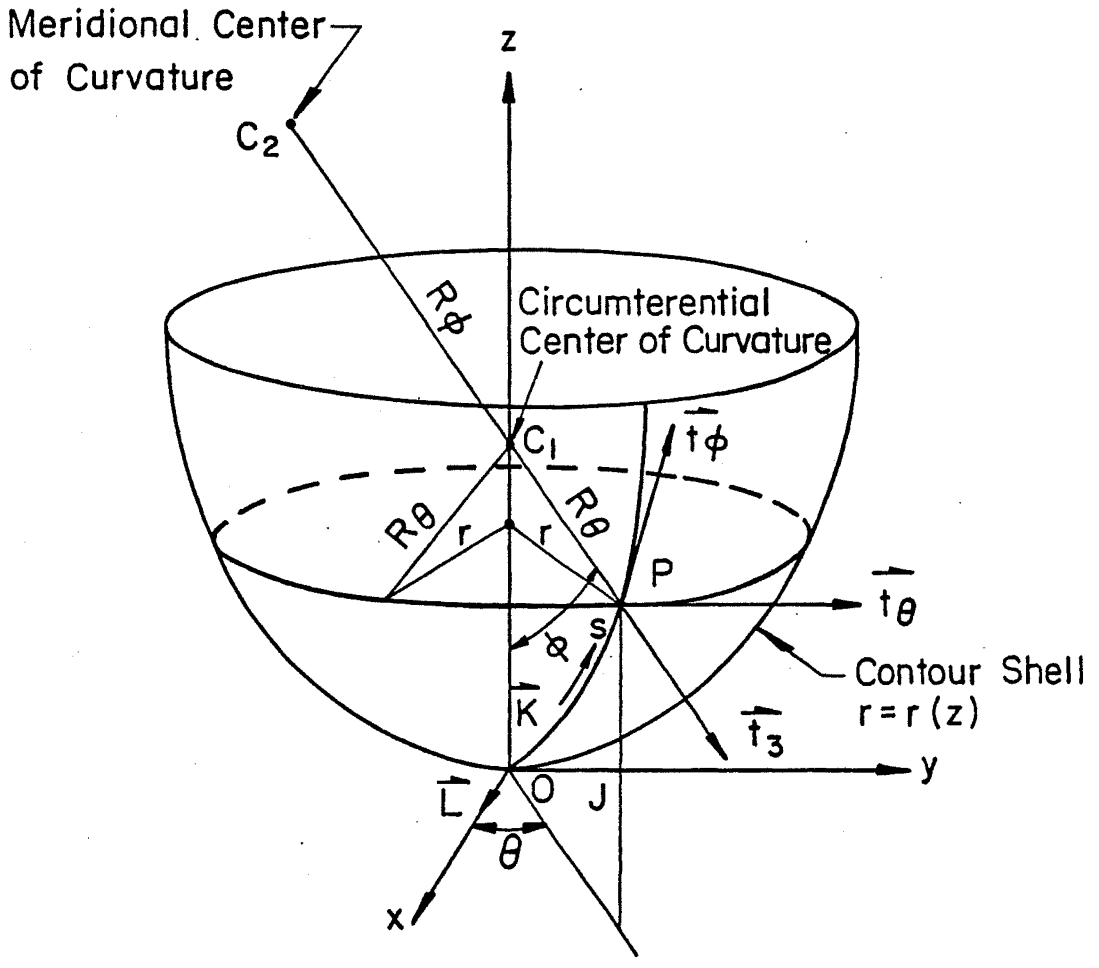

Fig. 6 Typical Geometry for an Axisymmetric Shell

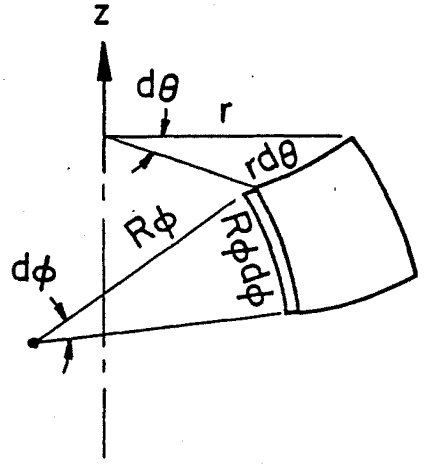

Fig. 7 Differential Element of An Axisymmetric Shell

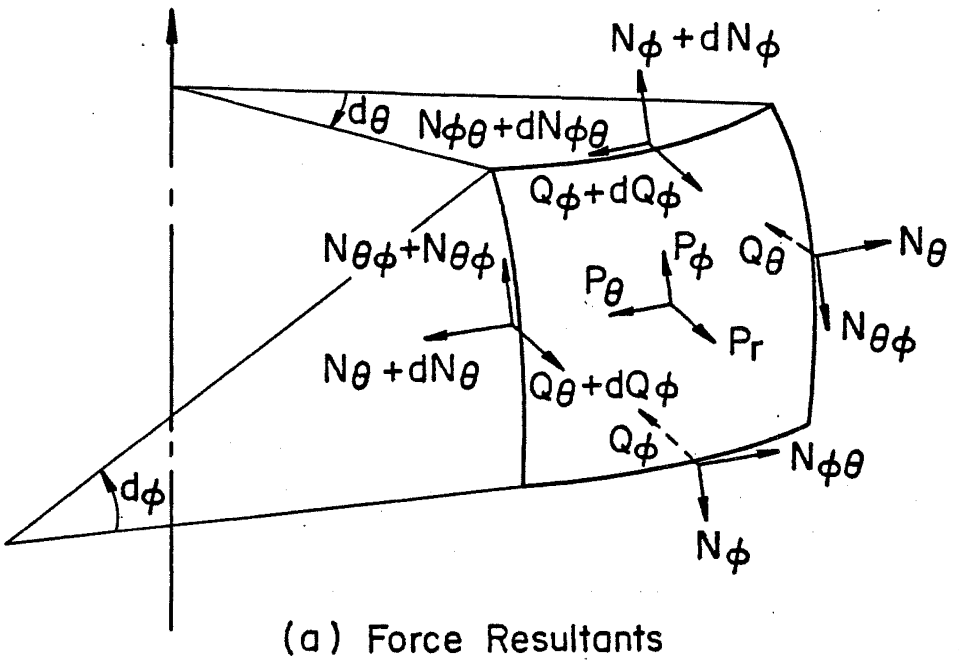

(a) Force Resultants

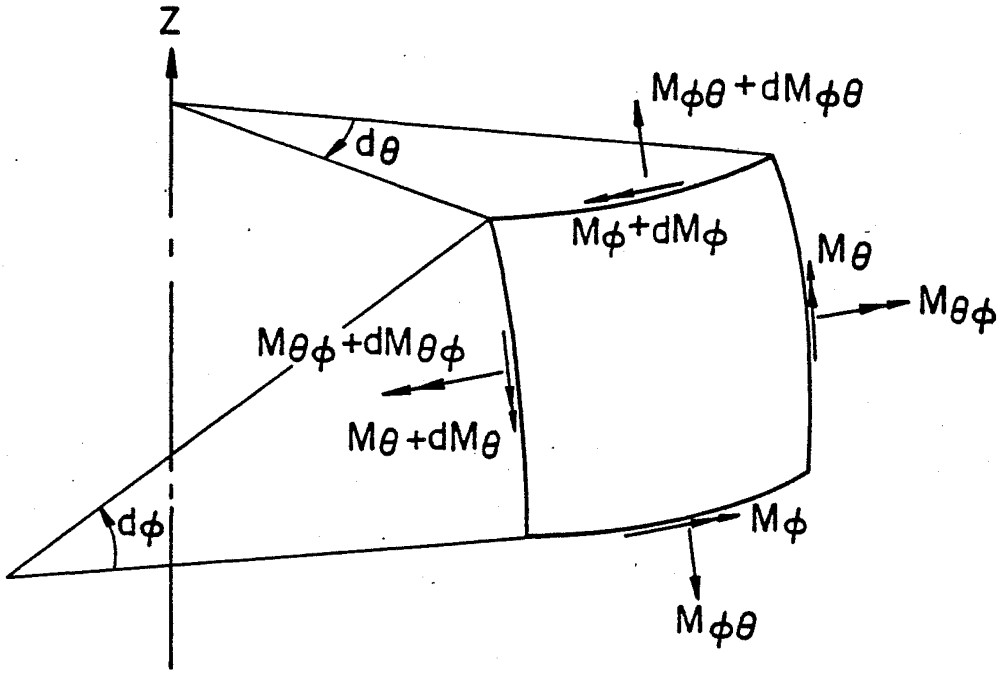

(b) Moment Resultants

Fig. 8 Force and Moment Resultants for an Element of an Axisymmetric Shell

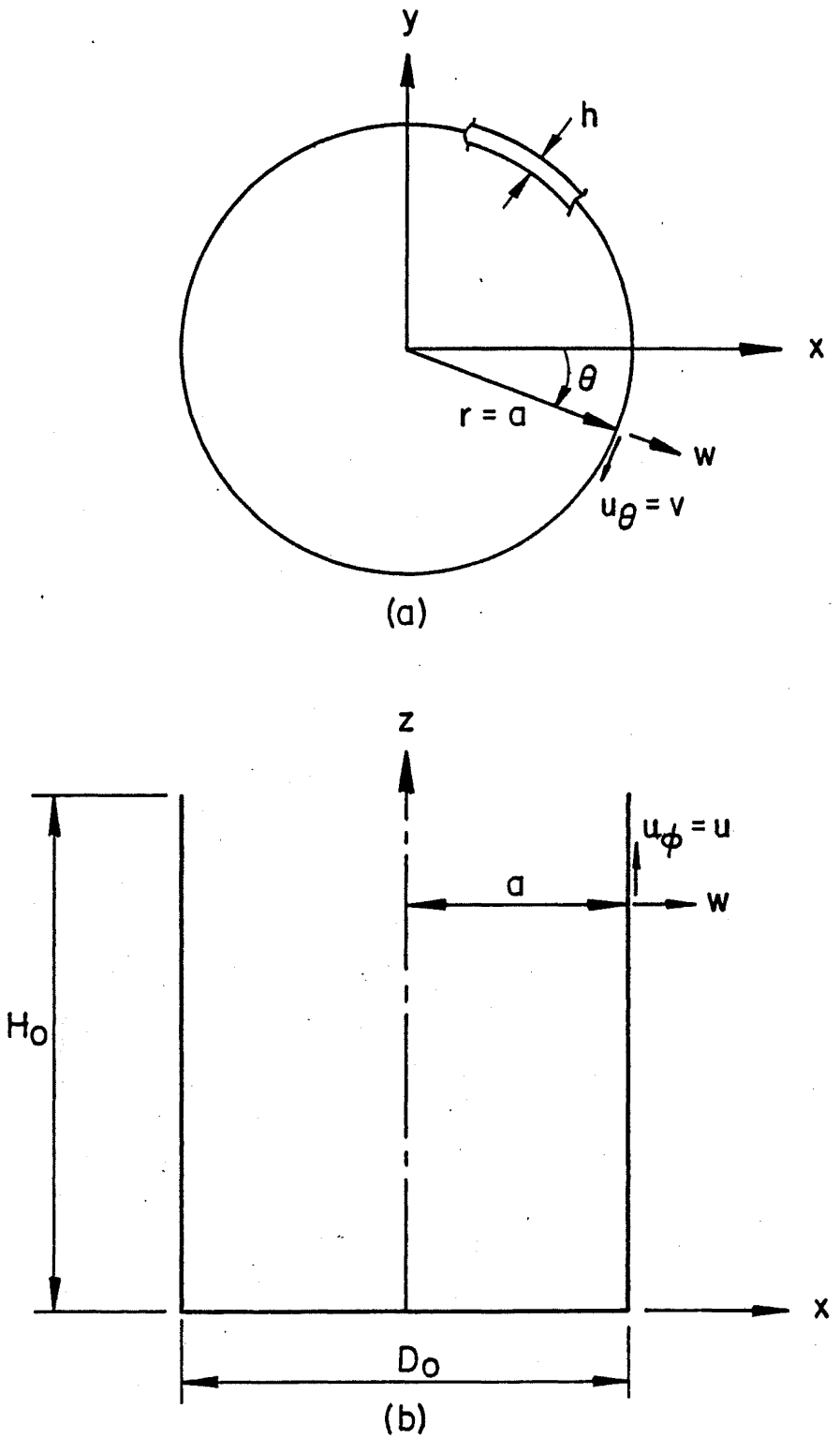

Fig. 9 Displacement Components and Dimensions for a Cylindrical Shell

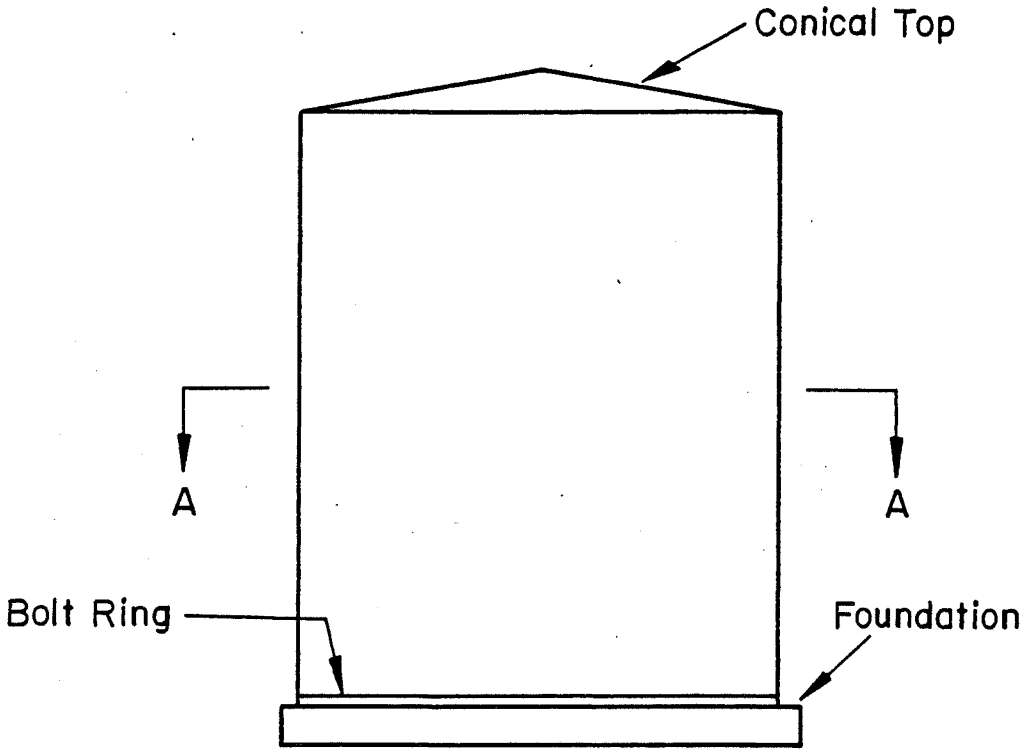

(a) Elevation

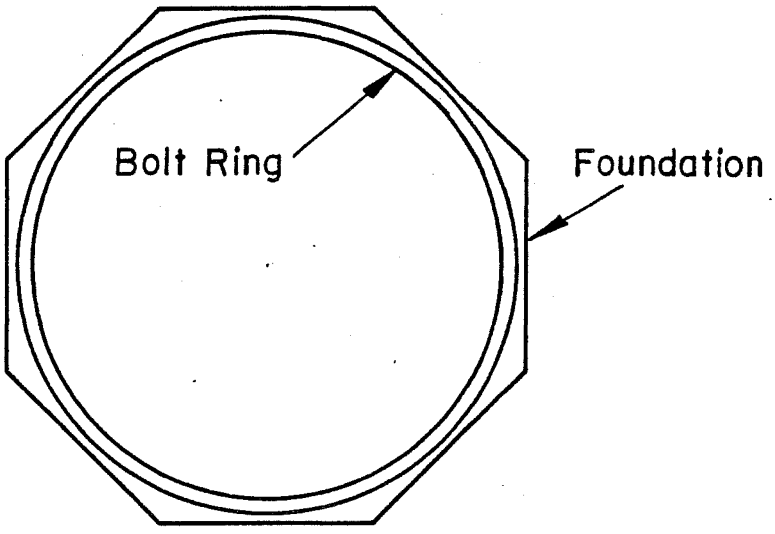

(b) Section A - A

Fig. 10 Typical Storage Tank Details

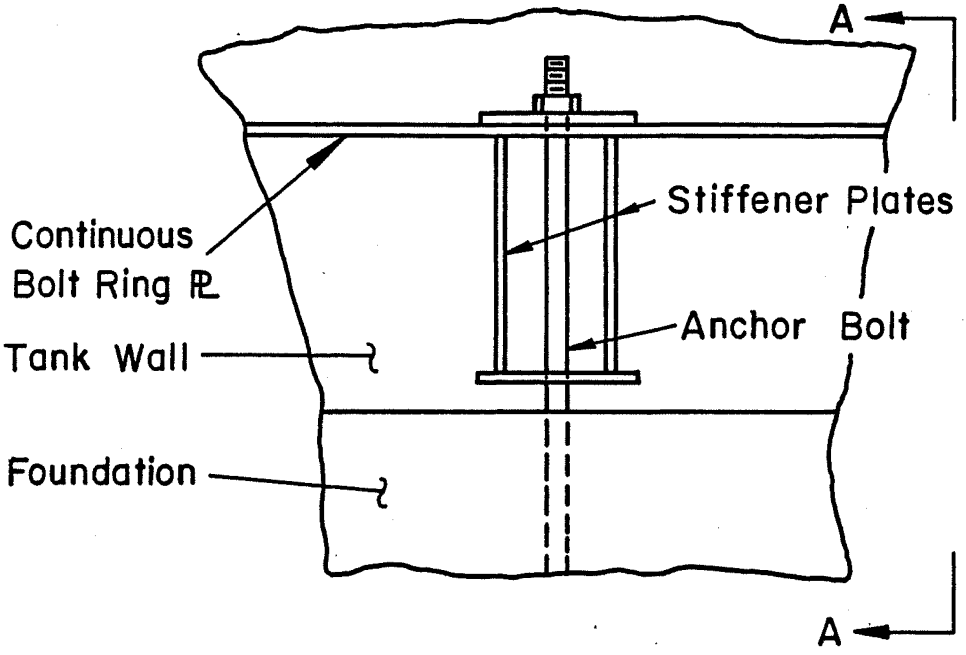

(a) Anchor Bolt Detail

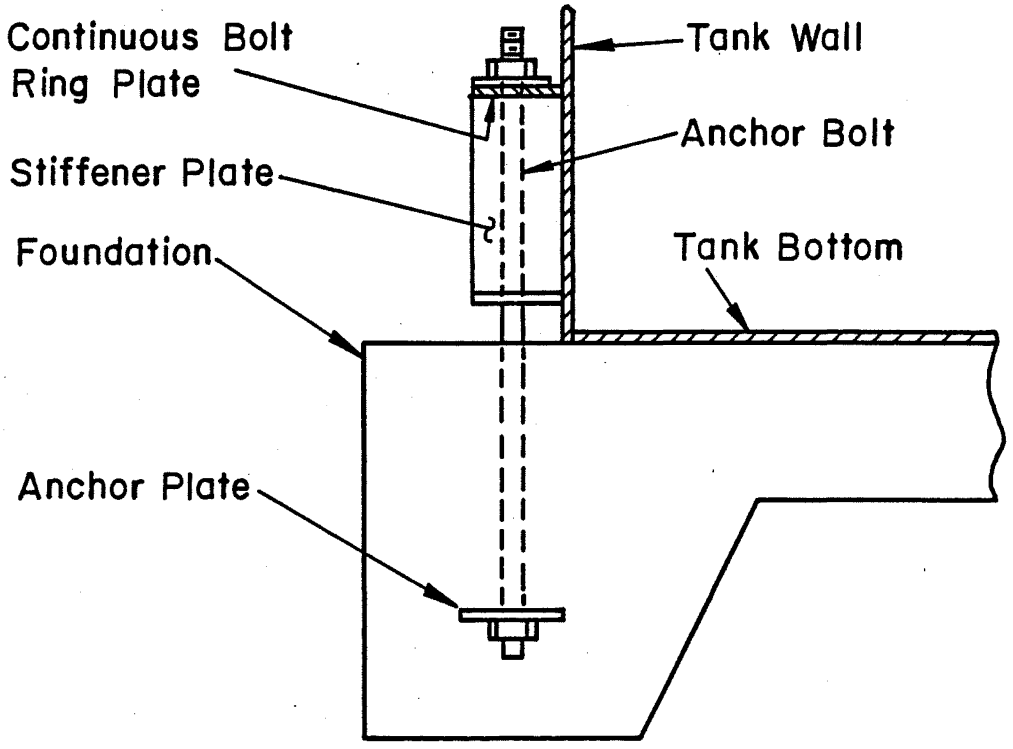

(b) Section AA

Fig. 11 Typical Anchor Bolt Details

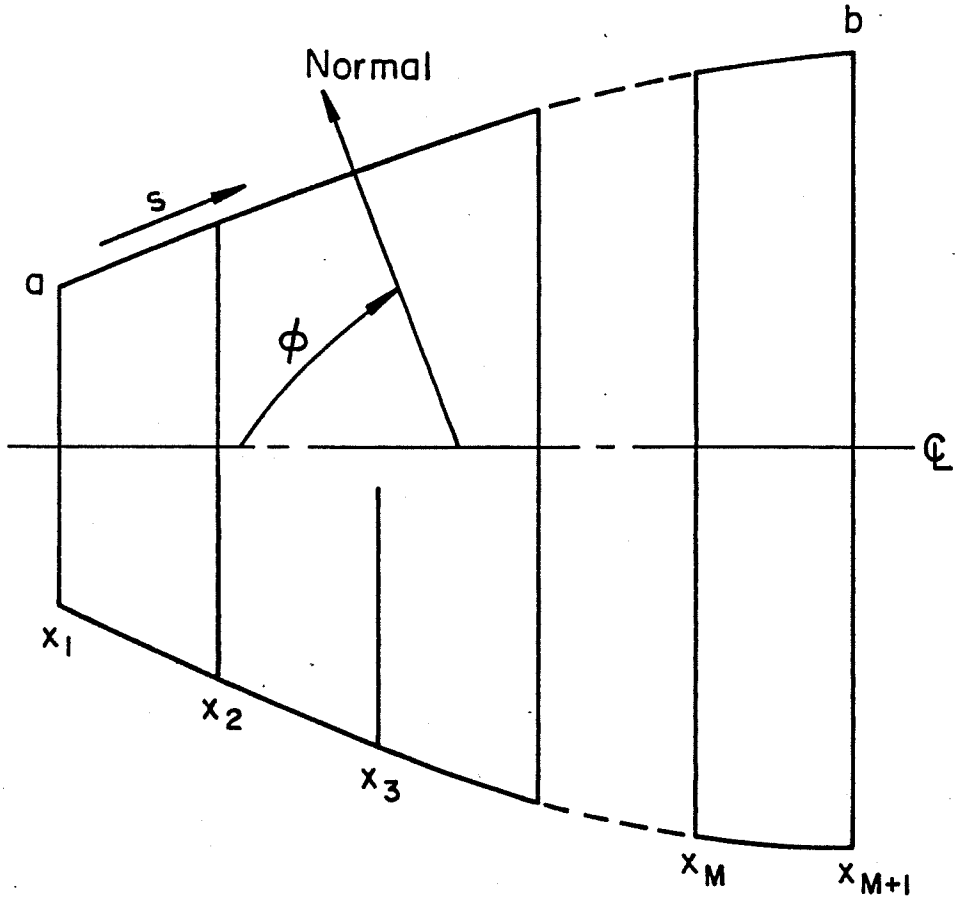

Fig. 12 Coordinates of an Axisymmetric Shell

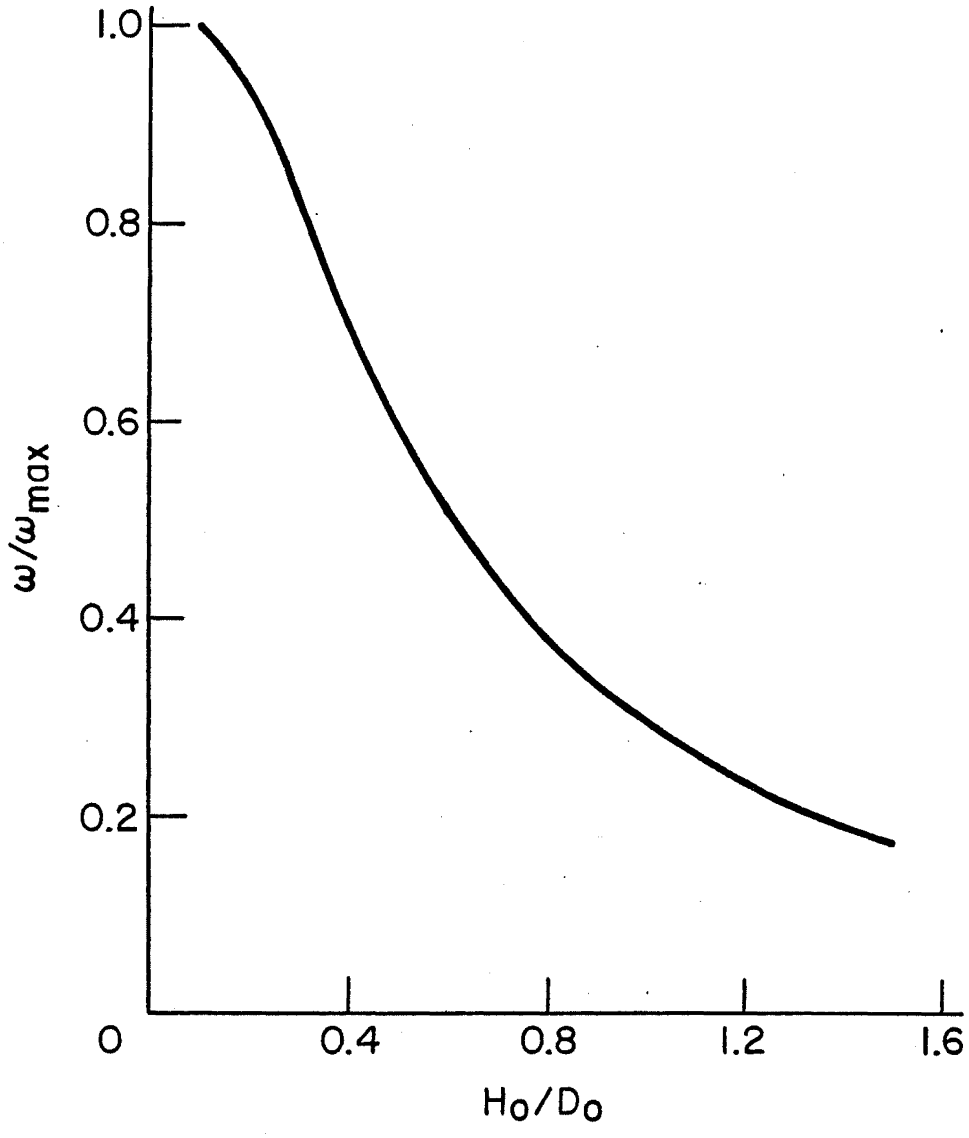

Fig. 13 Frequency versus Tank Aspect Ratio

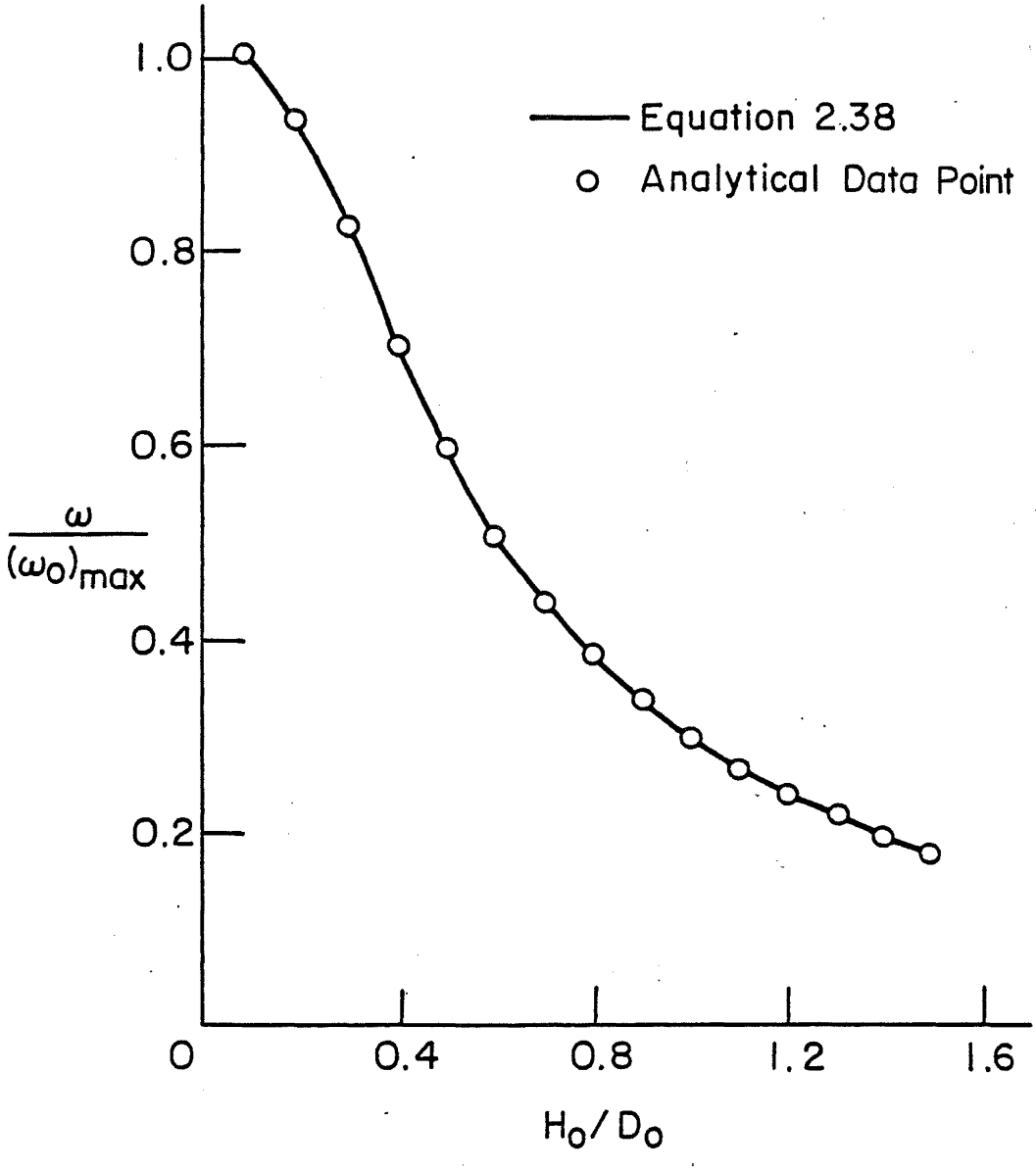

Fig. 14 Natural Frequencies of Open-Top Cylindrical Tanks

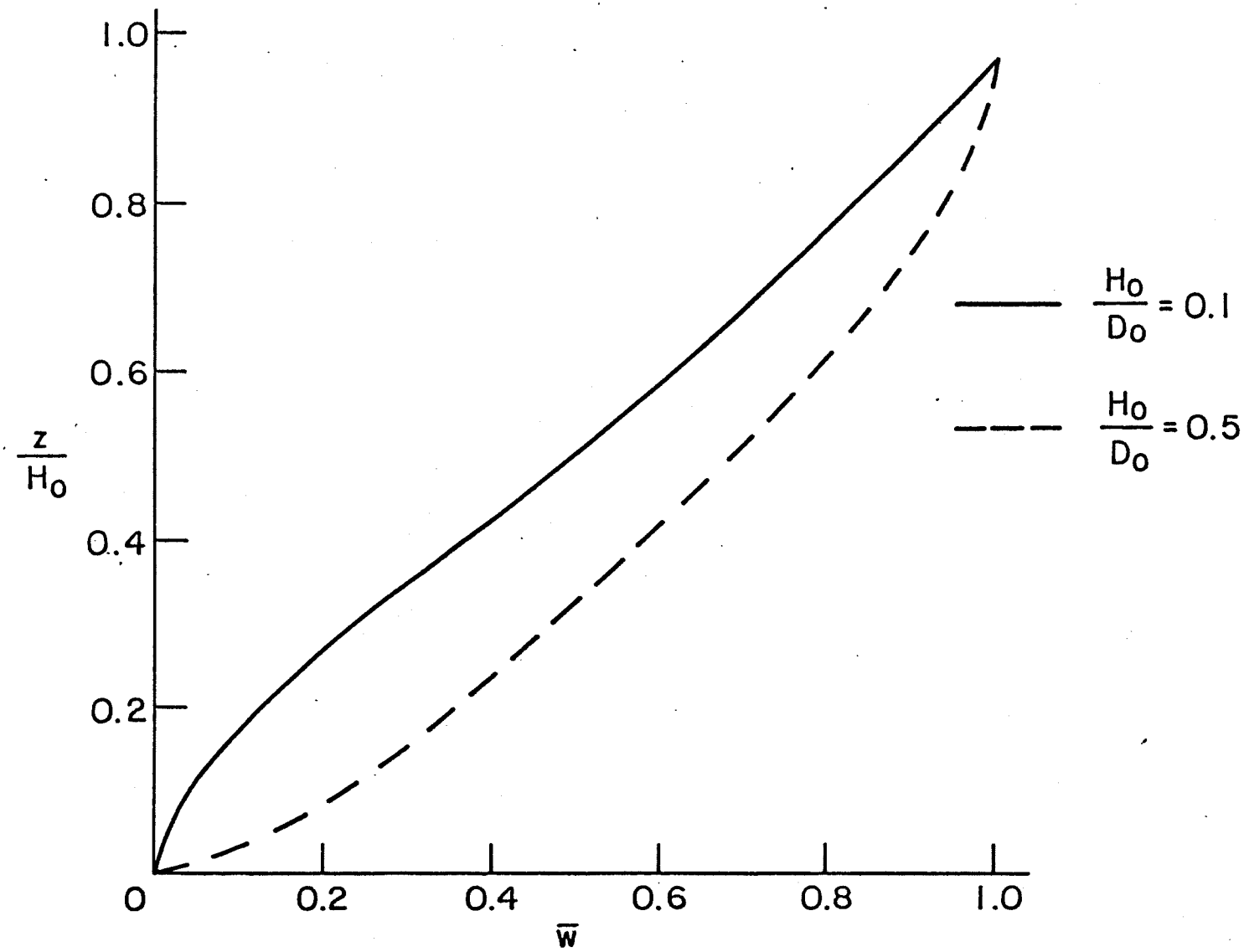

Fig. 15 Fundamental Vertical Mode Shape

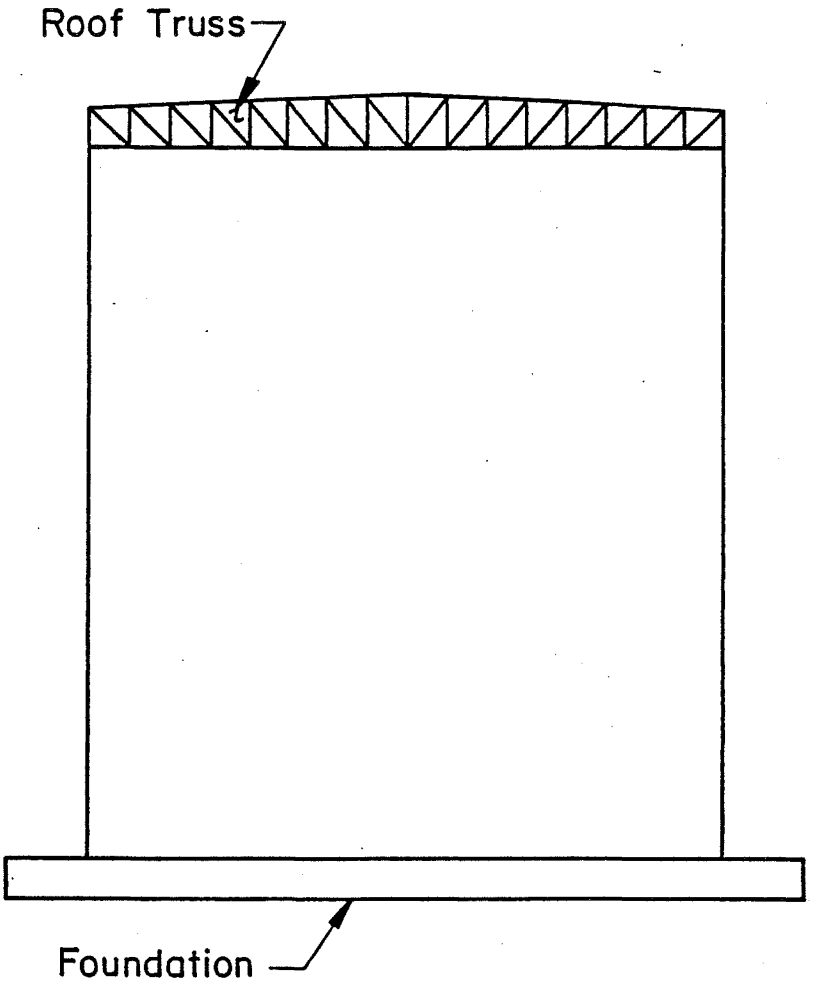

Fig. 16 Storage Tank with Supported Roof

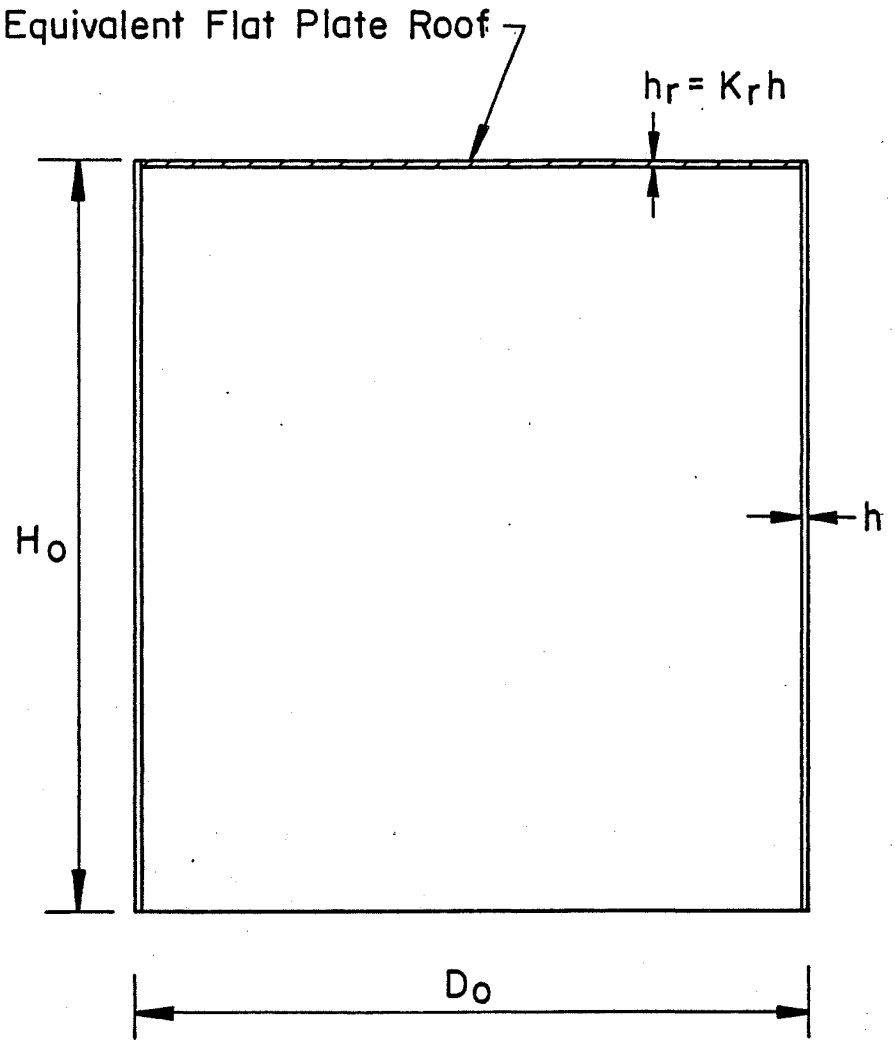

$$K_r = 4 \frac{m_r}{m_c} \left(\frac{H_o}{D_o} \right)$$

Fig. 17 Cylindrical Shell Model with Circular Plate Roof

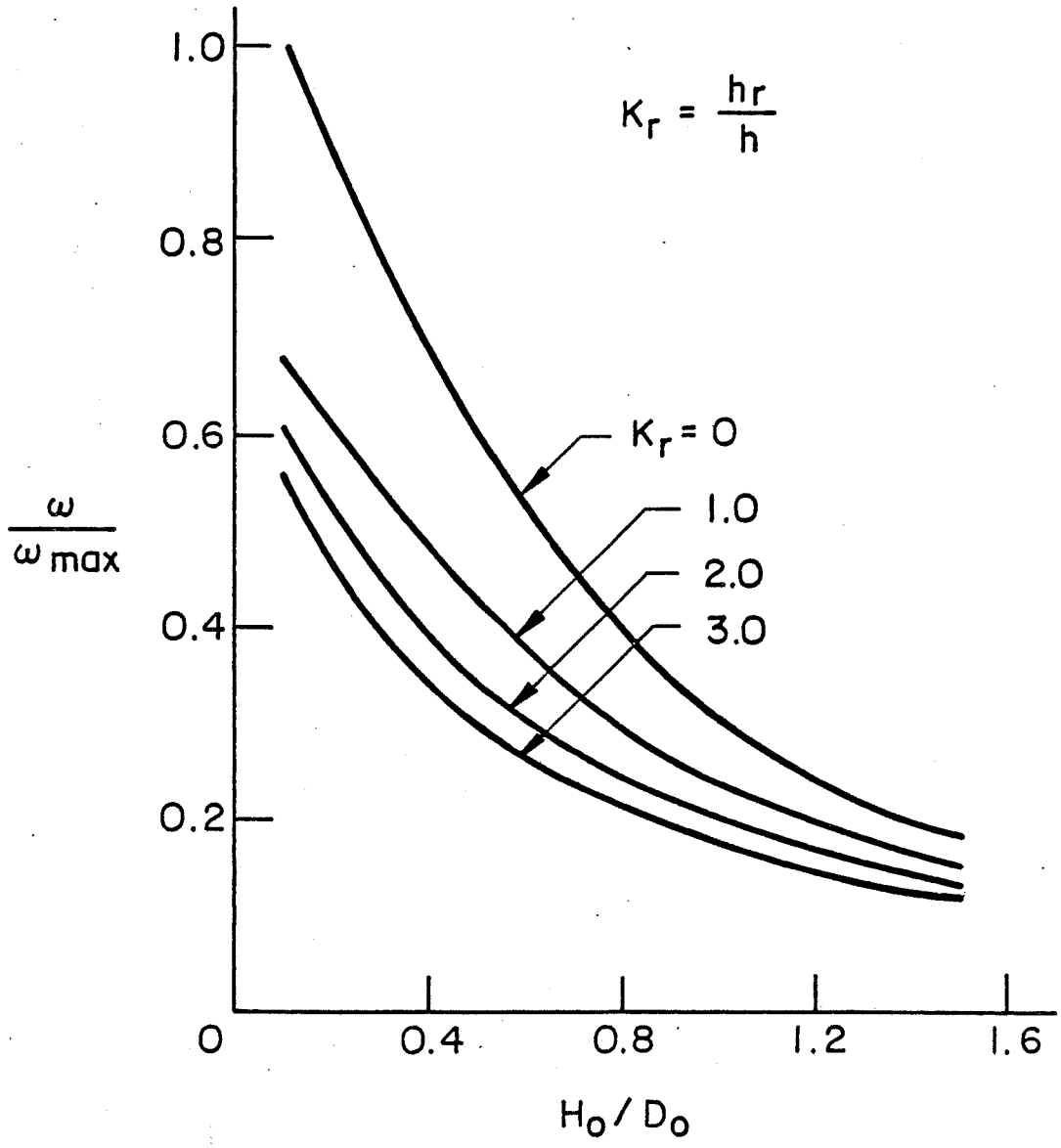

Fig. 18 Effect of Roof Mass on Natural Frequency of Cylindrical Storage Tanks

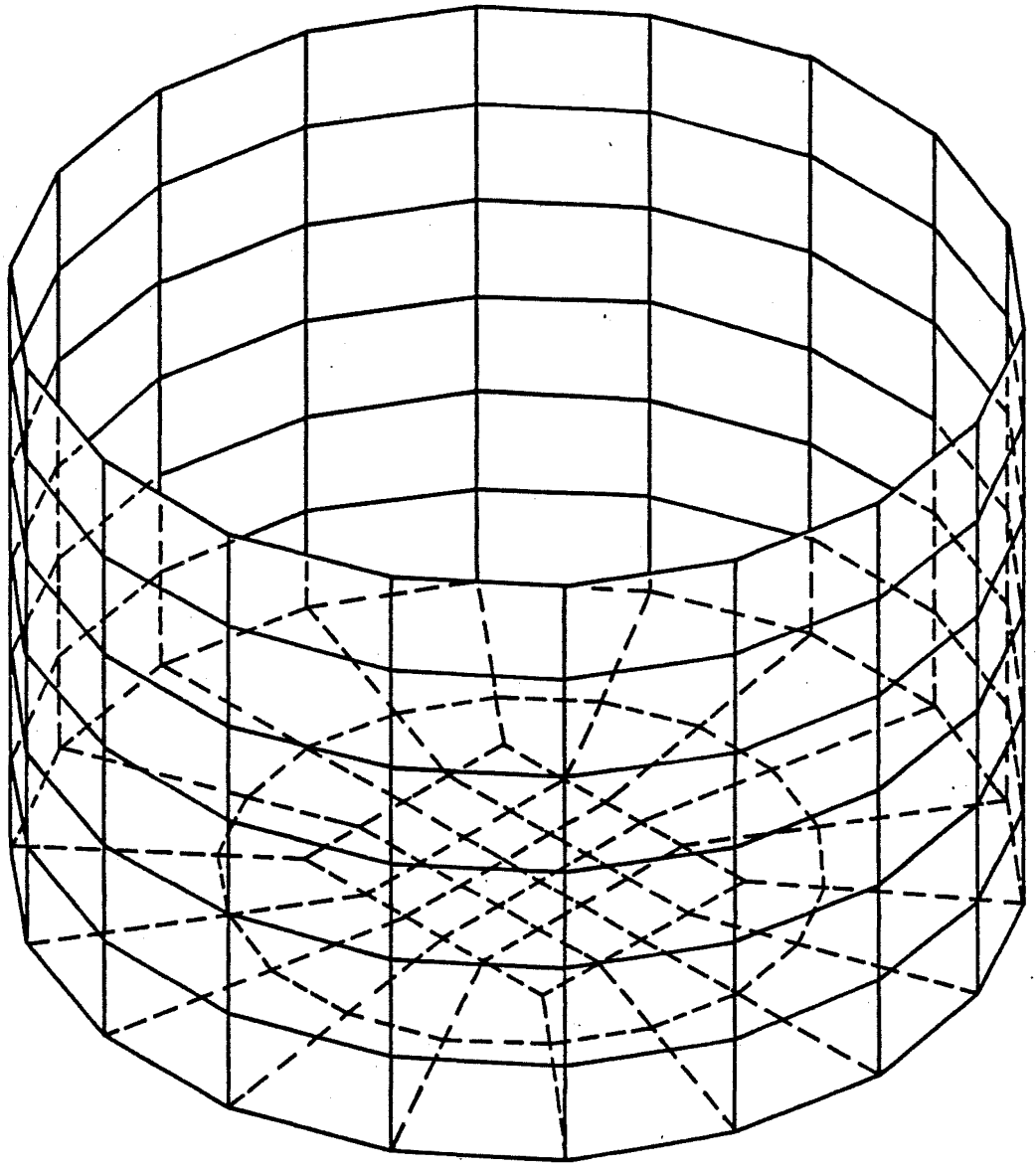

Fig. 19 Typical Discretization for Finite Element Parametric Study

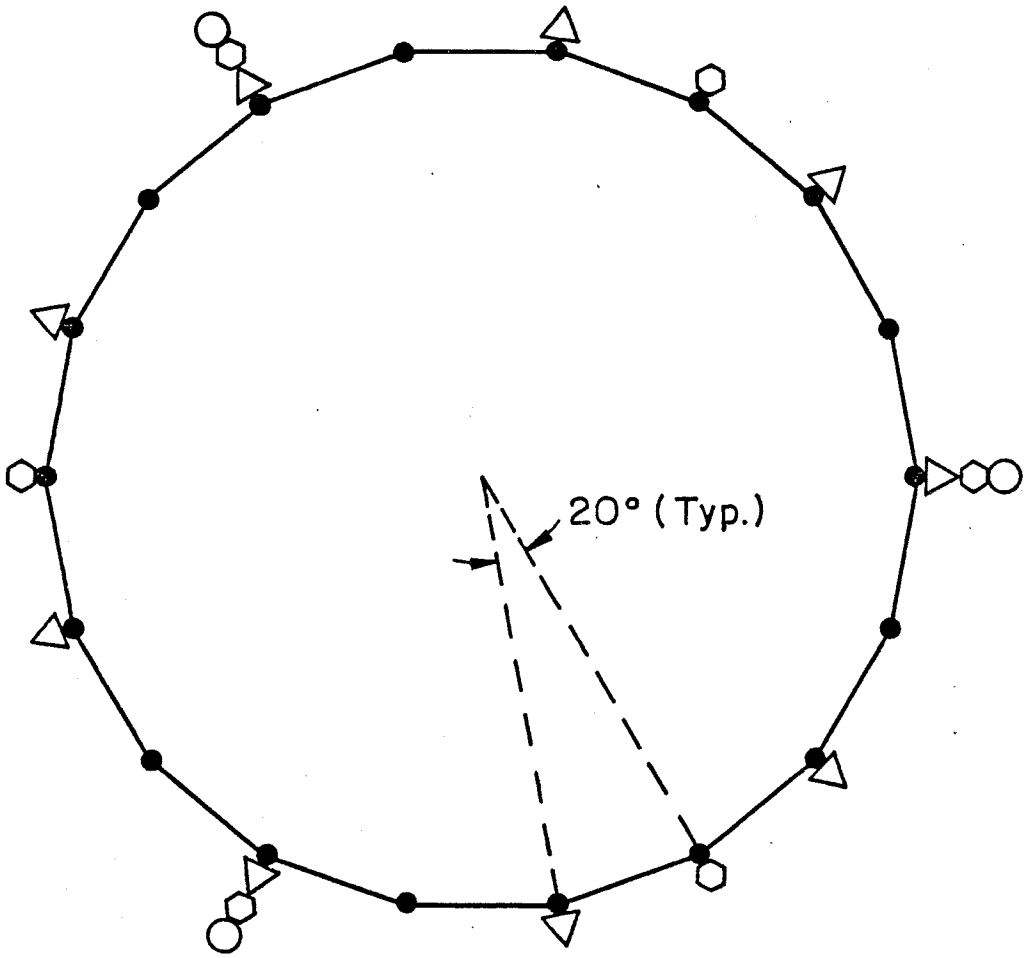

Fig. 20 Various Cases of Boundary Condition at Base of Cylindrical Storage Tank

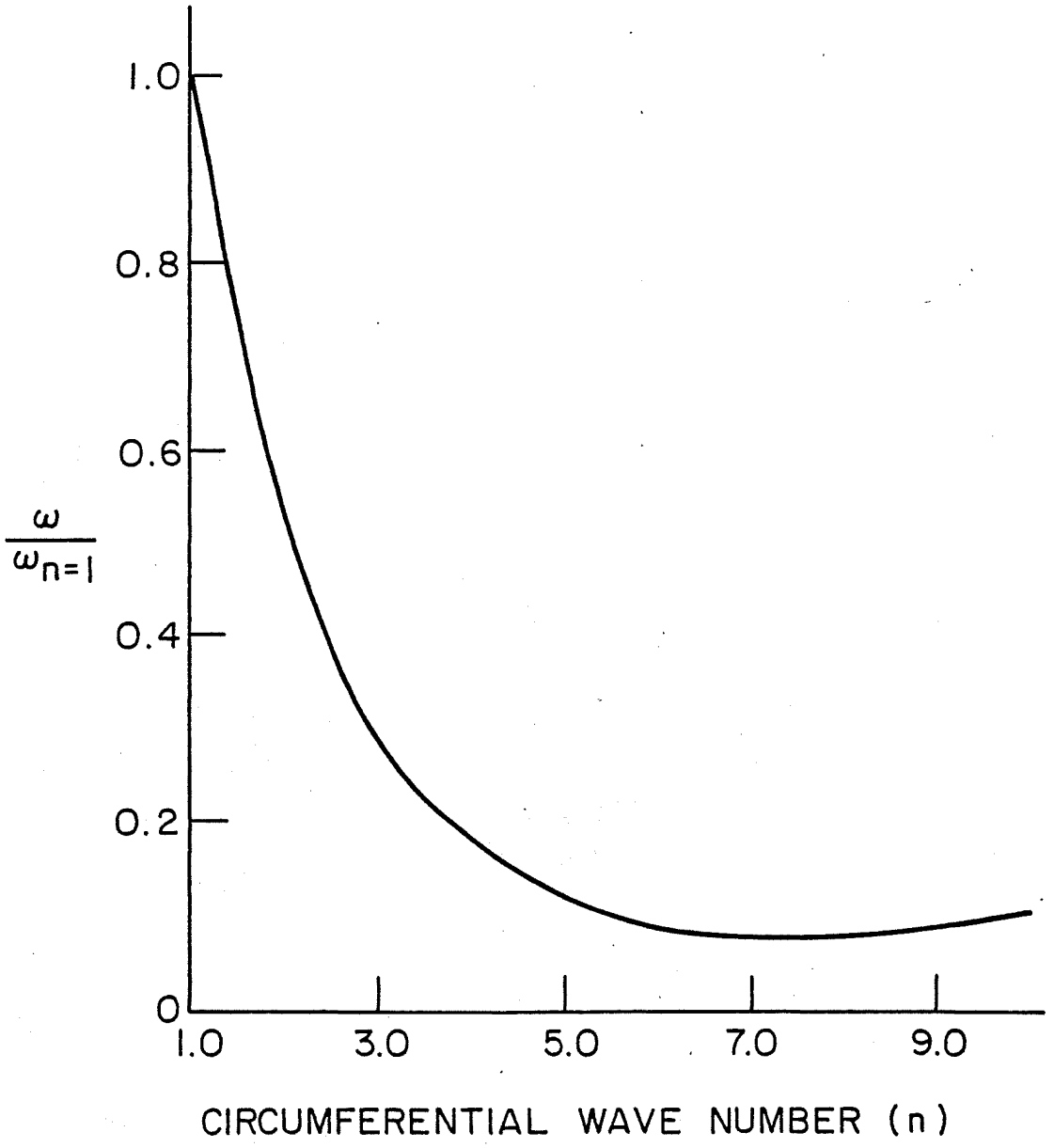

Fig. 21 Natural Frequency versus Number of Circumferential Waves

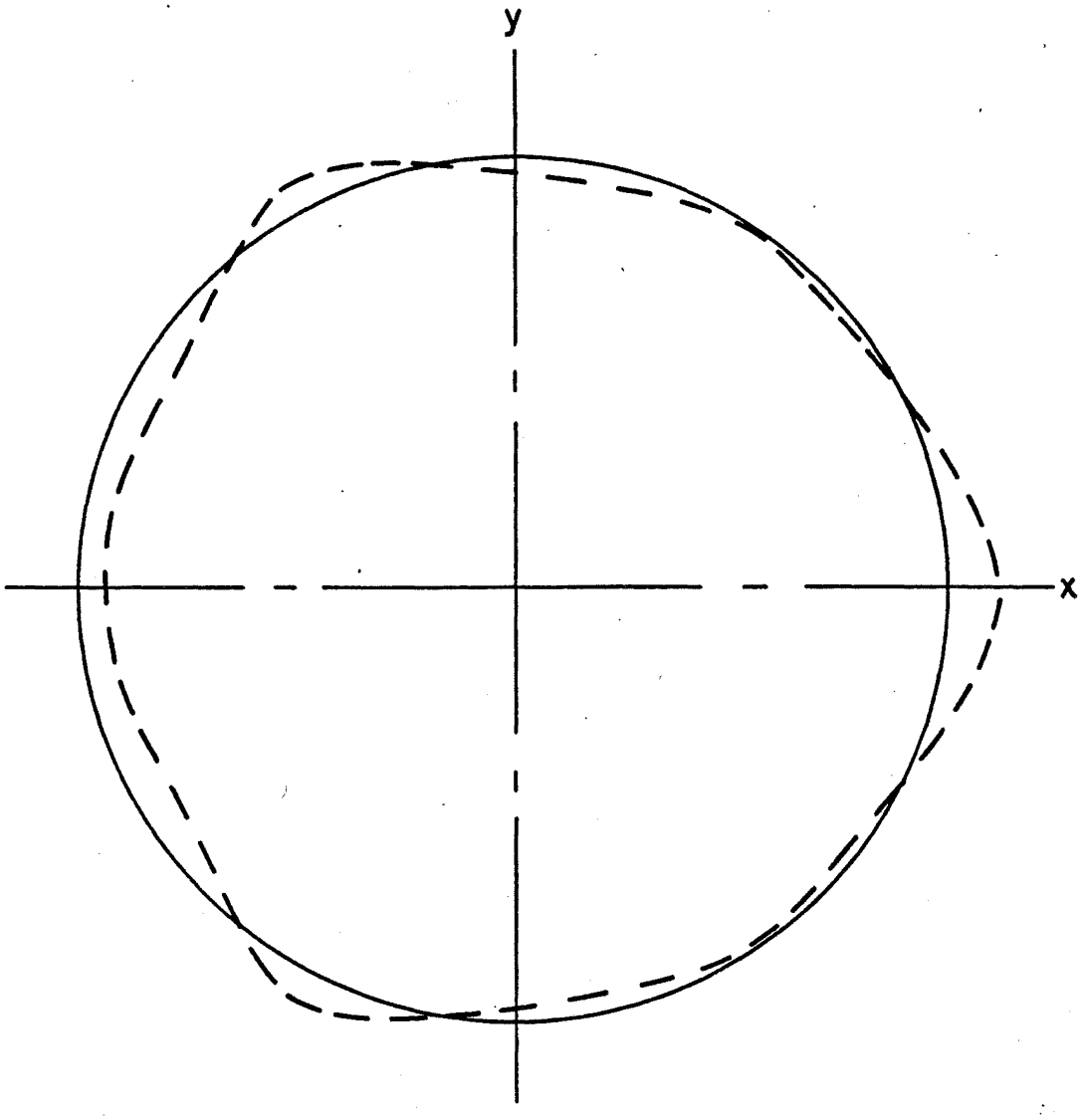

Fig. 22 Circumferential Mode Shape for Boundary Condition Case 2 (Anchors @ 40^{o})

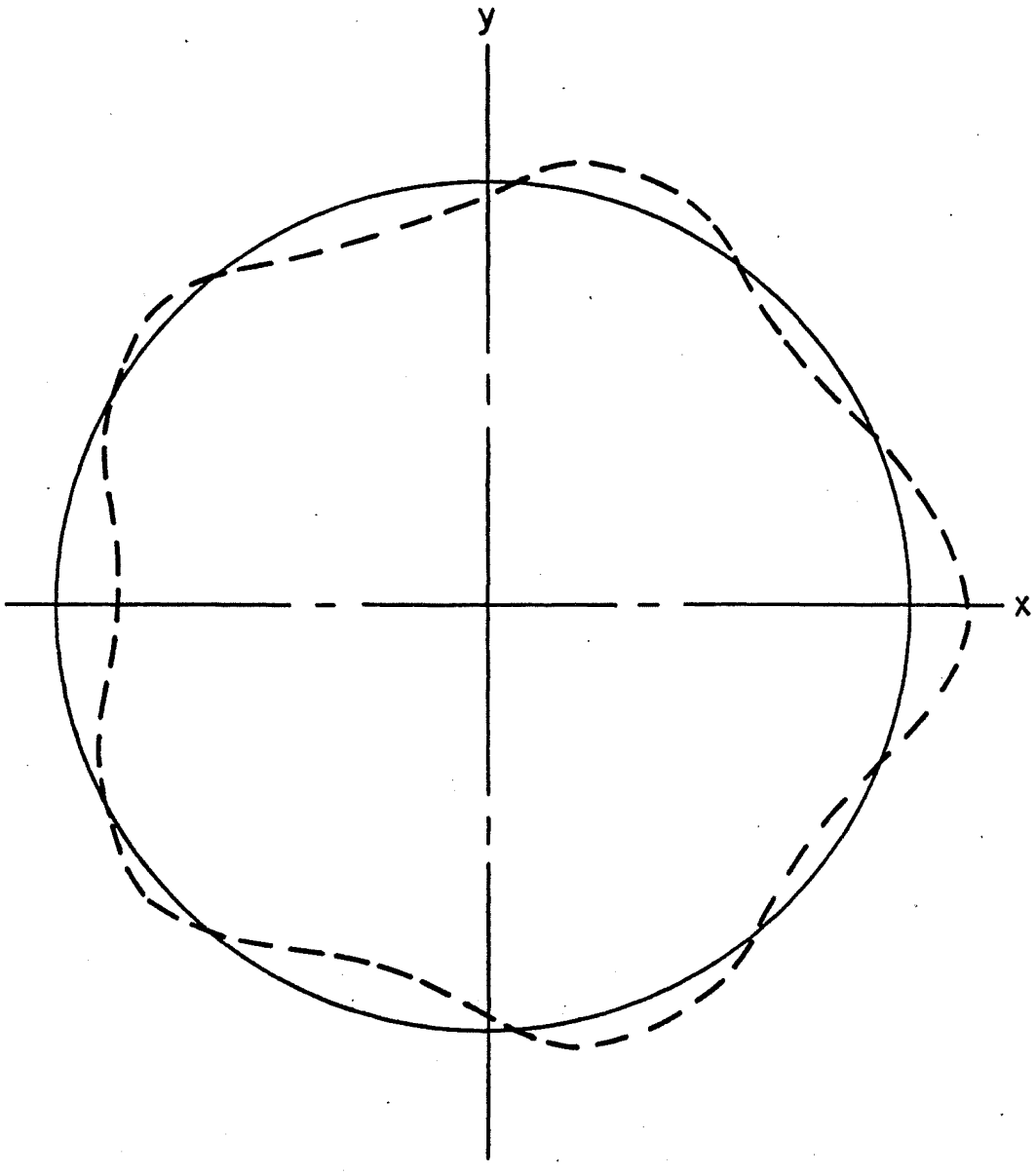

Fig. 23 Circumferential Mode Shape for Boundary Condition Case 3 (Anchors @ 60^{o})

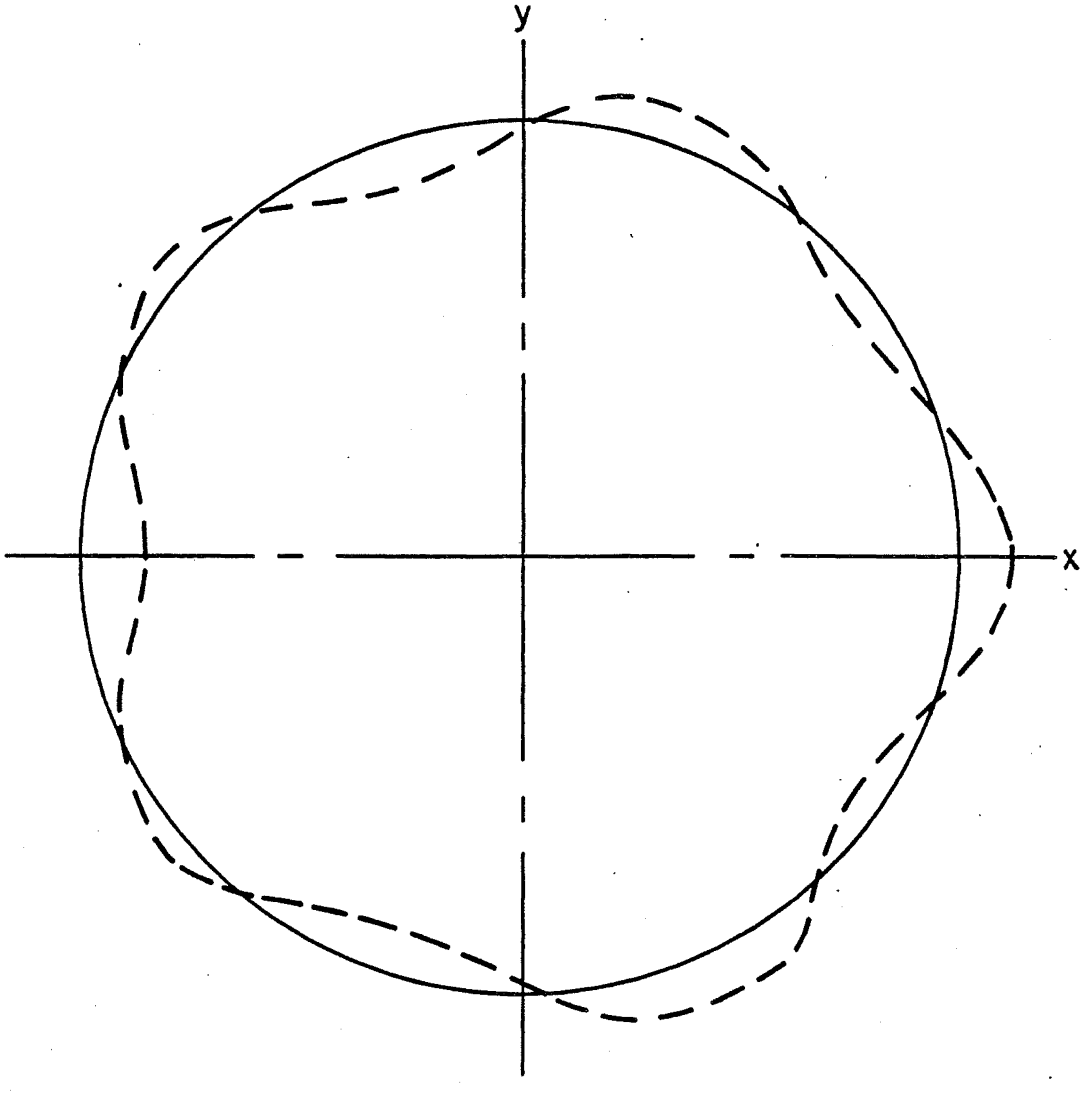

Fig. 24 Circumferential Mode Shape for Boundary Condition Case 4 (Anchors @ 120°)

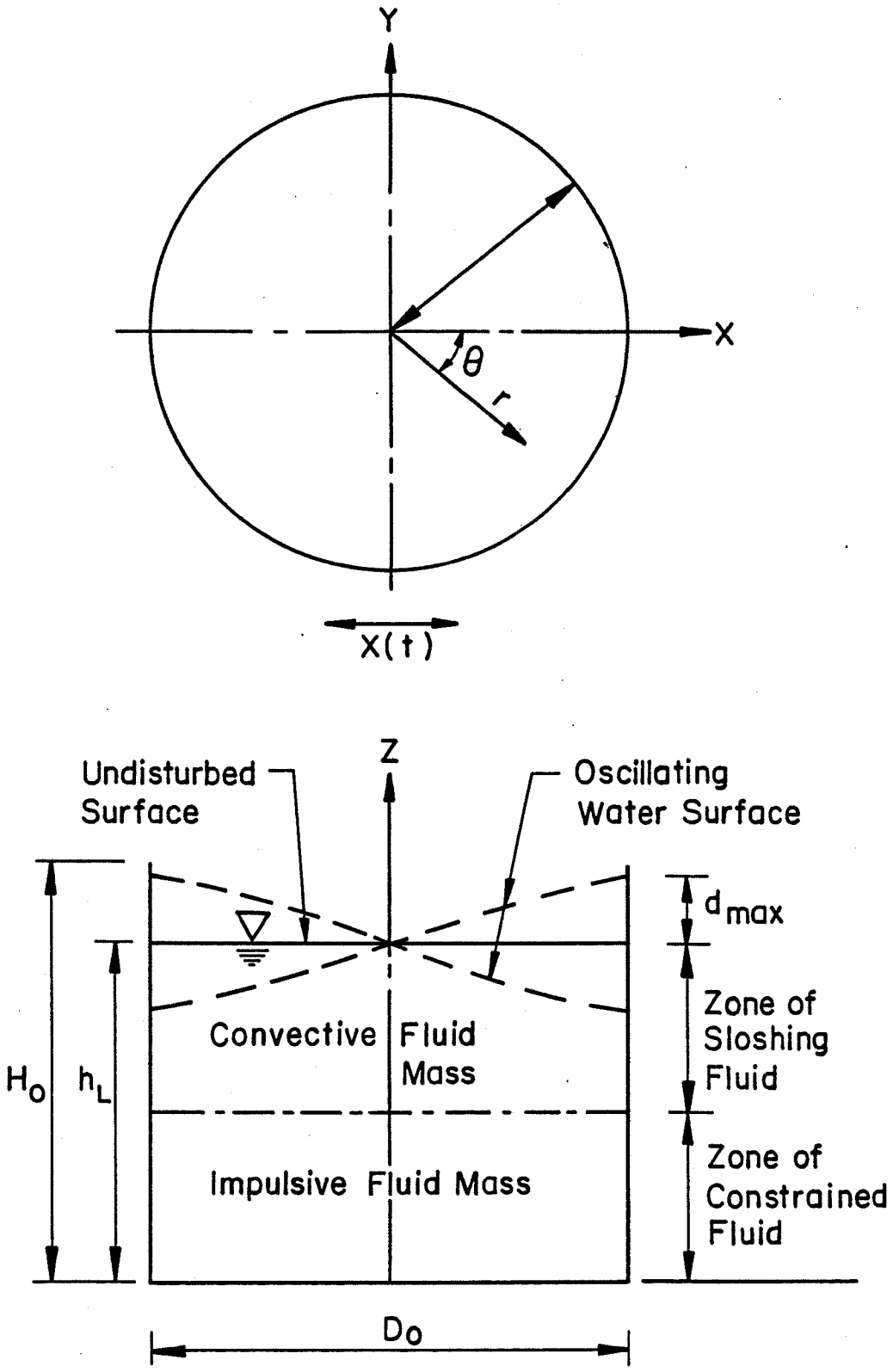

Fig. 25 Fluid Sloshing in a Cylindrical Tank

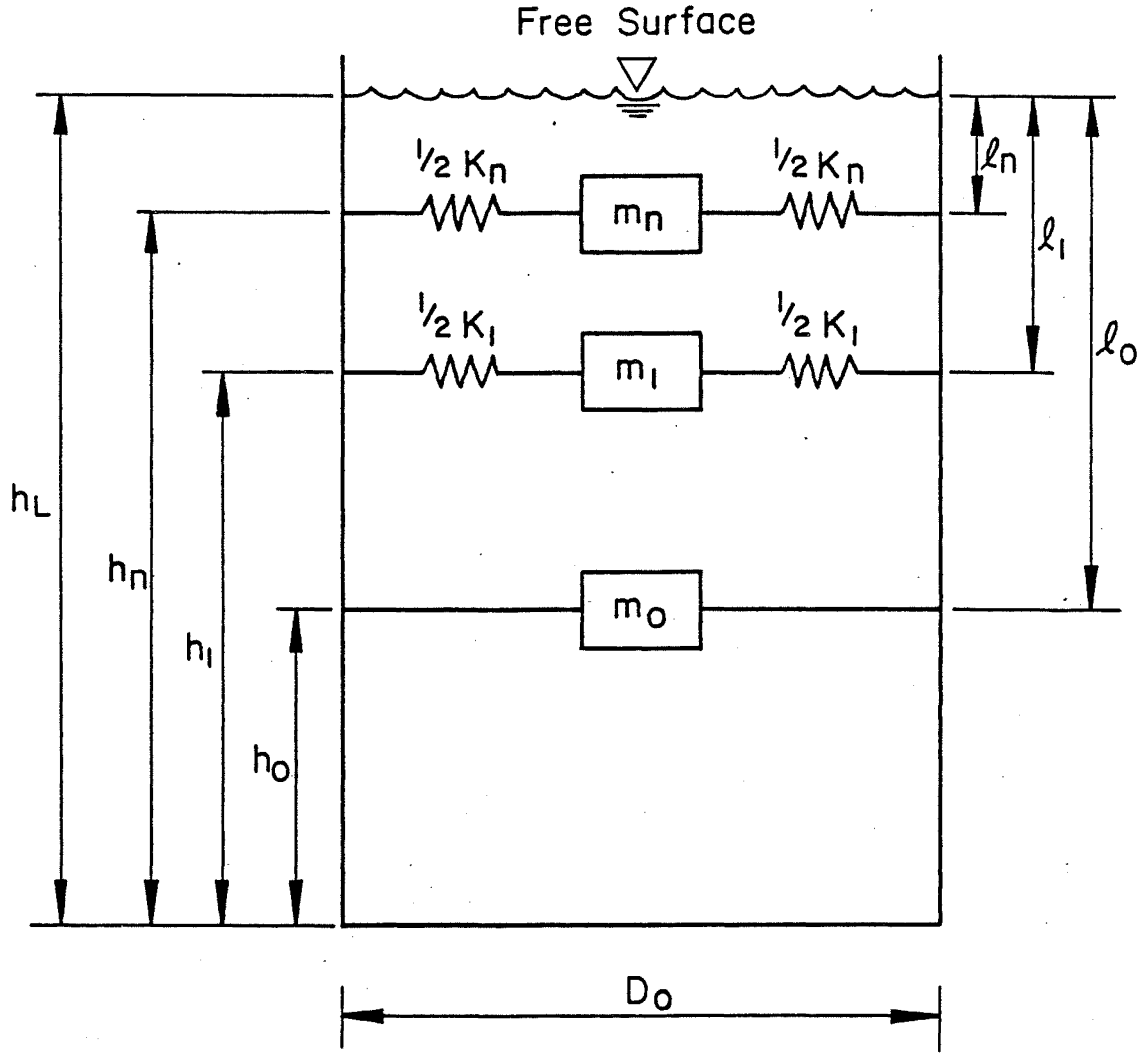

Fig. 26 Complex Mechanical Model for a Cylindrical Tank

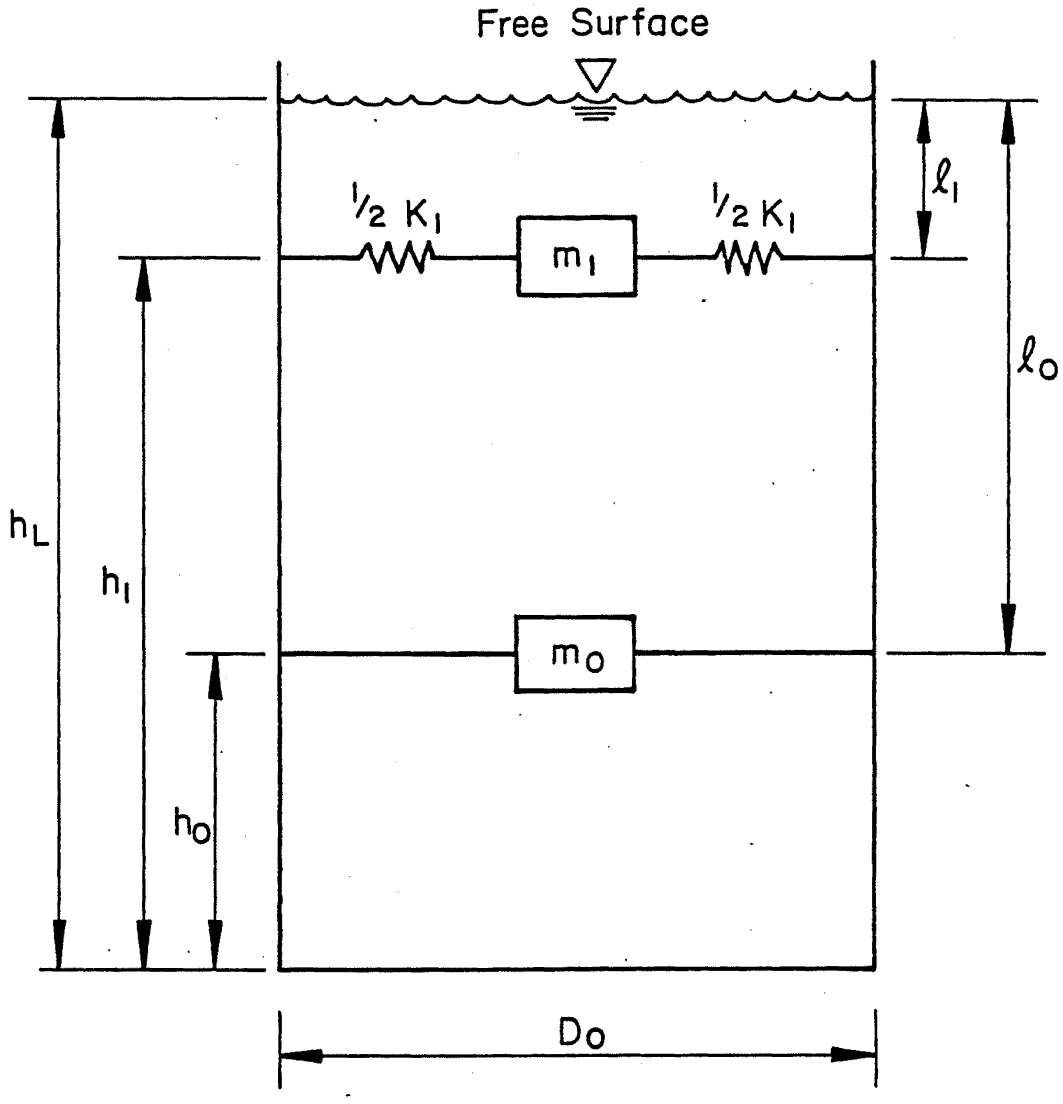

Fig. 27 Simple Mechanical Model for a Cylindrical Tank

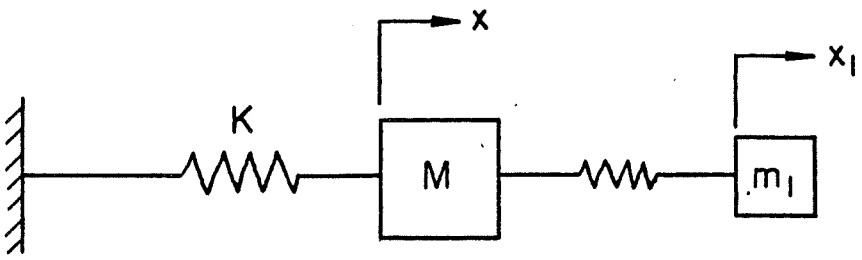

Fig. 28 Analytical Model of Shell-Liquid System

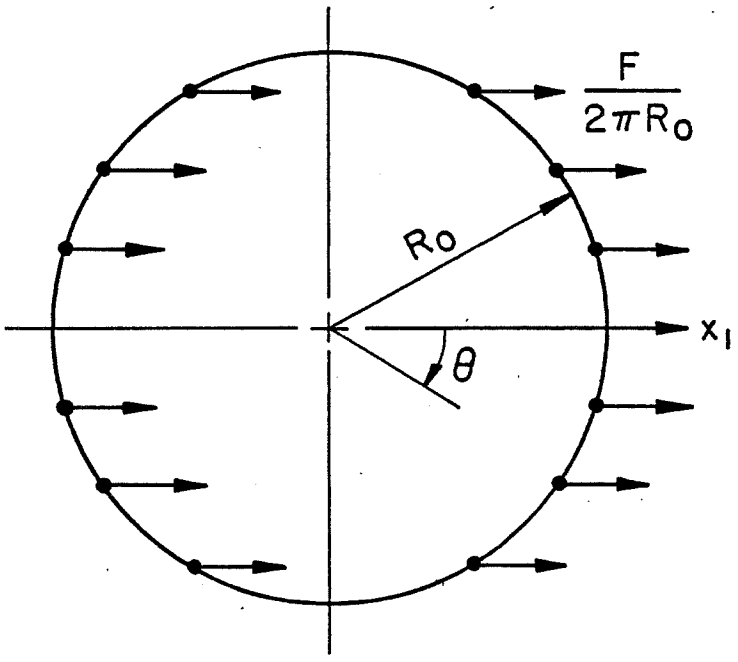

Fig. 29 Distribution of Sloshing Fluid Spring Force in the Shell

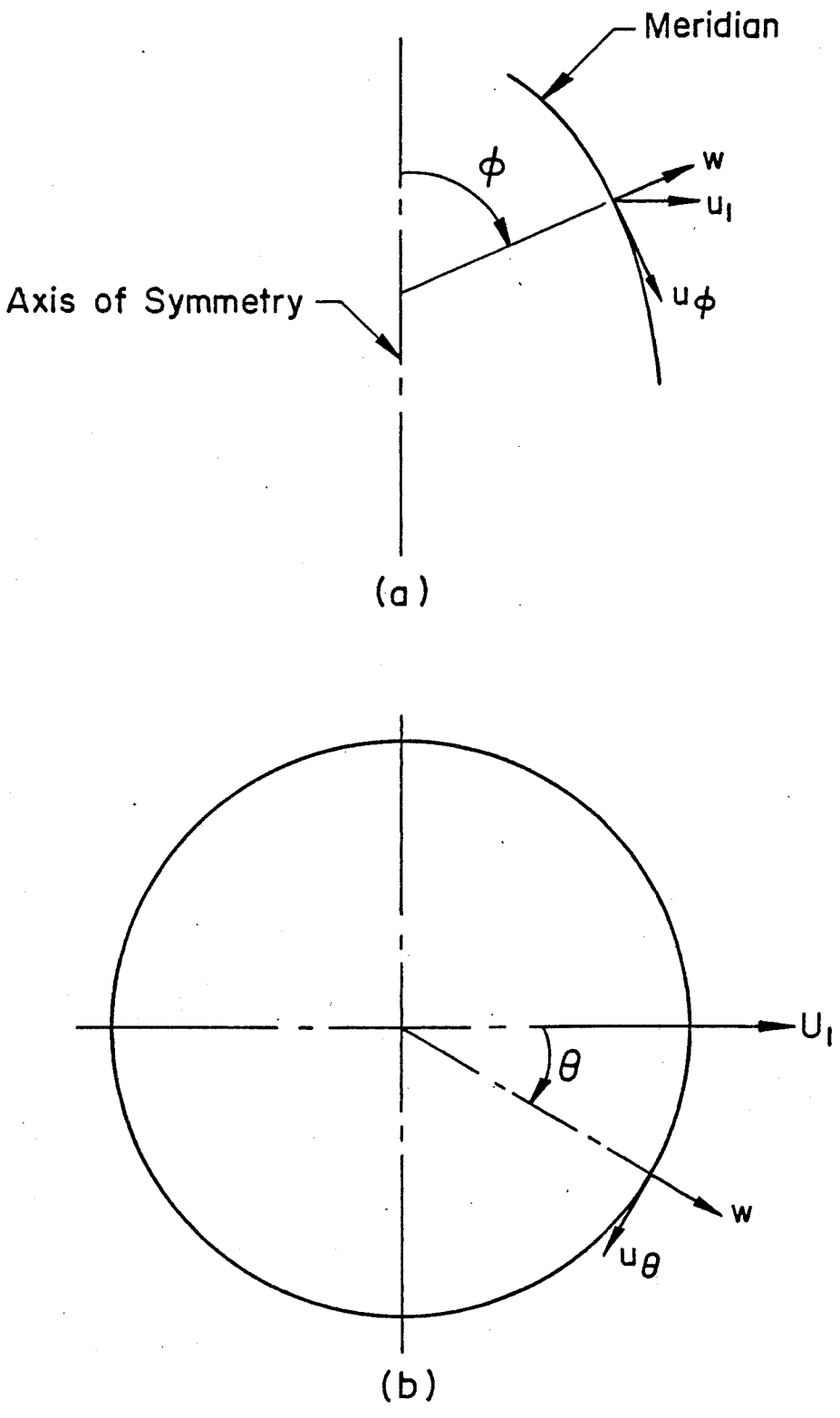

Fig. 30 Shell Displacement Components

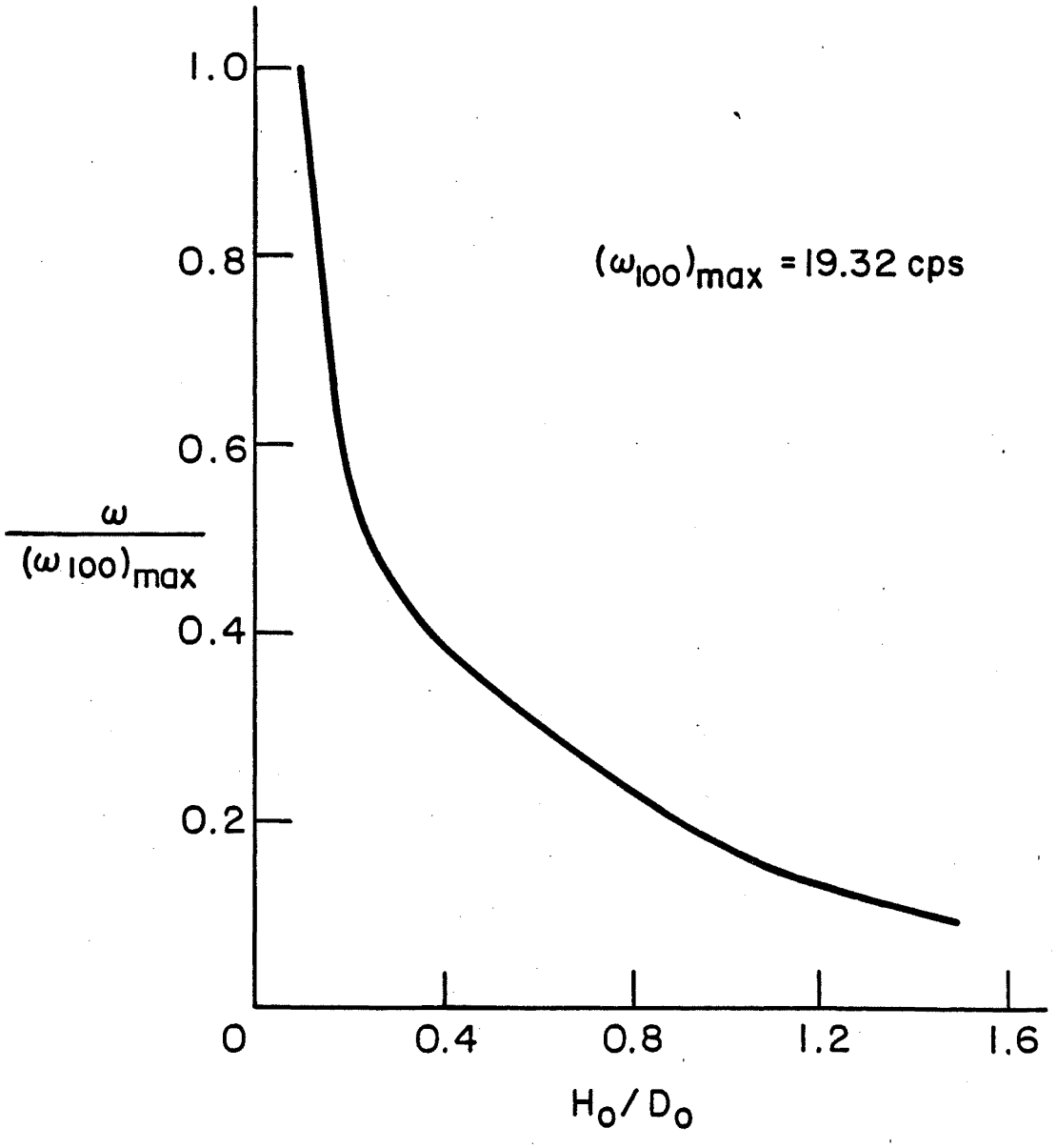

Fig. 31 Frequency versus Aspect Ratio for Cylindrical Tanks Full with Water

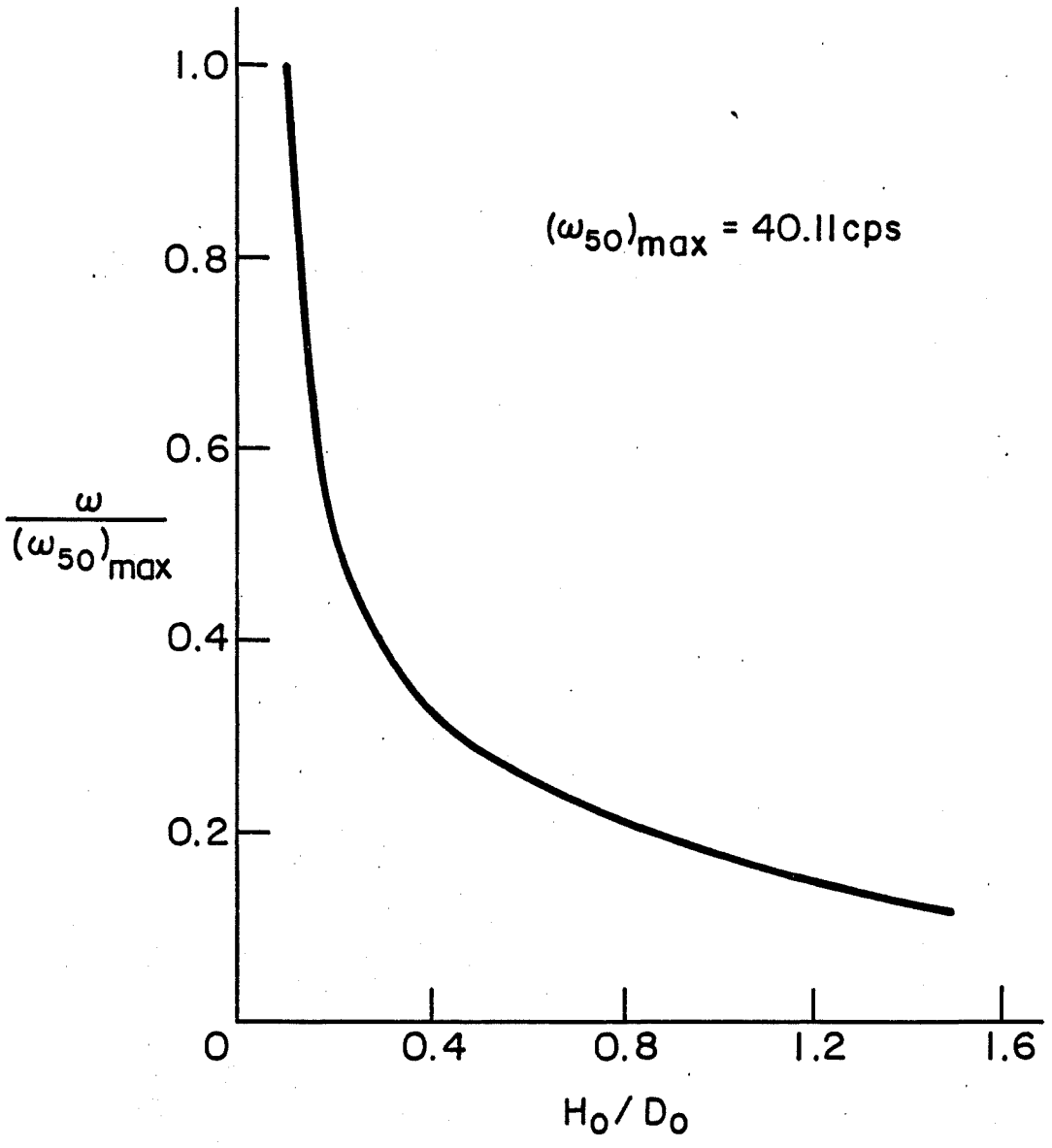

Fig. 32 Frequency versus Aspect Ratio for Cylindrical Tanks Half Full with Water

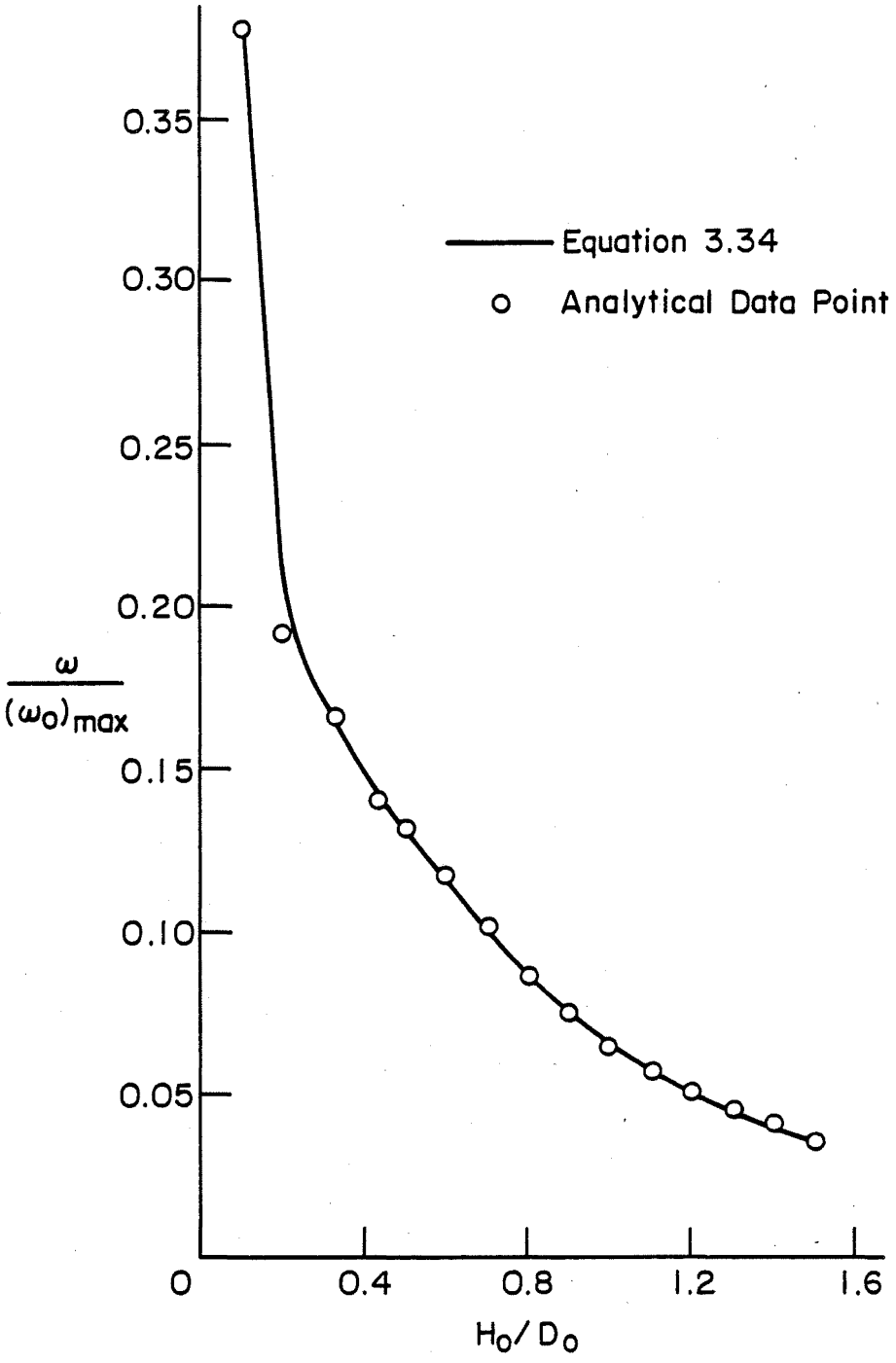

Fig. 33 Natural Frequencies of Tanks Full with Water

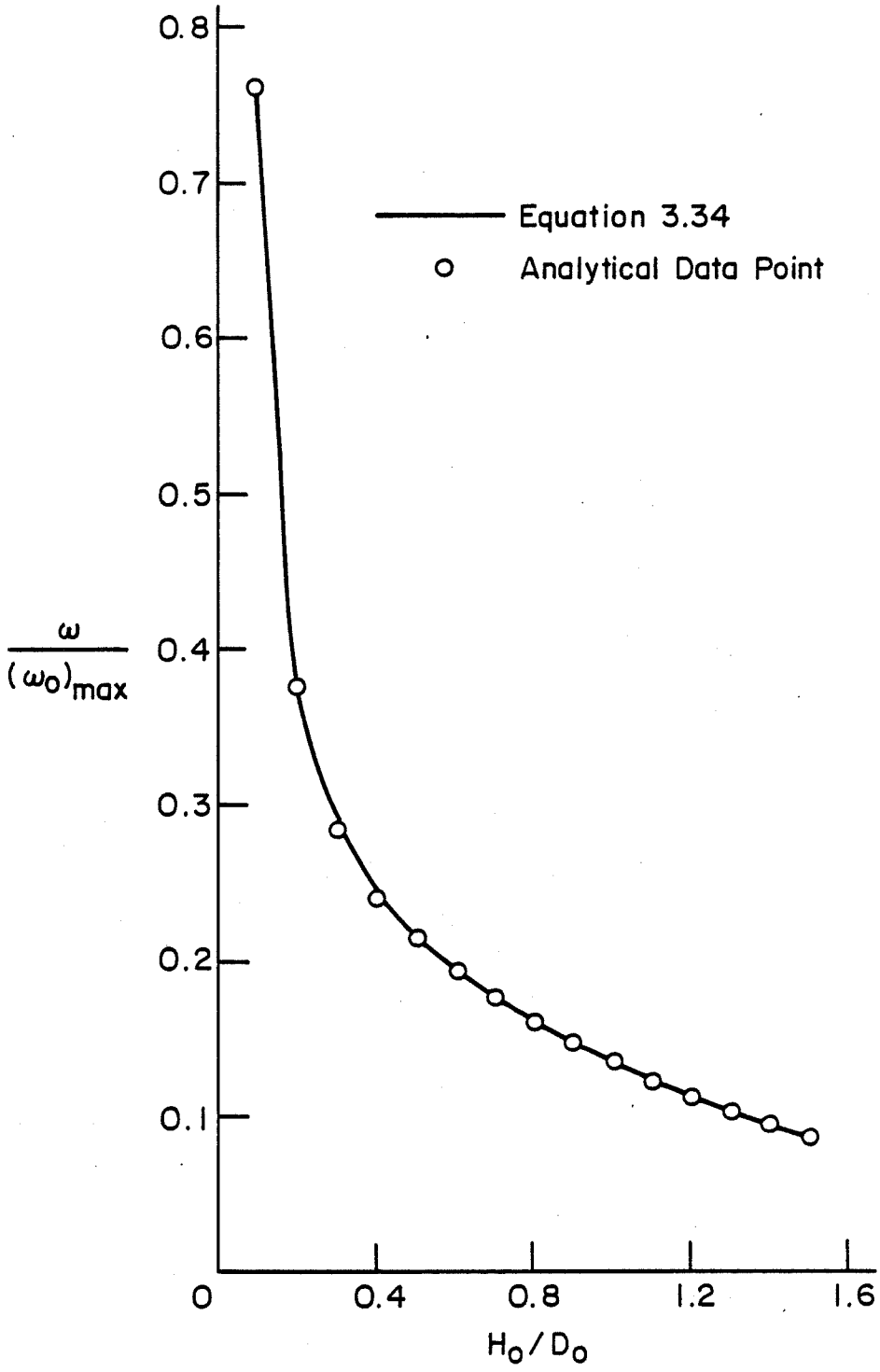

Fig. 34 Natural Frequencies of Tanks Half Full with Water

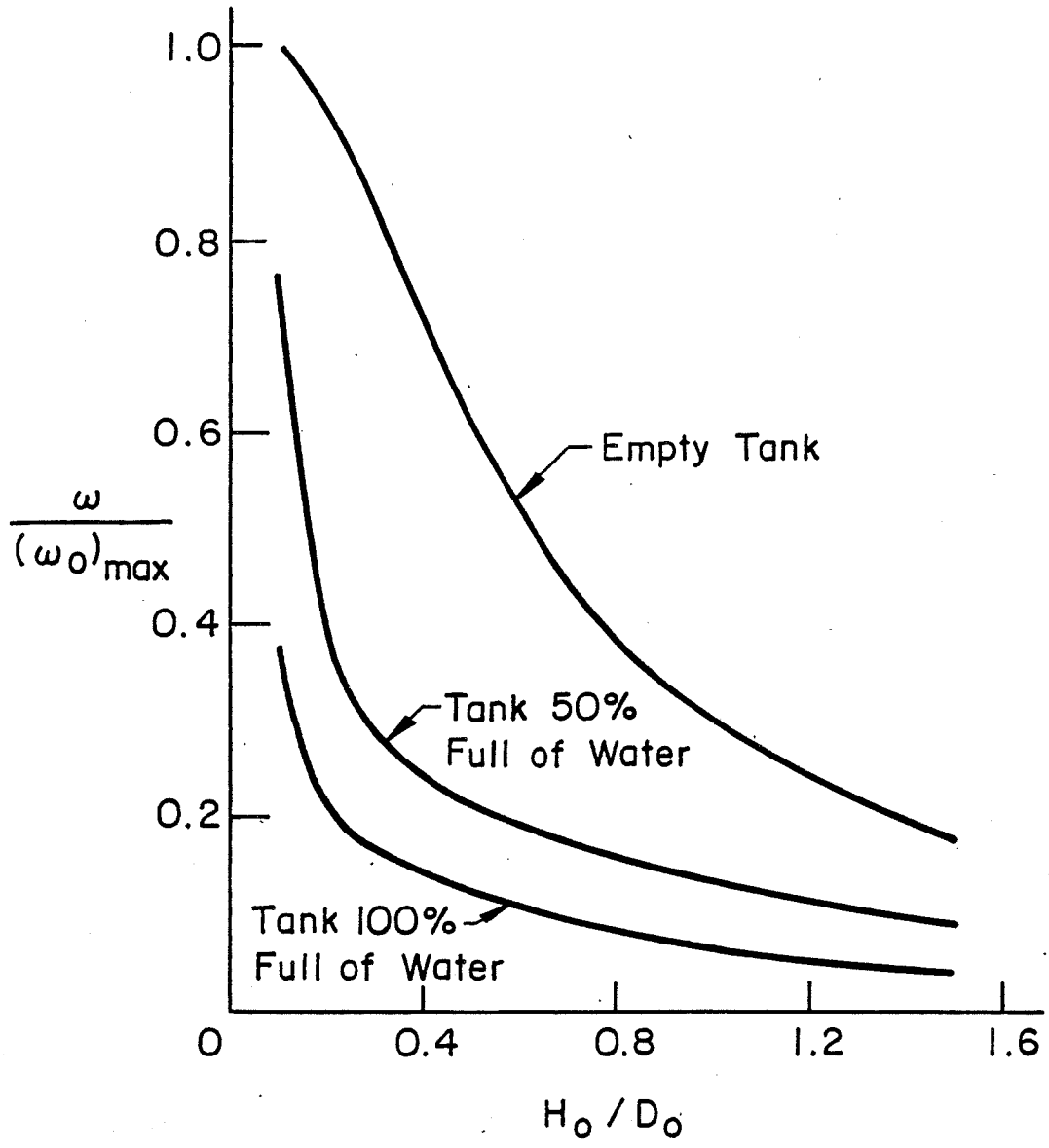

Fig. 35 Natural Frequencies of Empty, Half Full, and Completely Full Cylindrical Tanks

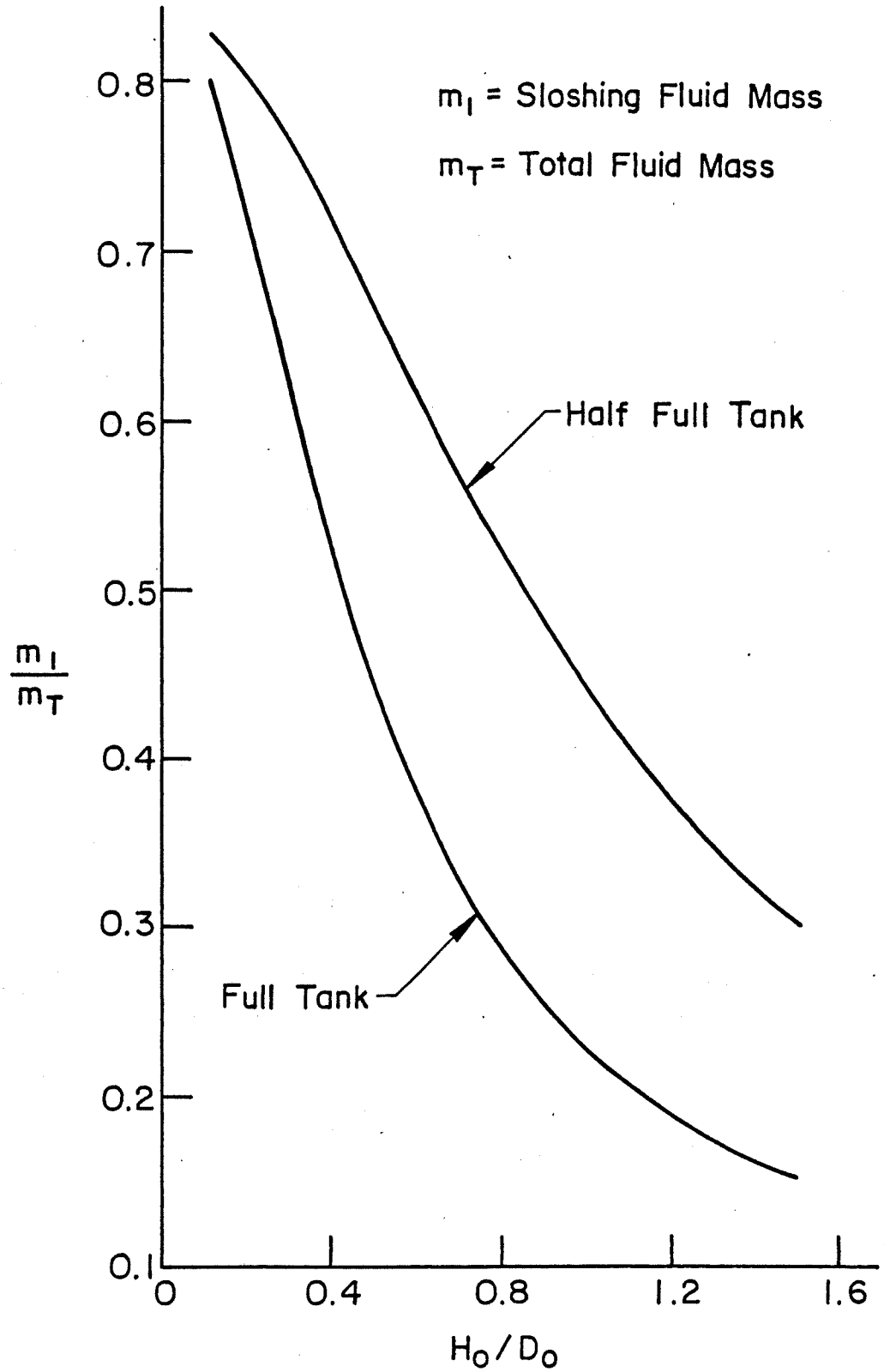

Fig. 36 Sloshing Fluid Mass versus Tank Aspect Ratio

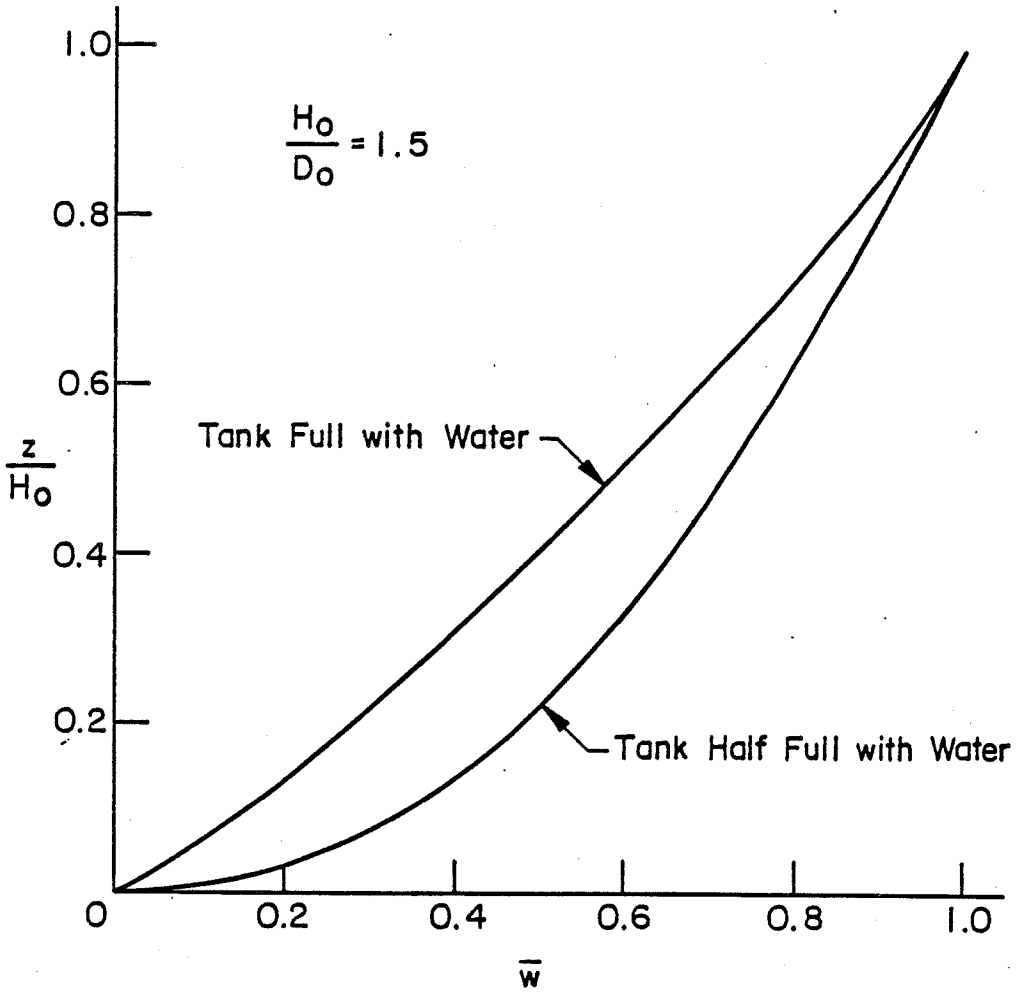

Fig. 37 Radial Displacement Mode Shapes for a Liquid-Filled Tall Tank

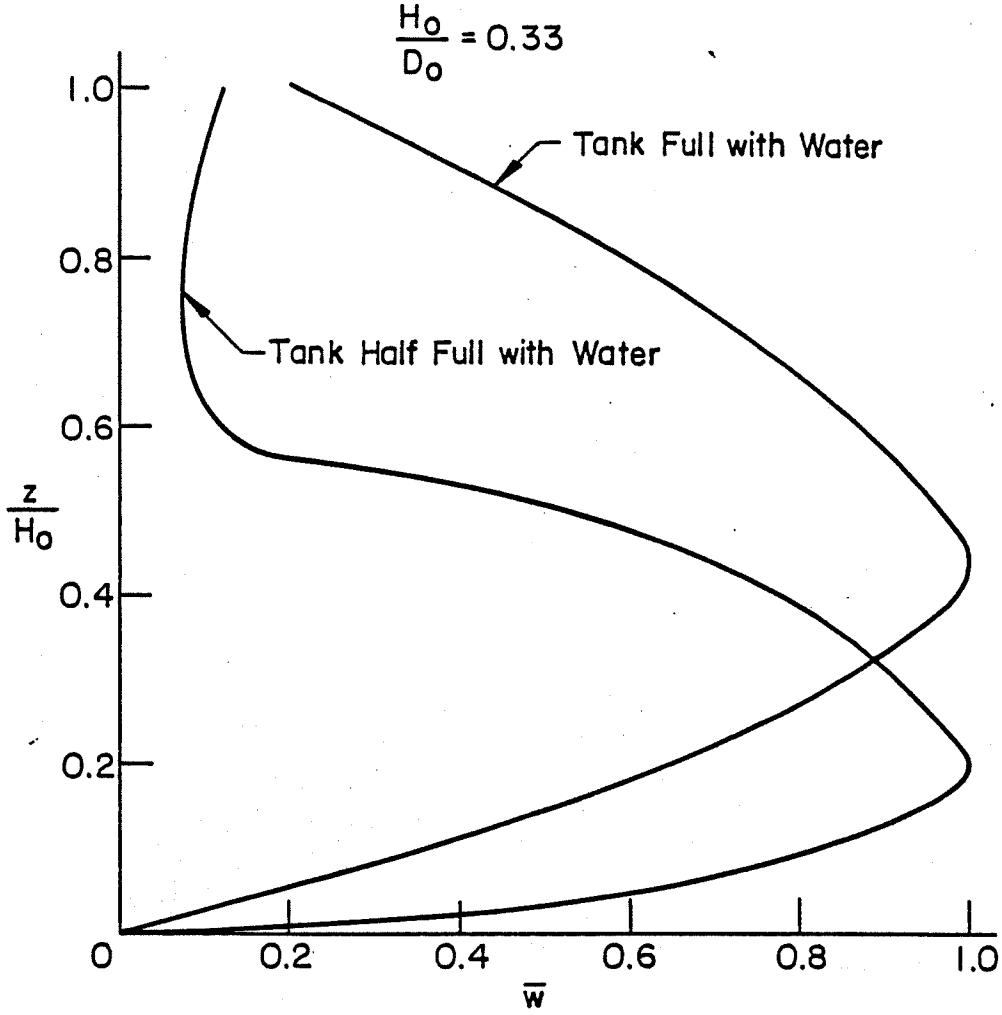

Fig. 38 Radial Displacement Mode Shapes for a Liquid-Filled Shallow Tank

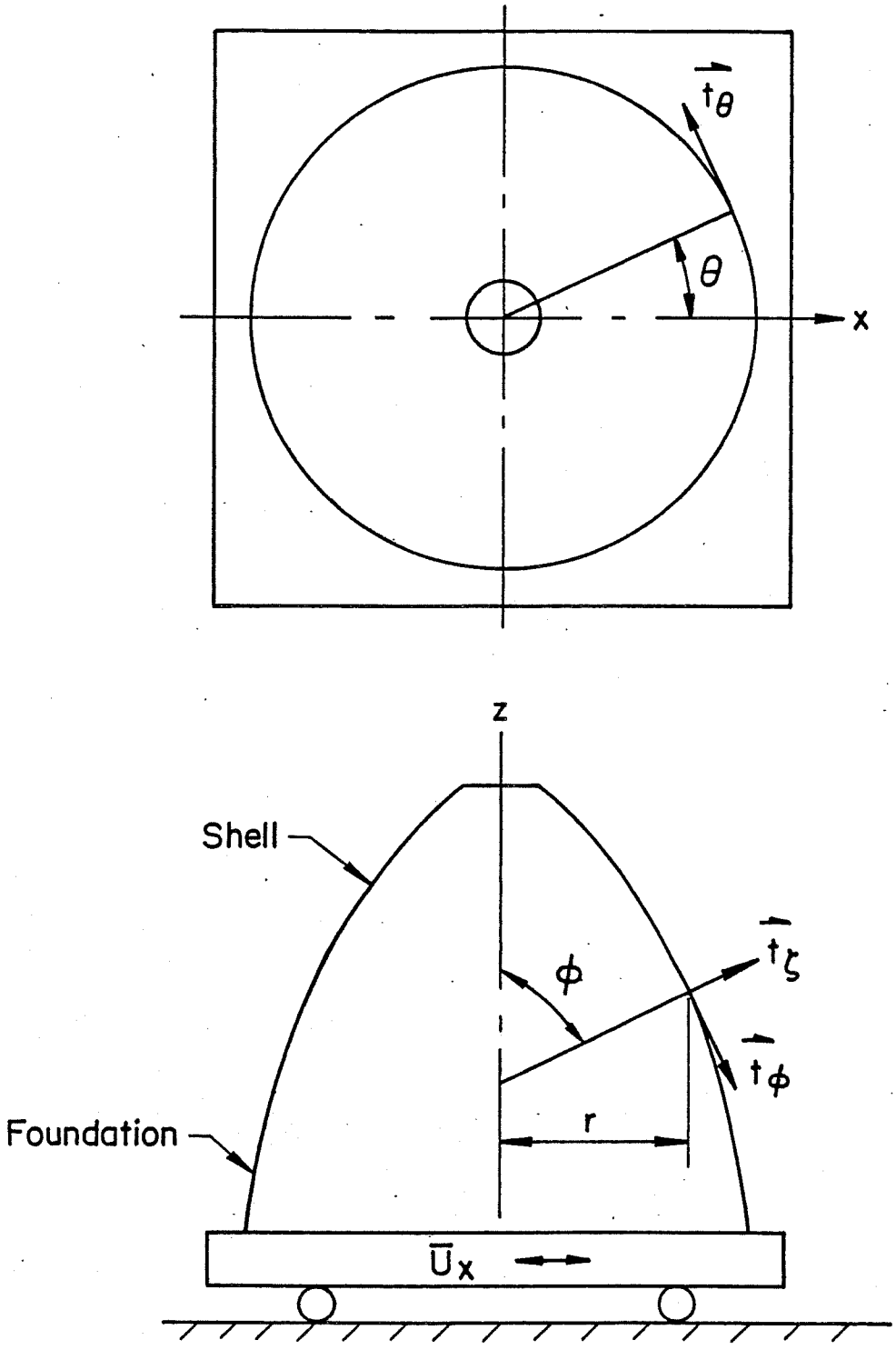

Fig. 39 Axisymmetric Shell on Moving Foundation

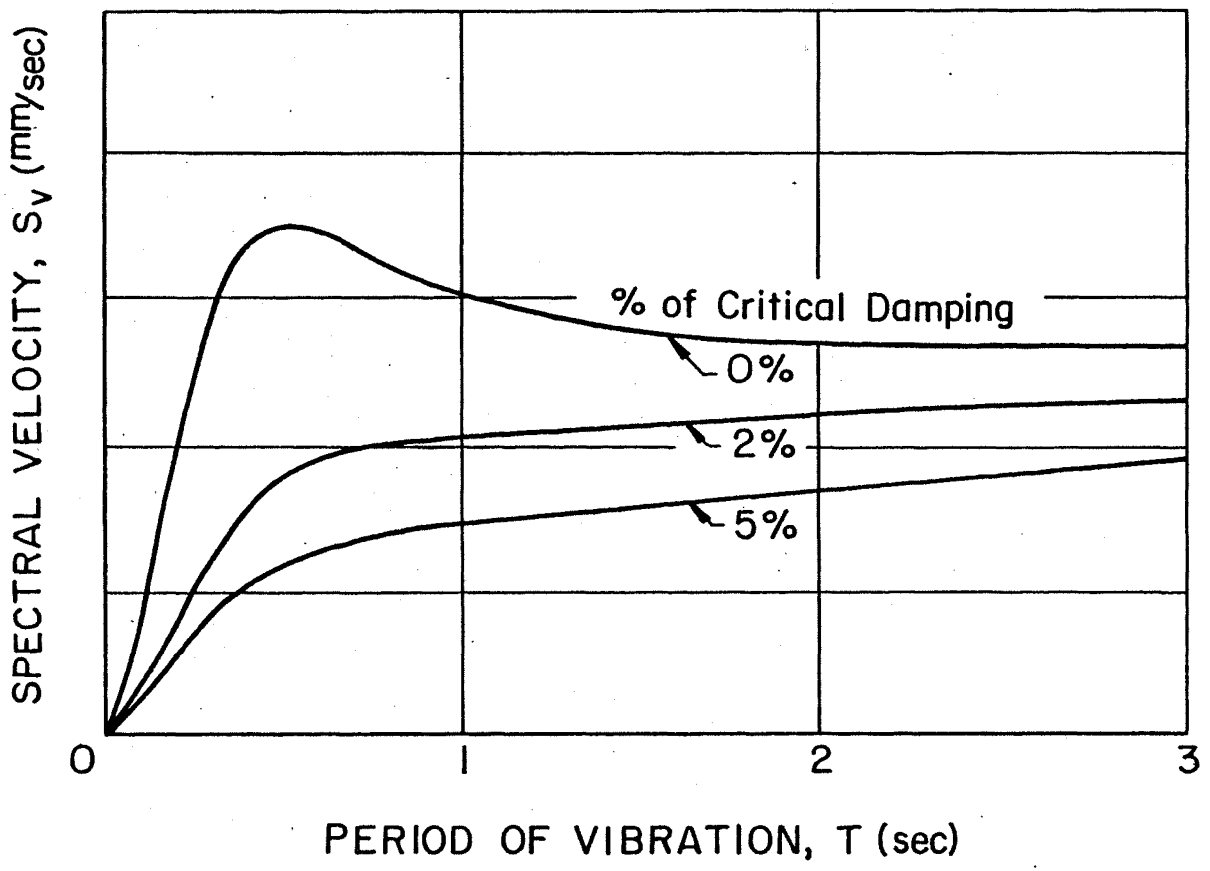

Fig. 40 Velocity Response Spectrum Curves, 1940 El Centro Intensity

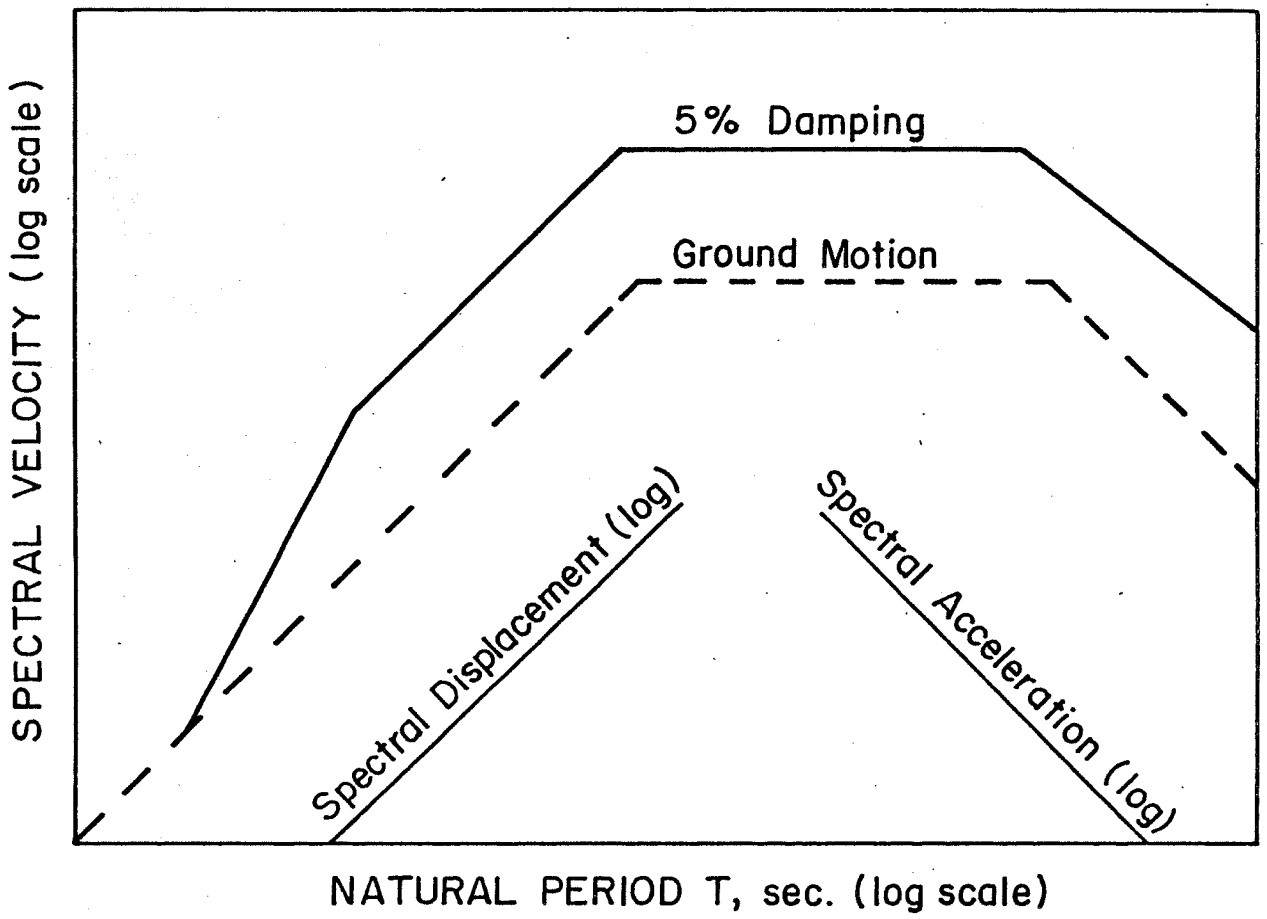

Fig. 41 Sample of Earthquake Design Spectrum

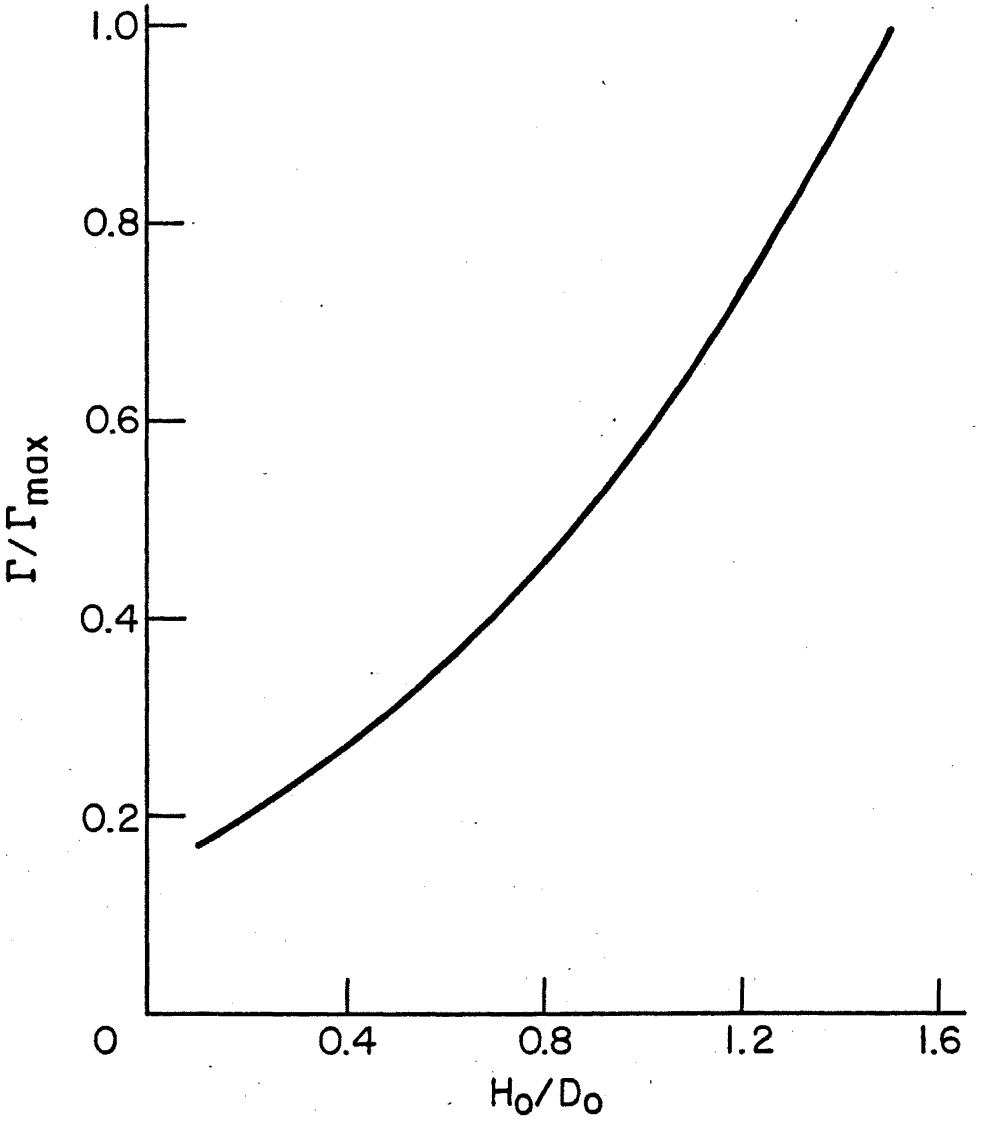

Fig. 42 Mode Participation Factor versus Tank Aspect Ratio

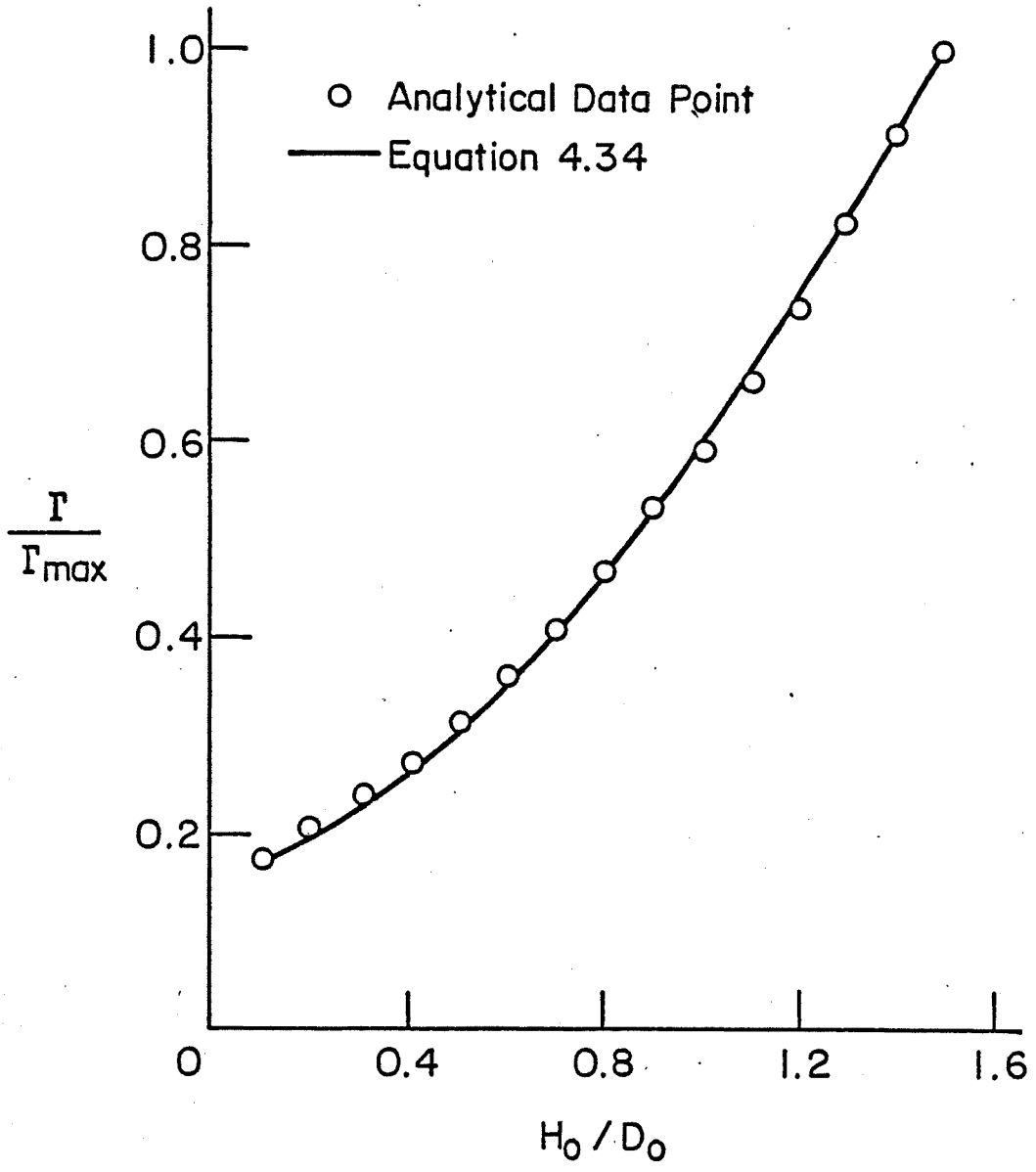

Fig. 43 Mode Participation Factor for Open-Top Cylindrical Tanks

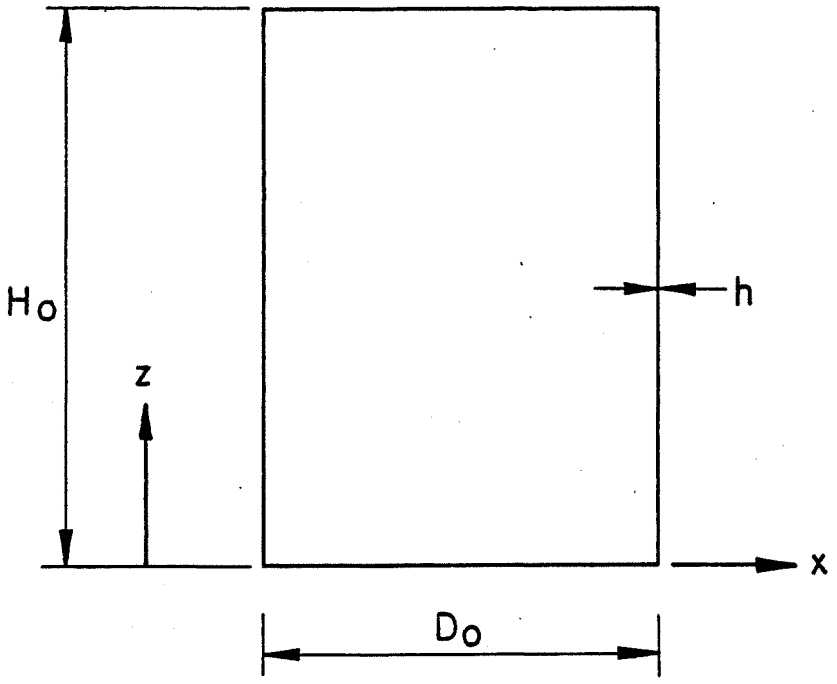

(a) Principal Designation

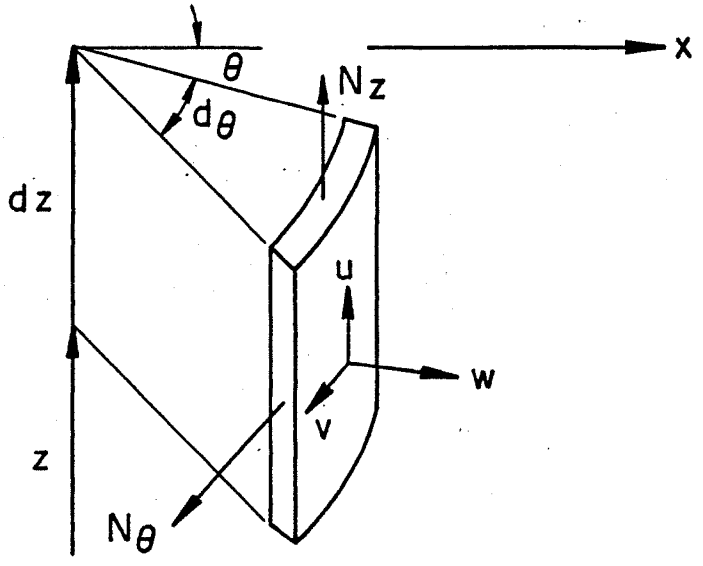

(b) Differential Element

Fig. 44 Cylindrical Shell Model

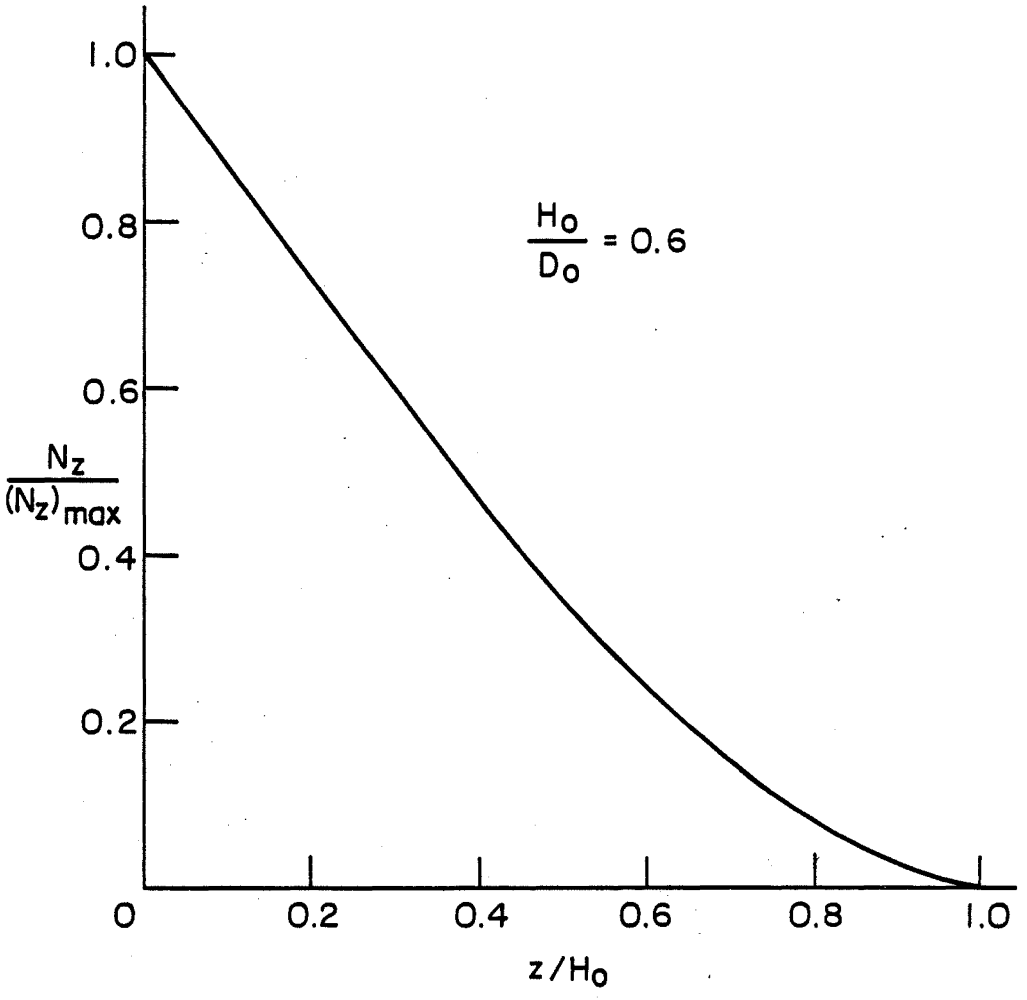

Fig. 45 Typical Axial Stress Resultant Distribution in an Empty Cylindrical Tank Undergoing Lateral Vibration

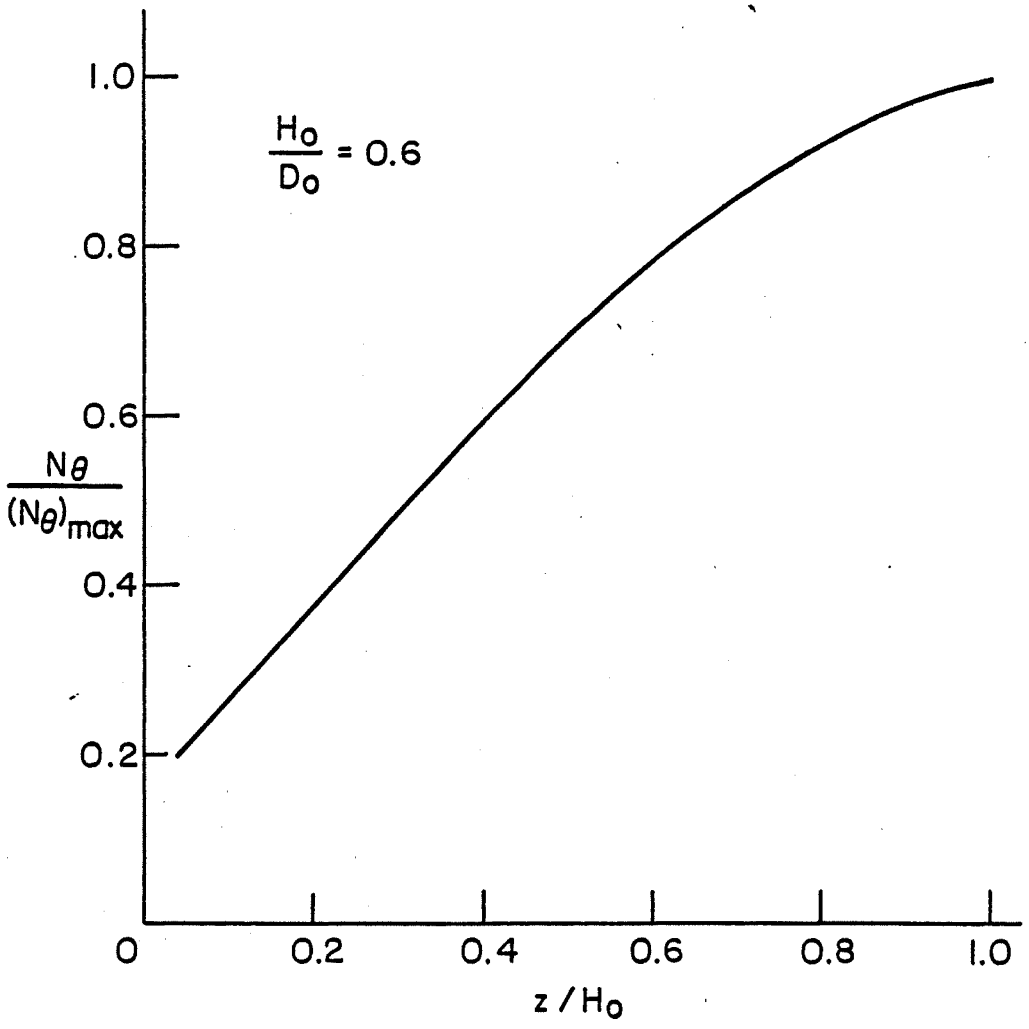

Fig. 46 Typical Circumferential Stress Resultant Distribution in an Empty Cylindrical Tank Undergoing Lateral Vibration

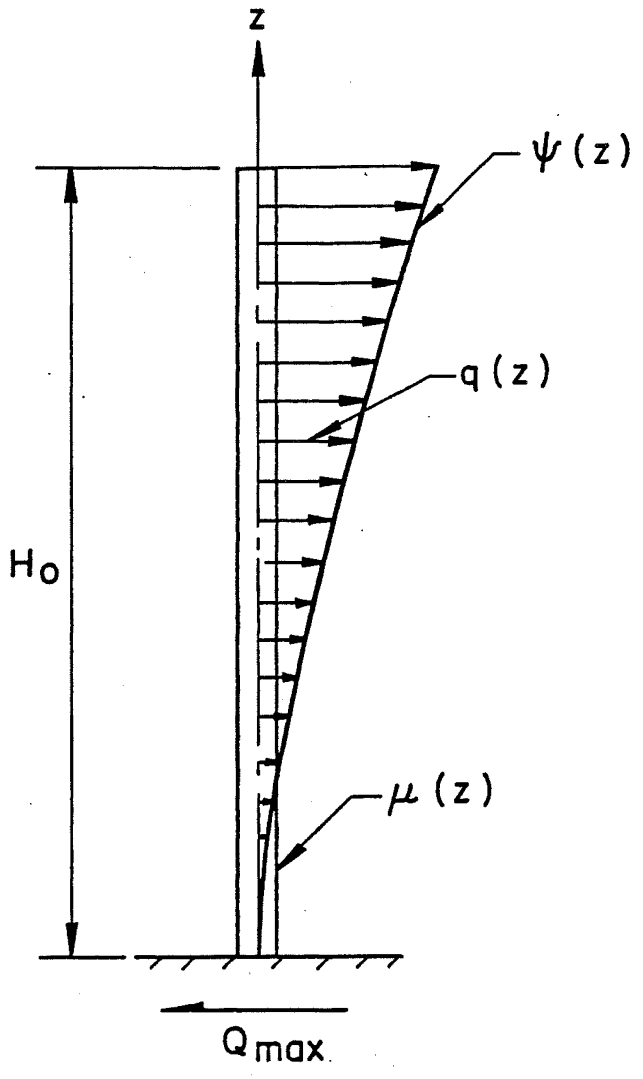

Fig. 47 Representation of Cylindrical Shell by an Equivalent Cantilever Column

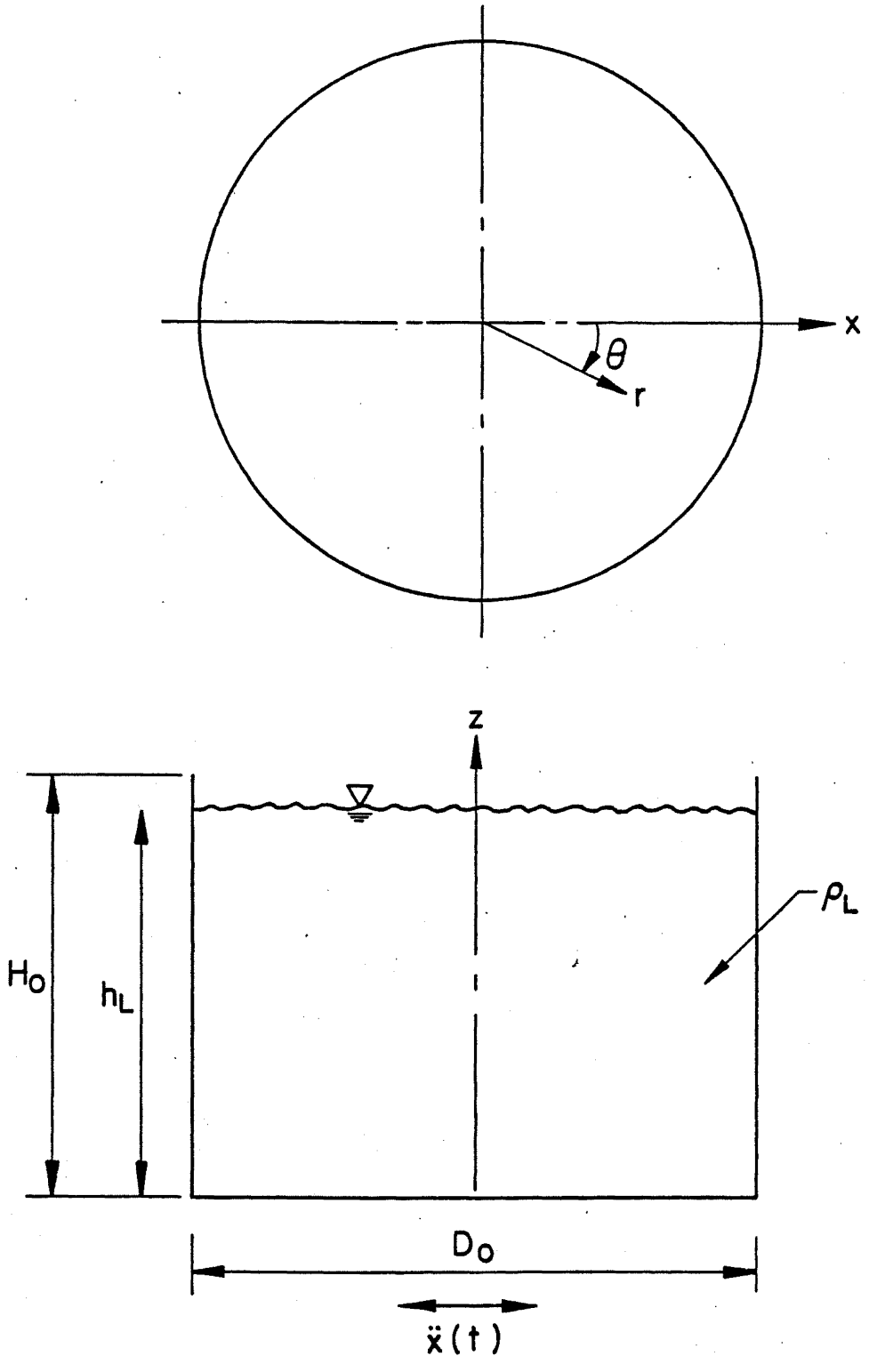

Fig. 48 Shell-Fluid System

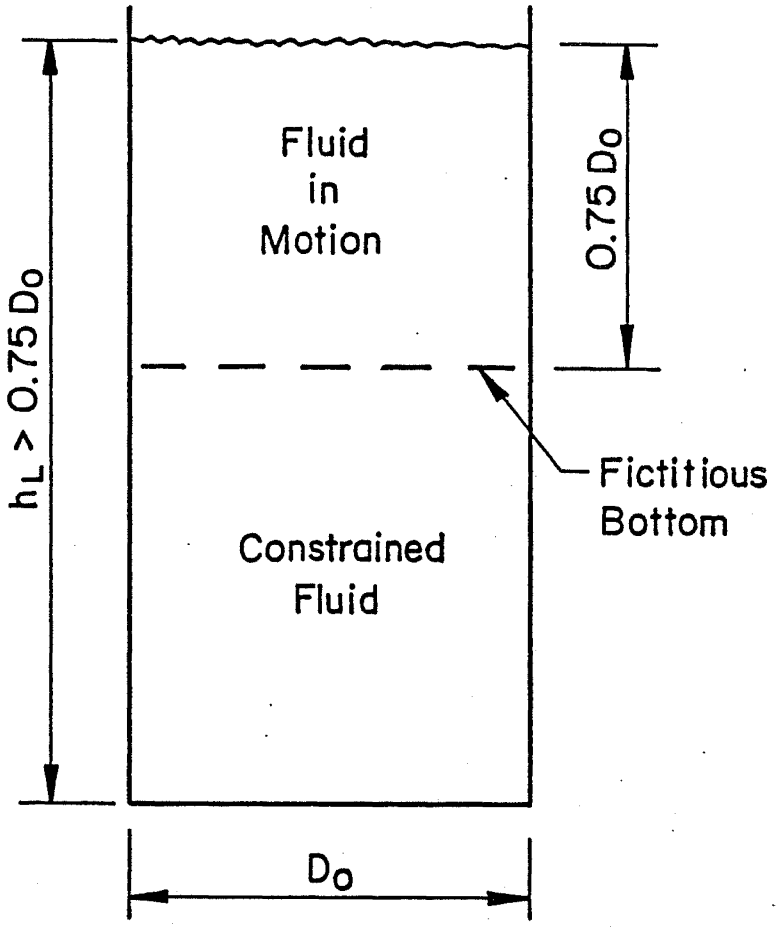

Fig. 49 Idealization for a Slender Container

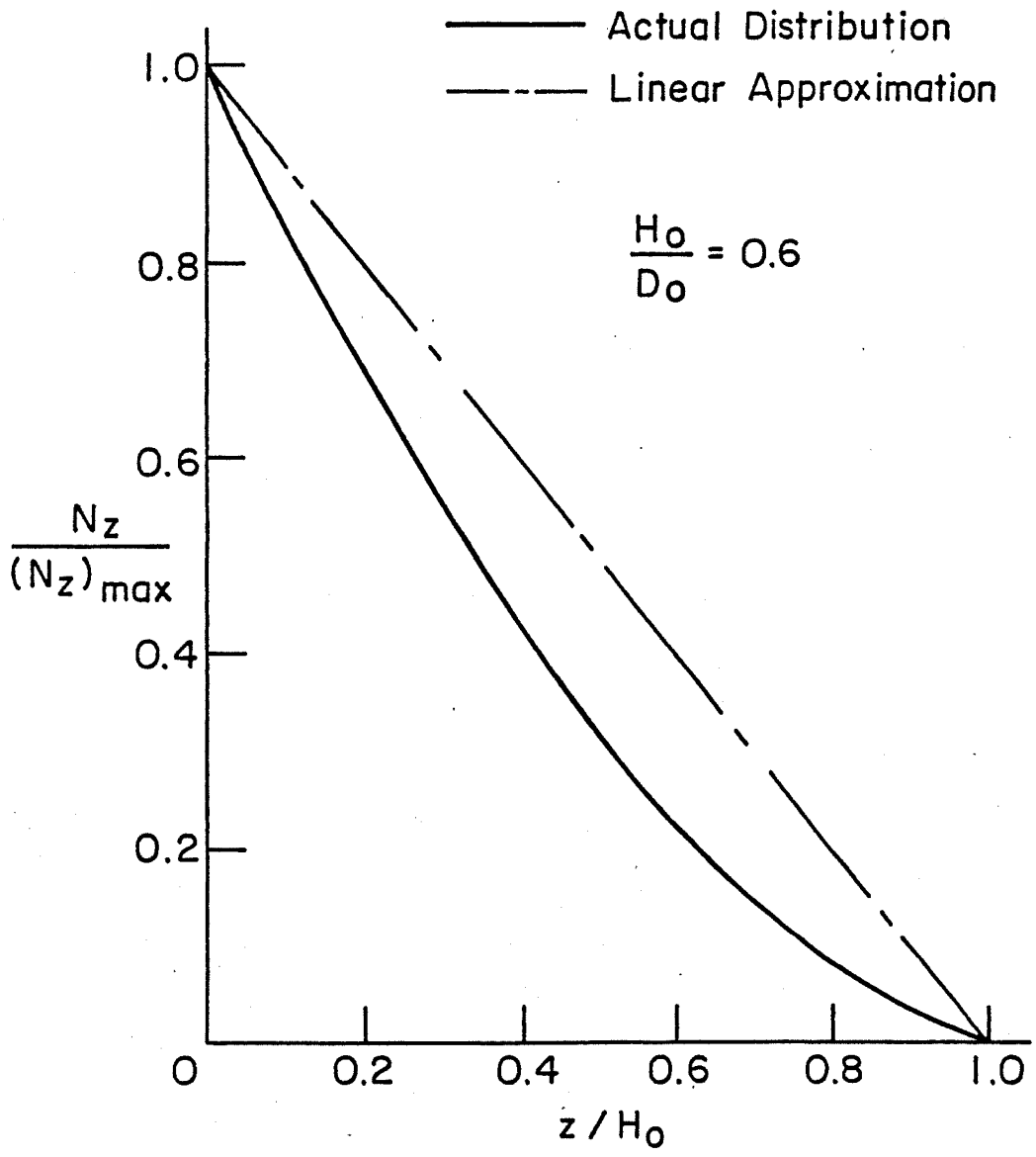

Fig. 50 Linear Approximation for Axial Stress Resultant Distribution in a Liquid-Filled Cylindrical Tank Undergoing Lateral Vibration

NOMENCLATURE

A = any desired variable (such as displacement or stress) of the forced vibration solution

A_i = polynomial coefficient

B = variable corresponding to A, taken from the free vibration solution

C_f = frequency constant (1600.2 in/sec; 5252 ft/sec)

C_i = polynomial coefficient

C_m = mode participation constant (0.0017952 in/sec; 0.0005472 ft/sec)

C_{N_θ} = circumferential stress constant ($\frac{10675.7}{D_o}$ MN/m^3; $\frac{5080000.0}{D_o}$ lb/in^3)

C_{N_z} = axial stress constant ($\frac{2933.7}{D_o}$ MN/m^3; $\frac{1396000.0}{D_o}$ lb/in.^{3})

C_w = radial displacement constant

D = shell elasticity constant ($D = Eh^3/12(1 - \nu^2)$)

D_o = diameter of a cylindrical tank

E = Young's modulus

E_s = Young's modulus for steel (206900.0 MN/m^3; 30,000 ksi)

F = horizontal force exerted by spring of sloshing fluid mass to shell wall

$F(t)$ = Duhamel integral

F_1 = generalized force for sloshing fluid mass

G = $1/(\frac{1 + D \sin^2\phi}{Kr^2})$

H = $\frac{1}{R_\phi} - \frac{\sin\phi}{r}$

I = moment of inertia about a cross section at the base of the tank

J = generalized force for an empty cylindrical shell

K = shell elasticity constant ($K = \frac{Eh}{1 - \nu^2}$)

K_n = spring stiffness of liquid mass participating in n^{th} sloshing mode

K_r = roof mass coefficient

K_1 = spring stiffness of liquid mass participating in first sloshing mode

L = characteristic length of shell

M = generalized mass for empty cylindrical shell

M_{BM} = bending moment about a cross section at the base of the tank

M_o = equivalent mass of shell and stationary fluid mass

$(M_{OTM})_c$ = convective hydrodynamic overturning moment

$(M_{OTM})_i$ = impulsive hydrodynamic overturning moment

M_1 = generalized mass for shell and stationary fluid mass

M_ϕ, M_θ, $M_{\phi\theta}$ = moment resultants

$\bar{N}(\frac{z}{H_o})$ = stress variable for N_z or N_θ

$\bar{\bar{N}}(\frac{z}{H_o})$ = non-dimensional stress function for N_z or N_θ

N_ϕ, N_θ, $N_{\theta\phi}$ = membrane stress resultants

P = $\frac{1}{R_\phi} + \nu\frac{\sin\phi}{r}$

Q_c = convective hydrodynamic base shear

Q_i = impulsive hydrodynamic base shear

Q_ϕ, Q_θ = transverse shear resultants

R_o = radius of the latitude circle at the location where the sloshing fluid mass spring is attached

R_ϕ = radius of curvature of the meridian

R_θ = length of the normal between any point on the reference surface and the axis of rotation

S = arclength along the meridian

S_a = maximum pseudo spectral acceleration

$(S_a)_1$ = spectral acceleration of fundamental sloshing fluid mass

S_d = maximum spectral displacement

$(S_d)_1$ = spectral displacement of fundamental sloshing fluid mass

S_v = maximum pseudo velocity

U_x = amplitude factor for horizontal foundation displacement

$\overline{U}_x$ = horizontal time dependent displacement of the foundation

U_1 = displacement of shell wall parallel to the x_1-axis at the location of the fundamental sloshing fluid mass spring

V = volume of the shell wall from the bottom of the shell to the point where the sloshing mass spring (K_1) is attached

a = radius of cylindrical shell

d_{max} = maximum water surface displacement

f = natural frequency, cycles per second

$\overline{f}(\frac{H_o}{D_o})$ = non-dimensional frequency function

$f_x(t)$ = time variation of horizontal foundation displacement

g = acceleration of gravity

h = shell wall thickness

h_L = height of liquid in tank

h_n = height to sloshing fluid mass, m_n, measured from the base of the tank

h_r = thickness of tank roof plate

h_o = height to stationary fluid mass, m_o, measured from the base of the tank

h_1 = height to fundamental sloshing fluid mass, m_1, measured from the base of the tank

$\vec{i}, \vec{j}, \vec{k}$ = unit vectors parallel to the x, y and z axes, respectively

ℓ_n = distance measured from the free surface of the liquid to the location of the n^{th} sloshing fluid mass, m_o

ℓ_o = distance measured from the free surface of the liquid to the location of the stationary fluid mass, m_o

ℓ_1 = distance measured from the free surface of the liquid to the location of the sloshing fluid mass participating in the first mode of vibration, m_1

m = axial wave number

m_c = mass of tank cylinder

m_n = mass of liquid participating in the n^{th} sloshing mode

m_r = mass of tank roof structure

m_T = total mass of fluid in tank

m_o = stationary liquid mass

m_1 = mass of liquid participating in the first sloshing mode

n = circumferential wave number

p_d = dynamic wall pressure

p_c = convective hydrodynamic wall pressure

p_i = impulsive hydrodynamic wall pressure

p_s = hydrostatic wall pressure

$\vec{p}$ = shell surface load vector

$q(t)$ = generalized coordinate for axisymmetric shell

$q(z)$ = effective inertia force per unit length of shell

r = radius of curvature of the parallel

r, θ, z = cylindrical coordinates

$\vec{r}$ = position vector from the origin of the Cartesian coordinate system to a point on the reference surface

$\vec{t}_1$ = unit tangent vector for the ζ_1 curve

$\vec{t}_2$ = unit tangent vector for the ζ_2 curve

$\vec{t}_3$ = unit vector determined from the cross product of $\vec{t}_1$ and $\vec{t}_2$

$\vec{t}_\phi, \vec{t}_\theta, \vec{t}_\zeta$ = triad of unit vectors tangent to the ϕ, θ and ζ coordinate curves, respectively

u_r = shell displacement perpendicular to the axis of symmetry

u_ϕ, u_θ, w = displacement of the middle surface in the meridional circumferential and radial directions, respectively

$\vec{u}$ = displacement vector of points lying on the reference surface

$\vec{u}_1$ = displacement vector of lowest mode of free vibration

$\bar{w}(\frac{z}{H_o})$ = corrected radial displacement functions (= $C_w \bar{\bar{w}}(\frac{z}{H_o})$)

$\bar{\bar{w}}(\frac{z}{H_o})$ = radial displacement function

$x(t)$ = horizontal component of earthquake ground motion

$\ddot{x}(t)$ = horizontal component of earthquake ground acceleration

$\ddot{x}$ = maximum value of horizontal earthquake ground acceleration

x, y, z = Cartesian coordinates

$[A(x)]$ = matrix of shell differential equation

$[I]$ = identity matrix

$[T(x)]$ = transformation matrix

$[W(x)]$ = matrix of homogeneous solutions to shell differential equations

$\{c\}$ = matrix of arbitrary constants

$\{d(x)\}$ = matrix containing particular solutions to shell differential equations

$\{y(x)\}$ = matrix of fundamental variables

Γ = mode participation factor

$\bar{\Gamma}(\frac{H_o}{D_o})$ = non-dimensional mode participation function

∇^2 = Laplace operator $(= \frac{\partial^2}{\partial r^2} + \frac{1}{r}\frac{\partial}{\partial r} + \frac{1}{r^2}\frac{\partial^2}{\partial \theta^2} + \frac{\partial^2}{\partial z^2})$

Φ = fluid velocity potential

$\psi(z)$ = shape function for determining wall accelerations in a fluid-filled tank

$\psi(\frac{z}{H_o})$ = deflection configuration for empty cylindrical tank

α_1 = metric component of ζ_1

α_2 = metric component of ζ_2

β_ϕ = angle of rotation of the normal in the meridional direction

β_θ = angle of rotation of the normal in the circumferential direction

β_ζ = describes change in thickness of shell wall

$\delta(x)$ = Dirac delta function

ε_ϕ, ε_θ = normal strains on the reference surface

ζ_1, ζ_2 = coordinates on the reference surface

θ = circumferential coordinate angle

θ_h = angular amplitude of free oscillations at the liquid surface

$\mu(z)$ = mass per unit length

ν = Poisson's ratio

$\vec{v}$ = displacement field for an axisymmetric shell

ρ = mass density of shell material

ρ_E = equivalent mass density of shell wall material plus stationary fluid mass

ρ_L = mass density of liquid in tank

ρ_{m_o} = density measure of stationary fluid mass over shell wall volume, V

ρ_s = mass density of steel (20.3 kg/m^3; 0.000733 $lb\text{-}sec^2/in^4$)

ρ_w = mass density of water (2.6 kg/m^3; 0.000094 lb-sec^2/in^4)

ρ_o = density measure of shell wall (= ρh)

ϕ = angle between the axis of symmetry of the shell and the shell normal

ω = natural circular frequency, radians per second

ω_M = natural frequency of coupled shell and stationary fluid mass

ω_n = natural frequency of fluid mass participating in the n^{th} sloshing mode

ω_1 = natural frequency of fluid mass participating in first sloshing mode

ω^I = sloshing fluid frequency (first mode) determined for the coupled shell-liquid system (from Eq. 3.13)

ω^{II} = natural frequency of shell and stationary fluid mass for the coupled shell-liquid system (from Eq. 3.13)

REFERENCES

1. Abramson, H. Norman
   THE DYNAMIC BEHAVIOR OF LIQUIDS IN MOVING CONTAINERS, NASA SP-106, 1966.

2. AN EVALUATION OF A RESPONSE SPECTRUM APPROACH TO SEISMIC DESIGN OF BUILDINGS, Applied Technology Council, San Francisco, California, 1974.

3. API STANDARD 620, RECOMMENDED RULES FOR DESIGN AND CONSTRUCTION OF LARGE, WELDED, LOW-PRESSURE STORAGE TANKS, American Petroleum Institute, Washington, D. C., 1977.

4. API STANDARD 650, WELDED STEEL TANKS FOR OIL STORAGE, 6th Edition, American Petroleum Institute, Washington, D. C., 1977.

5. Arnold, R. N. and Warburton, G. B.
   FLEXURAL VIBRATION OF THE WALLS OF THIN CYLINDRICAL SHELLS HAVING FREELY SUPPORTED ENDS, Proceedings of the Royal Society of London, Series A, Vol. 197, 1949, pp. 62-74.

6. Bathe, K. J. and Wilson, E. L.
   NUMERICAL METHODS IN FINITE ELEMENT ANALYSIS, Prentice-Hall, Inc., Englewood Cliffs, New Jersey, 1976.

7. Bathe, K. J., Wilson, E. L. and Peterson, F. E.
   SAP IV - A STRUCTURAL ANALYSIS PROGRAM FOR THE STATIC AND DYNAMIC RESPONSE OF LINEAR SYSTEMS, Earthquake Engineering Research Center Report No. 73-11, University of California, Berkeley, California, 1974.

8. Baker, E. H., Kovalevsky, L. and Rish, F. L.
   STRUCTURAL ANALYSIS OF SHELLS, McGraw Hill Book Company, New York, New York, 1972.

9. Bauer, H. F.
   FLUID OSCILLATIONS IN CONTAINERS OF A SPACE VEHICLE AND THEIR INFLUENCE ON STABILITY, NASA TR R-197, 1964.

10. Berg, G. V. and Stratta, J. L.
    ANCHORAGE AND THE ALASKA EARTHQUAKE OF 1964, American Iron and Steel Institute, July, 1974.

11. Biot, M. A.
ANALYTICAL AND EXPERIMENTAL METHODS IN ENGINEERING SEISMOLOGY, Transactions of the American Society of Civil Engineers, Vol. 108, 1943, pp. 365-408.

12. Blume, J. A., Newmark, N. M. and Corning, L. H.
DESIGN OF MULTISTORY REINFORCED CONCRETE BUILDINGS FOR EARTHQUAKE MOTIONS, Portland Cement Association, Skokie, Illinois, 1961.

13. Clough, D. P.
EXPERIMENTAL EVALUATION OF SEISMIC DESIGN METHODS FOR BROAD CYLINDRICAL TANKS, Department of Civil Engineering University of California, Berkeley, Report No. EERC/77-10, May, 1977.

14. Clough, R. W.
EARTHQUAKE RESPONSE OF STRUCTURES, in EARTHQUAKE ENGINEERING, Chapter 12, R. L. Wiegel, Editor, Prentice-Hall, Inc., Englewood Cliffs, New Jersey, 1970.

15. Clough, R. W. and Felippa, C. A.
A REFINED QUADRILATERAL ELEMENT FOR ANALYSIS OF PLATE BENDING, Proceedings of the 2nd Conference on Matrix Methods in Structural Mechanics, Wright Patterson Air Force Base, Ohio, 1968.

16. Clough, R. W. and Penzien, J.
DYNAMICS OF STRUCTURES, McGraw Hill, Inc., New York, New York, 1975.

17. COMBINING MODAL RESPONSES AND SPATIAL COMPONENTS IN SEISMIC RESPONSE ANALYSIS, Regulatory Guide 1.92, U. S. Nuclear Regulatory Commission, Washington, D. C., 1973.

18. DAMPING VALUES FOR SEISMIC DESIGN OF NUCLEAR POWER PLANTS, Regulatory Guide 1.61, U. S. Nuclear Regulatory Commission, Washington, D. C., 1973.

19. EARTHQUAKES
American Iron and Steel Institute, Washington, D. C., 1975.

20. Edwards, N. W.
A PROCEDURE FOR DYNAMIC ANALYSIS OF THIN WALLED CYLINDRICAL LIQUID STORAGE TANKS SUBJECTED TO LATERAL GROUND MOTIONS, Ph.D. Thesis, University of Michigan, Ann Arbor, Michigan, 1969.

21. Felippa, C. A.
THE FINITE ELEMENT ANALYSIS OF LINEAR AND NONLINEAR TWO-DIMENSIONAL STRUCTURES, SESM Report 66-2, Department of Civil Engineering, University of California, Berkeley, California, 1966.

22. Forsberg, K.
INFLUENCE OF BOUNDARY CONDITIONS ON THE MODAL CHARACTERISTICS OF THIN CYLINDRICAL SHELLS, AIAA Journal, Vol. 2, No. 12, 1964, pp. 2150-2157.

23. Graham, E. W. and Rodriquez, A. M.
THE CHARACTERISTICS OF FUEL MOTION WHICH AFFECT AIRPLANE DYNAMICS, Journal of Applied Mechanics, Vol. 19, 1952, pp. 381-388.

24. Hansen, H. M. and Chenea, P. F.
MECHANICS OF VIBRATION, John Wiley and Sons, Inc., New York, New York, 1959.

25. Hanson, R. D.
BEHAVIOR OF LIQUID STORAGE TANKS, THE GREAT ALASKA EARTHQUAKE OF 1964, National Academy of Sciences, Vol. 7, 1973.

26. Haroun, M. A.
DYNAMIC ANALYSIS OF LIQUID STORAGE TANKS, EERL 80-04, Earthquake Engineering Research Laboratory, California Institute of Technology, Pasedena, California, February, 1980.

27. Housner, G. W.
DYNAMIC PRESSURES ON ACCELERATED FLUID CONTAINERS, Bulletin of the Seismological Society of America, Vol. 47, No. 1, January, 1957.

28. Housner, G. W.
THE DYNAMIC BEHAVIOR OF WATER TANKS, Bulletin of the Seismological Society of America, Vol. 53, No. 2, February, 1963, pp. 381-387.

29. Housner, G. W., Martel, R. R. and Alford, J. L.
SPECTRUM ANALYSIS OF STRONG MOTION EARTHQUAKES, Bulletin of the Seismological Society of America, Vol. 43, 1953, pp. 97-119.

30. Hunt, B. and Priestly, N.
SEISMIC WATER WAVES IN A STORAGE TANK,
Bulletin of the Seismological Society of America,
Vol. 68, No. 2, April, 1978, pp. 487-499.

31. Jacobsen, L. S.
IMPULSIVE HYDRODYNAMICS OF FLUID INSIDE A CYLINDRICAL
TANK AND OF FLUID SURROUNDING A CYLINDRICAL PIER,
Bulletin of the Seismological Society of America,
Vol. 39, July, 1949, pp. 189-203.

32. Jacobsen, L. S. and Ayre, R. S.
IMPULSIVE HYDRODYNAMICS OF FLUIDS INSIDE A CYLINDRICAL
TANK, Bulletin of the Seismological Society of America,
Vol. 39, 1949, pp. 189-203.

33. Kalnins, A.
FREE VIBRATION OF ROTATIONALLY SYMMETRIC SHELLS,
Journal of the Acostical Society of America, Vol. 36,
No. 7, 1964, pp. 1355-1365.

34. Kalnins, A.
KSHEL - A COMPUTER PROGRAM FOR THE ANALYSIS OF PLATES
AND SHELLS, Department of Mechanical Engineering and
Mechanics, Lehigh University, Bethlehem, Pennsylvania,

35. Kalnins, A.
STRESS ANALYSIS OF BEAMS, PLATES AND SHELLS, Department
of Mechanical Engineering and Mechanics, Lehigh
University, Bethlehem, Pennsylvania

36. Kalnins, A.
VIBRATION AND STABILITY OF PRESTRESSED SHELLS, Nuclear
Engineering and Design, Vol. 20, 1972, pp. 131-147.

37. Kalnins, A.
VIBRATION OF FLUID-FILLED THIN SHELLS, Transactions
of the 5th International Conference on Structural
Mechanics in Reactor Technology, Paper B4/8, Berlin,
Germany, August, 1978.

38. Kalnins, A. and Dym, C. L.
VIBRATION OF BEAMS, PLATES AND SHELLS, Hutchinson
and Ross, Inc., Strousburg, Pennsylvania, 1976.

39. Kalnins, A. and Godfrey, D. A.
SEISMIC ANALYSIS OF THIN SHELL STRUCTURES,
Nuclear Engineering and Design, Vol. 27, 1974,
pp. 68-76.

40. Kostem, C. N.
STRENGTHING OF TALL CHIMNEYS IN EARTHQUAKE ZONES, Proceedings of the International Conference on Lightweight Shell and Space Structures for Normal and Seismic Zones, Vol. 2, IASS, Alma-Ata, MIR Publishers, U.S.S.R., 1977.

41. Kostem, C. N. and Tedesco, J. W.
ON THE ACCURACY OF THE FINITE ELEMENT ANALYSIS OF THE VIBRATIONAL CHARACTERISTICS OF SHALLOW CYLINDRICAL TANKS, World Congress on Shell and Spatial Structures, Vol. 1, Madrid Spain, September, 1979, pp. 2.33-2.43.

42. Kostem, C. N. and Tedesco, J. W.
VIBRATIONAL CHARACTERISTICS OF SHALLOW CYLINDRICAL TANKS, Proceedings of the 7th World Conference on Earthquake Engineering, Istanbul, Turkey, Part II, Structural Aspects, Vol. 5, September, 1980, pp. 513-520.

43. Kraus, H.
THIN ELASTIC SHELLS, John Wiley and Sons, Inc., New York, New York, 1967.

44. Kraus, H. and Kalnins, A.
TRANSIENT VIBRATION OF THIN ELASTIC SHELLS, Journal of the Acostical Society of America, Vol. 38, No. 6, December, 1965, pp. 994-1002.

45. Kumar, A.
STUDIES OF DYNAMIC AND STATIC RESPONSE OF CYLINDRICAL LIQUID STORAGE TANKS, Ph.D. Dissertation, Department of Civil Engineering, Rice University, 1981.

46. Lord Rayleigh,
THE THEORY OF SOUND, Vol. 1, 2nd Edition, Maxmillan, London, and Basingstoke, 1926.

47. Love, A. E. H.
A TREATISE ON THE MATHEMATICAL THEORY OF ELASTICITY, 4th Edition, Cambridge University Press, 1927.

48. Miles, R. W.
PRACTICAL DESIGN OF EARTHQUAKE RESISTANT STEEL RESERVOIRS, The Current State of Knowledge of Lifeline Earthquake Engineering, A.S.C.E., New York, New York, 1977, pp. 168-182.

49. Newmark, N. M.
DESIGN CRITERIA FOR NUCLEAR REACTORS SUBJECT TO EARTHQUAKE HAZARDS, University of Illinois Report, Urbana, Illinois, May 25, 1964.

50. Newmark, N. M.
EARTHQUAKE RESPONSE ANALYSIS OF REACTOR STRUCTURES, Nuclear Engineering and Design, Vol. 20, No. 2, 1972, pp. 303-322.

51. Newmark, N. M., Blume, J. A. and Kapur, K. K.
DESIGN RESPONSE SPECTRA FOR NUCLEAR POWER PLANTS, U. S. Atomic Energy Report, 1973.

52. Newmark, N. M. and Hall, W. J.
VIBRATION OF STRUCTURES INDUCED BY GROUND MOTION, SHOCK AND VIBRATION HANDBOOK, Chapter 29, Harris, C. M. and Crede, E. S. Editors, McGraw Hill, Inc., 1976.

53. Newmark, N. M. and Rosenblueth, E.
FUNDAMENTALS OF EARTHQUAKE ENGINEERING, Prentice-Hall, Inc., Englewood Cliffs, New Jersey, 1971.

54. Niwa, A.
SEISMIC BEHAVIOR OF TALL LIQUID STORAGE TANKS, Earthquake Engineering Research Center, Report No. UCB/EERC-78/04, February, 1978.

55. Parmelee, R. A.
RESEARCH NEEDS IN LIFELINE EARTHQUAKE ENGINEERING, The Current State of Knowledge of Lifeline Earthquake Engineering, A.S.C.E., New York, New York, 1977, pp. 454-458.

56. Pearson, C. E., editor
HANDBOOK OF APPLIED MATHEMATICS, Van Nostrand Reinhold Company, New York, New York, 1974.

57. Rinnie, J. F.
OIL STORAGE TANKS, The Prince William Sound, Alaska Earthquake of 1964 and Aftershocks, Vol. IIA, U. S. Coast and Geodetic Survey, Environmental Science Service Administration, 1967.

58. Rosenblueth, E.
DESIGN OF EARTHQUAKE RESISTANT STRUCTURES, John Wiley and Sons, Inc., New York, New York, 1980.

59. Ross, E. W., Jr.
ON INEXTENSIONAL VIBRATIONS OF THIN SHELLS, ASME, Journal of Applied Mechanics, Vol. 35, 1968, pp. 516-523.

60. Shaban, S. H. and Nash, W. A.
RESPONSE OF AN EMPTY CYLINDRICAL GROUND SUPPORTED LIQUID STORAGE TANK TO BASE EXCITATION, University of Massachusetts Report to National Science Foundation, August, 1975.

61. Thomas, W. T.
THEORY OF VIBRATIONS WITH APPLICATIONS, 2nd Edition, Prentice-Hall, Inc., Englewood Cliffs, New Jersey, 1981.

62. Tse, F. S., Morse, I. E. and Hinkle, R. T.
MECHANICAL VIBRATIONS, THEORY AND APPLICATIONS, 2nd Edition, Allyn and Bacon, Inc., Boston, 1978.

63. U. S. Atomic Energy Commission
NUCLEAR REACTORS AND EARTHQUAKES, TID-7024, Office of Technical Service, Washington, D. C., 1963.

64. Veletsos, A. S.
SEISMIC EFFECTS IN FLEXIBLE LIQUID STORAGE TANKS, Proceedings of the 5th World Conference on Earthquake Engineering, Vol. 1, Rome, Italy, 1974, pp. 630-639.

65. Veletsos, A. S. and Yang, J. Y.
EARTHQUAKE RESPONSE OF LIQUID STORAGE TANKS, Advances in Civil Engineering Through Engineering Mechanics, Proceedings of the EMD Specialty Conference, Rayleigh, North Carolina, ASCE, 1977, pp. 1-24.

66. Wang, C. T.
APPLIED ELASTICITY, McGraw Hill, Inc., New York, New York, 1953.

67. Wu, C. I., Mouzahis, T., Nash, W. A. and Colonell, J. W.
NATURAL FREQUENCIES OF CYLINDRICAL LIQUID STORAGE CONTAINERS, Department of Civil Engineering, University of Massachusetts, June, 1975.

68. Yang, J. Y.
DYNAMIC BEHAVIOR OF FLUID-TANK SYSTEMS, Ph.D. Dissertation, Department of Civil Engineering, Rice University, 1976.

69. Aslam, M., Godden, W. G. and Scalise, D. T.
EARTHQUAKE SLOSHING IN ANNUAL AND CYLINDRICAL TANKS, Journal of the Engineering Mechanics Division, ASCE, Vol. 105, No. EM3, June, 1979, pp. 371-389.

70. Epstein, H. I.
SEISMIC DESIGN OF LIQUID STORAGE TANKS, ASCE, Journal of the Structural Division, Vol. 102, No. ST9, September, 1976, pp. 1659-1671.

ACKNOWLEDGEMENTS

The authors are indebted to Professor Arturs Kalnins for the invaluable technical advice provided during various phases of the study.

The computer work for the study was performed at the Lehigh University Computing Center and the cooperation of the staff, especially Carol Rauch, Dean Krause, Paul Kern, Janice Polenchar and Lori A. Laubach, is appreciated.

Special thanks are extended to Mrs. Dorothy Fielding for her expert typing of the manuscript and to Mr. J. Gera for inking the figures.